2019

Metastable-State Photoacids: Synthesis, Properties, and Applications

Parth Patel
University of Central Florida

METASTABLE-STATE PHOTOACIDS: SYNTHESIS, PROPERTIES, AND APPLICATIONS

by

PARTH K. PATEL
B.S. University of Central Florida, 2014
M.S. University of Central Florida, 2017

A dissertation submitted in partial fulfillment of the requirements
for the degree of Doctor of Philosophy
in the Department of Chemistry
in the College of Sciences
at the University of Central Florida
Orlando, Florida

Fall Term
2019

Major Professor: Karin Y. Chumbimuni-Torres

ABSTRACT

Reversible photochromic compounds have the ability to reversibly change its color when it absorbs photons of a particular wavelength. This process of color change is a consequence of structural changes within the compound, such as cis-trans photo-isomerization. Some examples of photochromic compounds are spiropyrans, spirooxazines, diarylethenes and azobenzenes. These compounds have been extensively studied for decades, and are used in various applications such as biomedicine, chemical sensors and harvesting solar energy. However, majority of photochromic compounds are initially activated by ultraviolet (UV) light. The use of UV light is harmful for biological applications and photo-degrade the compound over repeated use. To overcome these limitations, a new class of reversible photochromic compound was introduced, called metastable-state photoacid (mPAH). In brief, mPAH is a photochromic compound which can photo-dissociate its protons under visible light and can thermally re-capture the released protons efficiently in the dark. Based on this unique property, in this research, we (1) synthesized different mPAH, and (2) studied and characterized their physicochemical (acidity, kinetics, and optical) properties. Additionally, we (3) applied different visible light activated mPAHs towards light controllable polymeric-based ion-selective optodes for detection of calcium ions and sodium ions, and modulate fluorescence with pH. The research presented herein opens new avenues towards the synthesis of mPAH derivatives and could be applied to any proton-transfer process related applications which requires wireless controllability with high sensitivity.

To my loving family and lovely wife.

Thanks for providing endless support throughout this “carefree” journey.

ACKNOWLEDGMENTS

I would like to express my sincerest gratitude to my mentor, Dr. Karin Y. Chumbimuni-Torres. There are still no words to describe how much it means when she welcomed me to her group, Nano-BioElectrochemistry Lab (NBEL). I really appreciate that she gave me the liberty to undertake this very challenging research early on, and entrusted me to other projects and the lab itself. Without her full support and guidance through numerous hardships, the success of this research would not have been possible.

I would like to give my sincerest thanks to all the committee members for providing support throughout my graduate studies and taking the time from the busy schedule to serve as a committee member. A special thanks to Dr. Florencio Hernandez for sharing his knowledge about fluorescence spectroscopy, and allowing me to use the very expensive fluorescence instrument for lifetime studies. A special thanks to Dr. Swadeshmukul Santra and Dr. Woo Hyoung Lee for sharing their knowledge during many collaborative meetings and exposing me on how to combat real-life problems. I am very grateful to be a part of a great collaboration. A special thanks to Dr. Melanie Beazley for sharing important information for which I truly appreciate.

Special thanks to Joseph Dejesus (now Dr. Dejesus) and Dr. Valentine Johns for exposing me to the world of metastable-state photoacids. Lastly, special thanks to all former and current NBEL members for the great support and hard work you have provided. You all made me go through every possible emotions there can be; and the journey we had in the lab was all worth it and irreplaceable. Thank you all, it means a lot.

TABLE OF CONTENTS

LIST OF FIGURES

LIST OF TABLES

LIST OF SCHEMES

LIST OF MEDIA

CHAPTER 1 GENERAL INTRODUCTION

1.1 Motivation

Media 1-1 Visual illustration of a colored solution in response to light. See supplemental file to view Media 1-1.

As shown in Media 1-1, a solution contains an organic dye initially exhibiting a yellow color. When this solution was irradiated with blue LED light and just after switching off the light source, the yellow solution turned almost clear. Interestingly, the near clear solution slowly regains the original yellow color after some time. Also, this color change can be switched back forth and it amazed me. Likewise, a bunch of questions arose. What dye was used and why the color changed? How can we apply such a dye to advance today's technology? Answering these simple

fundamental questions is what inspired me to pursue research about this interesting dye called metastable-state photoacid.

1.2 Reversible Organic Photochromic Compounds

Reversible organic photochromic compounds have a unique property. These compounds can reversibly undergo molecular structural or electronic configuration changes by absorbing photons of a particular wavelength of light.[1-3] Likewise, structural transformation in response to the non-invasive stimuli (light), these compounds are able to remotely modulate physicochemical properties; such as color, fluorescence, dipole moment, electrical property and/or acidity.[4-13] Also, the use of light provides spatial and temporal control over the processes involved.[14,15] To name a few, spiropyrans, spirooxazines, azobenenzes and diarylethenes are some of the most extensively studied reversible organic photochromic compounds (Figure 1-1).

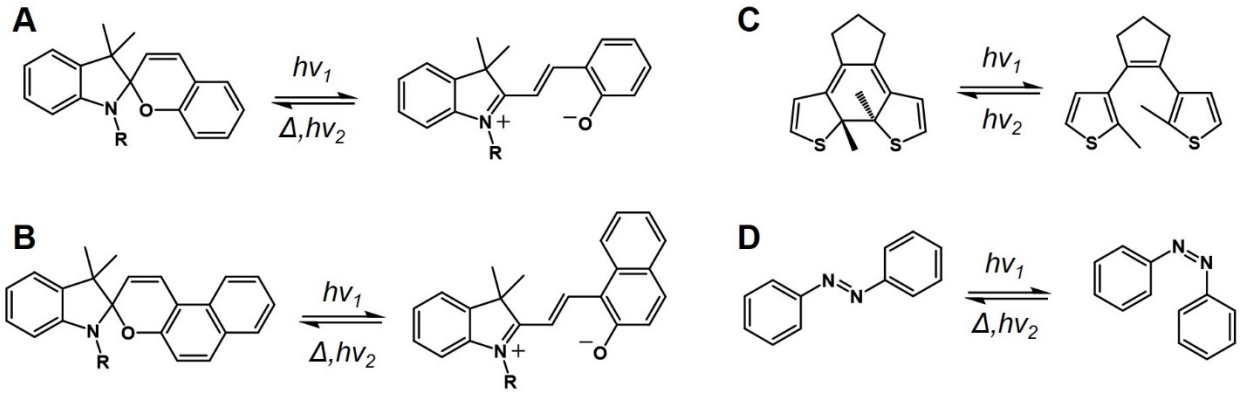

Figure 1-1 Examples of light responsive organic photochromic compound (A) spiropyran, (B) spirooxazine, (C) diarylethene, and (D) azobenzene.

These compounds have been applied towards designing light-responsive materials for various applications; for instance, chemical sensors, energy conversion, actuators, opticoelectronic devices or drug delivery applications.[16-24] However, most organic-based photochromic compounds use high-energy ultraviolet light (UV) for promoting changes in physicochemical property.[25] As a result of employing highly energetic light source to activate these compounds, its use in biological applications could prove detrimental.[26,27] Additionally, these organic photochromic compounds exhibit fatigueness in response of repeated activation by UV light.[25]

1.3 Reversible Organic Photo-acidochromic Compounds

The physicochemical property that is most intriguing is the reversible modulation of acidity or proton-transfer by light. This is because proton-transfer dependent chemical reaction is one of the most common reaction found in nature.[28] It is responsible for the production of adenosine triphosphate and controlling the photosynthetic pathway in plants.[29-31] Moreover, proton-transfer plays a vital role towards regulating many pH-dependent enzymes.[32-36] Therefore, controlling this important process by light could prove extremely beneficial for any proton-dependent applications. Since light can be applied remotely and non-invasively, is energy efficient, and provides spatiotemporal control.[37] As so, extensive research has been undertaken to artificially create reversible proton-gradient by light. This can be achieved by using pH and light-sensitive organic compounds, such as photobases (example: sipropyrans) and photoacids (example: excited-state photoacids and metastable-state photoacids).[13,38-45] A distinction must be made between these pH and light-sensitive organic compounds.

When a spiropyran compound (Sp) absorb UV light, it converts to its more basic merocyanine form (Mc); hence, a photobase (Figure 1-2).[13,38] Still under UV light, this merocyanine form can capture protons thermodynamically from an external proton source which is governed by the acidity constants and diffusion of protons. Additionally, protonated merocyanine (McH^+) is visible light sensitive.[13,38] Therefore, once UV light ceases and the visible light is exposed, McH^+ can than photo-release the protons back to the original source. Nonetheless, the use of UV light as mentioned previously could hinder its potential use.[26,27]

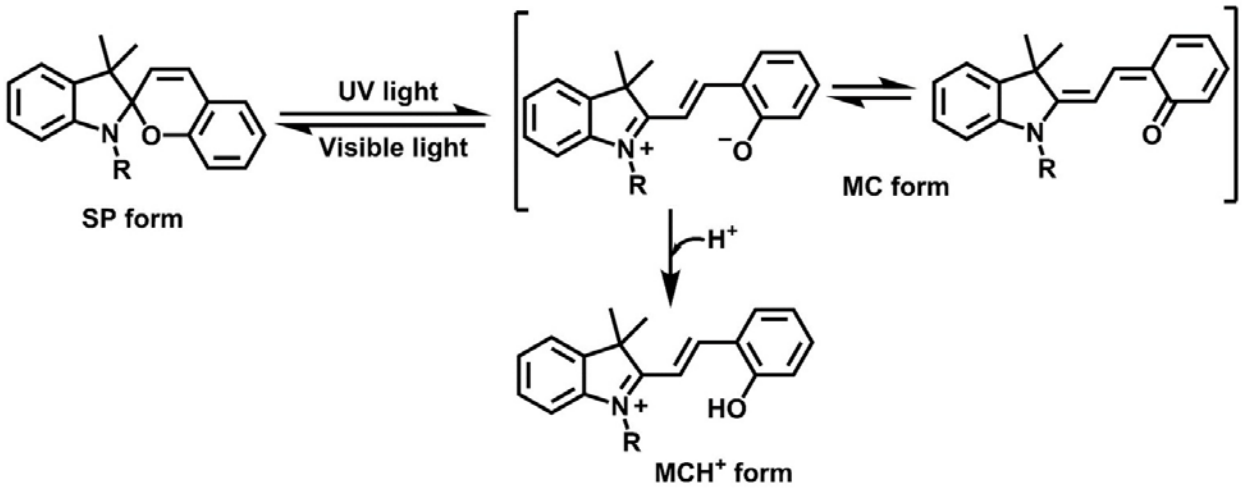

Figure 1-2 Reversible photo-acidochromic behavior of spiropyran.

On the other hand, photoacids in general behave like a strong acid under light activation.[28] They can photo-release their protons and can be re-captured when the light is switch off. Of the two types of reversible photoacids, excited-state photoacids (Figure 1-3) photo-release their protons from an electronically high-acidity excited state upon light activation.[39-42] When the light is switched off, the high-acidity excited state undergoes extremely fast relaxation (proton re-capture

process) to the original low-acidity ground state; thereby, hindering large change in proton gradient.[28] Hence, this type of photoacid may not be an ideal candidate for applications that rely on slow diffusion mediated proton-transfer reactions.

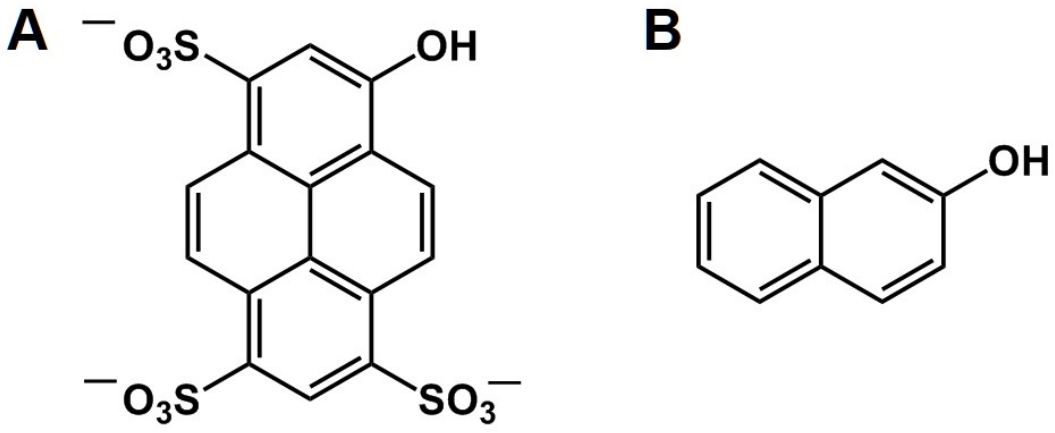

Figure 1-3 Examples of excited-state photoacid (A) Pyranine, and (B) 1-Naphthol.

1.4 Metastable-state Photoacids

Contrary to excited-state photoacids,[39-42] a new class of visible light activated photoacid, called metastable-state photoacid, was first introduced by Liao and co-workers in 2011.[43] This is the type of compound that was used to illustrate color changing behavior (Media 1-1). As shown in Figure 1-4, there are two types of metastable-state photoacids: merocyanine-type (Mer-mPAH) and tricyanofuran-type (TCF-mPAH).[43-45] Both these metastable-state photoacid were designed by connecting an electron-accepting moiety to a weakly acidic nucleophilic moiety by a trans-double bond.[28] In brief, these compounds are able to change color and photo-release their protons under

visible light activation via trans-cis photoisomerization followed by nucleophilic reaction between the two moieties.[28] When visible light is switched off, the color is regained and the photo-dissociated metastable-state photoacid displays thermodynamically driven long relaxation (proton re-capture process).[28]

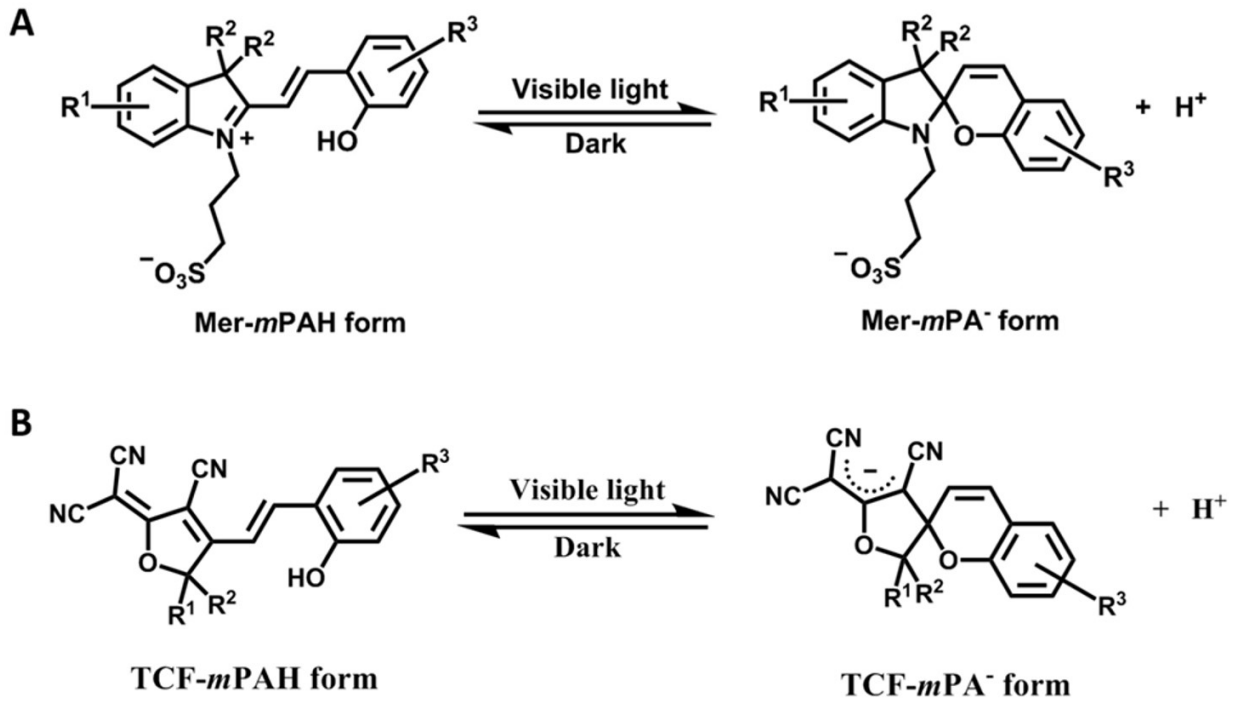

Figure 1-4 Reversible photo-acidochromic behavior of metastable-state photoacids (A) Merocyanine-type (Mer-mPAH), and (B) Tricyanofuran-type (TCF-mPAH).

This relaxation process is greatly slower than compared to the excited-state photoacids. Due to the improved stability of the photo-dissociated metastable-state photoacid, the photo-released protons can theoretically be used for any proton-transfer based applications. Furthermore, metastable-state photoacids can cause a large pH change with high efficiency and good reversibility. Due to these

unique factors, metastable-state photoacids have found numerous applications in recent years. To name a few, they have been applied towards controlling supramolecular structures,[46-48] killing bacteria,[49] used as an acid-catalyst,[43,50] activate ion-channels,[51] release fragrant molecules,[52] ATP production,[53] and manage waste[54].

Hence, presented in the following chapters, different visible light activated metastable-state photoacids (merocyanine- and tricyanofuran-type) were synthesized to meet the applications' requirement. These modified metastable-state photoacids were characterized and evaluated in terms of its optical properties, acidity, reversibility, and stability. In accordance to the evaluations, they were then applied towards cation-selective optode sensors,[55-57] and fluorescence and pH modulations[58].

1.5 References

1 R. Exelby, R. Grinter, *Chem. Rev.*, **1965**, *65*, 247.

2. M. Irie, *Chem. Rev*., **2000**, *100*, 1683.

3 H. Bouas-Laurent, H. Durr, *Pure Appl. Chem.*, **2001**, *73*, 639.

4 E. Orgiu, P. Samorì, *Adv. Mater*, **2014**, *26*, 1827.

5 F. Ercole, T. P. Davis, R. A. Evans, *Polym. Chem.*, **2010**, *1*, 37.

6 F. M. Raymo, M. J. Tomasulo, J. *Phys. Chem. A*, **2005**, *109*, 7343.

7 M. Natali, S. Giordani, *Chem. Soc. Rev.*, **2012**, *41*, 4010.

8 G. Callierotti, A. Bianco, C. Castiglioni, C. Bertarelli, G. Zerbi, *J. Phys. Chem. A*, **2008**, *112*, 7473.

9 F. L. E. Jakobsson, P. Marsal, S. Braun, M. Fahlman, M. Berggren, J. Cornil, X. Crispin, *J. Phys. Chem. C*, **2009**, *113*, 18396.

10 P. Toman, W. Bartkowiak, S. Nešpůrek, J. Sworakowski, R. Zaleśny, *Chem. Phys.*, **2005**, *316*, 267.

11 T. Tsujioka, M. Irie, *J. Photochem. Photobiol. C*, **2010**, *11*, 1.

12 M. Irie, T. Fukaminato, K. Matsuda, S. Kobatake, *Chem. Rev.*, **2014**, *114*, 12174.

13 L. Kong, H. L. Wong, A. Y. Y. Tam, W. H. Lam, L. Wu, V. W. W. Yam, *ACS Appl. Mater. Interfaces*, **2014**, *6*, 1550.

14 R. Göstl, A. Senf, S. Hecht, *Chem. Soc. Rev.*, **2014**, *43*, 1982.

15 P. Ceroni, A. Credi, M. Venturi, *Chem. Soc. Rev.*, **2014**, *43*, 4068.

16 X. J. Xie, G. Mistlberger, E. Bakker, *J. Am. Chem. Soc.*, **2012**, *134*, 16929.

17 X. J. Xie, G. Mistlberger, E. Bakker, *Anal. Chem.*, **2013**, *85*, 9932.

18 A. Balamurugan, H. Lee, *Macromolecules*, **2016**, *49*, 2568-2574.

19 S. Jia, W. Fong, B. Graham, B. J. Boyd, *Chem. Mater*., **2018**, *30*, 2873.

20 W. A. Velema, W. Szymanski, B. L. Feringa, *J. Am. Chem. Soc*., **2014**, *136*, 2178.

21 M. M. Lerch, M. J. Hansen, G. M. van Dam, W. Szymanski, B. L. Feringa, *Angew. Chem., Int. Ed.*, **2016**, *55*, 10978.

22 L. Wang, Q. Li, *Chem. Soc. Rev*., **2018**, *47*, 1044.

23 X. Xie, E. Bakker, *Phys. Chem. Chem. Phys*., **2014**, *16*, 19781.

24 M. Wei, Y. Gao, X. Li, M. J. Serpe, *Polym. Chem*., **2017**, *8*, 127.

25 S. Helmy, F. A. Leibfarth, S. Oh, J. E. Poelma, C. J. Hawker, J. Read de Alaniz, *J. Am. Chem. Soc*., **2014**, **136**, 8169.

26 V. Adler, A. Schaffer, J. Kim, L. Dolan, Z. Ronai, *J. Biol. Chem*., **1995**, *270*, 26071 -26077.

27 D. E. Brash, J. A. Rudolph, J. A. Simon, A. Lin, G. J. McKenna, H. P. Baden, A. J. Halperin, J. Pontén, *Proc. Natl. Acad Sci*., **1991**, *88*, 10124.

28 Y. Liao, Y. *Acc. Chem. Res*., **2017**, *50*, 1956.

29 V. I. Vullev, *J. Phys. Chem. Lett*., **2011**, *2*, 503.

30 N. Nelson, A. Ben-Shem, *Nat. Rev. Mol. Cell Biol*., **2004**, *5*, 971.

31 Y. Cheng, G. R. Fleming, *Annu. Rev. Phys. Chem.*, **2009**, *60*, 241.

32 T. Millat, H. Janssen, H. Bahl, R. Fischer, O. Wolkenhauer, *Microb. Biotechnol*., **2013**, *6*, 526.

33 Y. Zhang, J. Desharnais, S. E. Greasley, G. P. Beardsley, D. L. Boger, I. A. Wilson, Biochemistry, **2002**, *41*, 14206.

34 C. Malet, A. Planas, *Biochemistry*, **1997**, *36*, 13838.

35 H. Chahinian, T. Snabe, C. Attias, P. Fojan, S. B. Petersen, F. Carrière, *Biochemistry*, **2006**, *45*, 993.

36 S. Kohse, A. Neubauer, A. Pazidis, S. Lochbrunner, U. Kragl, *J. Am. Chem. Soc*., **2013**, *135*, 9407.

37 H. Nie, J. L. Self, A. S. Kuenstler, R. C. Hayward, J. Read de Alaniz, *Adv. Opt. Mater*., **2019**, 7, 1900224.

38 M. Hammarson, J. R. Nilsson, S. Li, T. Beke-Somfai, J. Andréasson, *J. Phys. Chem. B*, **2013**, *117*, 13561.

39 J. F. Ireland, P. A. H. Wyatt, *Advances in Physical Organic Chemistry*, Gold, V., Ed. Academic Press: **1976**, *12*, 131.

40 H. Shizuka, *Acc. Chem. Res*, **1985**, *18*, 141.

41 P. Wan, D. Shukla, *Chem. Rev*., **1993**, *93*, 571.

42 L. M. Tolbert, K. M. Solntsev, *Acc. Chem. Res*, **2002**, *35*, 19.

43 Z. Shi, P. Peng, D. Strohecker, Y. Liao, *J. Am. Chem. Soc*., **2011**, *133*, 14699.

44 V. K. Johns, P. Peng, J. DeJesus, Z. Wang, Y. Liao, *Chem. – Eur. J*., **2014**, *20*, 689.

45 C. Yang, T. Khalil, Y. Liao, *RSC Adv*., **2016**, *6*, 85420.

46 C. Maity, W. E. Hendriksen, J. H. van Esch, R. Eelkema, *Angew. Chem., Int. Ed.*, **2015**, *54*, 998.

47 D. Samanta, R. Klajn, *Adv. Opt. Mater*., **2016**, *4*, 1373.

48 X. Li, J. Fei, Y. Xu, D. Li, T. Yuan, G. Li, C. Wang, J. Li, *Angew. Chem., Int. Ed.*, **2018**, *57*, 1903.

49 Y. Luo, C. Wang, P. Peng, M. Hossain, T. Jiang, W. Fu, Y. Liao, M. Su, *J. Mater. Chem. B*, **2013**, *1*, 997.

50 C. Fu, J. Xu, C. Boyer, *Chem. Commun*., **2016**, *52*, 7126.

51 O. S. Shafaat, J. R. Winkler, H. B. Gray, D. A. Dougherty, *ChemBioChem*, **2016**, *17*, 1323.

52 Z. Wang, V. K. Johns, Y. Liao, *Chem. – Eur. J*., **2014**, *20*, 14637.

53 Y. Xu, J. Fei, G. Li, T. Yuan, Y. Li, C. Wang, X. Li, J. Li, *Angew. Chem., Int. Ed.*, **2017**, *56*, 12903.

54 L. A. Tatum, J. T. Foy, I. Aprahamian, *J. Am. Chem. Soc*., **2014**, *136*, 17438.

55 V. K. Johns, P. K. Patel, S. Hassett, P. Calvo-Marzal, Y. Qin, K. Y. Chumbimuni-Torres, *Anal. Chem*., **2014**, *86*, 6184.

56 P. K. Patel, V. K. Johns, D. M. Mills, J. E. Boone, P. Calvo-Marzal, K. Y. Chumbimuni-Torres, *Electroanalysis*, **2015**, *27*, 677.

57 P. K. Patel, K. Y. Chumbimuni-Torres, *Analyst*, **2016**, *141*, 85-89.

58 P. K. Patel, J. E. Arias, R. S. Gongora, F. E. Hernandez, A. Moncomble, S. Aloïse, K. Y. Chumbimuni-Torres, *Phys. Chem. Chem. Phys*., **2018**, *20*, 26804.

CHAPTER 2 VISIBLE-LIGHT ACTIVATED METASTABLE-STATE PHOTOACID POLYMER FOR CALCIUM DETECTION UNDER NON-EQUILIRIUM CONDITIONS

Reprinted with permission from Johns, V. K.; Patel, P. K.; Hassett, S.; Calvo-Marzal, P.; Qin, Y.; Chumbimuni-Torres, K. Y., "Visible Light Activated Ion Sensing Using a Photoacid Polymer for Calcium Detection.", *Analytical Chemistry*, **2014**, *86*, 6184-6187.

2.1 Abstract

Presented here is a sensing membrane consisting of a modified merocyanine photoacid polymer and a calcium ionophore in plasticized poly(vinyl chloride). This membrane is shown to actively exchange protons with calcium ions when switched ON after illumination at 470 nm, and the exchange can be followed by UV−vis spectroscopy. The sensing membrane shows no response in the ON state when calcium ions are absent. The limit of detection of the sensor is 5.0×10^{-4} M with an upper detection limit of 1.0 M. Thus, we demonstrate for the first time the use of a visible light activated, lipophilic photoacid polymer in an ion-sensing membrane for calcium ions, which highly discriminates potassium, sodium, and magnesium ions.

2.2 Introduction

A sensor that uses the change in absorption or emission of a dye provides a means for detecting analytes using different methods.[1-4] When the dye is a photoactive molecule, it promises control

over the sensor's characteristics using light as a noninvasive stimulus. Readily available monochromatic light sources, advances in photochemistry, and synthetic methods open the door for the use of such photoactive molecules in sensors.

Umezawa's group pioneered the use of photoswitchable molecules in potentiometric sensing[5] while other researchers have used different types of photoactive species in optical ion sensors.[6-9] A typical cation selective sensor consists of a lipophilic polymer membrane such as plasticized poly(vinyl chloride) (PVC) containing an ion-exchanger and two ionophores: one designed to bind to a cation of interest and the other is a pH indicator (chromoionophore) that interacts with a reference ion (H^+) and changes its optical properties. This change is related to the activity of the ion of interest. These sensors typically function under conditions of mass transfer equilibria and are passive in nature. However, they can be made dynamic by the use of photoactive compounds. For instance, Bakker and co-workers replaced the chromoionophore in a traditional optode with a spiropyran that photoisomerizes to a zwitterionic merocyanine form with increased basicity.[10,11] In order to be used as a sensor for cations, they had to introduce an external source of protons to protonate the photoisomerized merocyanine.[12] In contrast, the use of molecules that photorelease protons could eliminate the need for an external source of H^+.

There are two main types of molecules that release protons upon illumination: photoacid generators (PAGs) and photoacids (PAHs). PAGs undergo proton photodissociation irreversibly,[13,14] while PAHs are molecules that undergo proton photodissociation and thermal reassociation, hence promising reversibility.[15-17] Shvarev et al. recently used a PAG to perturb the

equilibrium of a conventional ion-sensing optode; however, to the best of our knowledge, no one has used a PAH in such sensing systems.[18] This ability to switch proton fluxes back and forth using light makes PAHs better candidates for use in reusuable optical ion sensors and, at the same time, obviates the need for conditioning prior to use.

Recently, a new PAH was reported that undergoes proton dissociation under visible light and thermal reassociation over multiple cycles with no observable fatigue and has a long-lived high-acidity state.[19,20] In addition, this PAH was shown to change the volume of a hydrogel upon photoillumination, used to inhibit bacterial growth,[21] and change the conductivity of a polymer.[22] The long-lived proton dissociated state allows for this PAH to be used in diffusion controlled processes. In contrast, most known PAHs have short-lived high acidity states,[15] hence limiting the use of these compounds in diffusion controlled states. We envision the introduction of this photoacid in optical ion sensors that can substitute the chromoionophore as well as serve to switch the sensor ON only when desired. Thus, this work presents our results toward a "first of a kind" cation-selective sensor based on a polymerized PAH reported before.[23]

2.3 Results and Discussion

The PAH mentioned before[19] is useful in applications which involve hydrophilic matrices, being incompatible with sensing membranes based on lipophilic components such as in optodes. A previous study described the synthesis of a copolymer between a PAH unit and methyl acrylate.[23] Acrylates are viable monomers for the synthesis of polymers used in optical sensing membranes.[24,25] Thus, the covalent attachment of the PAH unit to a lipophilic acrylic polymer

backbone might allow the introduction of this photoacid into a lipophilic sensing membrane. These membranes are typically composed of an inert polymer such as PVC dissolved in a plasticizer such as dioctylsebacate (DOS) or o-nitrophenyl octyl ether (o-NPOE). The proper choice of a plasticizer is very important as it fixes the dielectric constant, improves the selectivity, ensures a fast response, and elongates the lifetime of the sensor.[26] With a few modifications, polymer 1 (Scheme 2-1) was synthesized with ~10% PAH component (in blue) and ~90% methyl acrylate (in black) which was optimal for the lipophilic requirements of the PVC/DOS or o-NPOE membrane matrix described in this work. Higher percentages of photoacid polymer were synthesized but were not appropriate for PVC/DOS or PVC/o-NPOE matrix due to solubility problems.

Scheme 2-1 shows the likely mechanism of the sensor. The sensor can be activated (switched ON) upon irradiation at 470 nm for 5 min, where polymer 1 photocyclizes to polymer 2 with the concomitant release of protons. Incorporation of a cation selective ionophore (L) results in an exchange of protons with the cation of choice. The photogenerated protons should actively undergo two processes once the light is switched OFF. One is the recombination of the protons with polymer 2 to form polymer 1, and the second, the exchange of protons with the ion analyte, which should occur to maintain electroneutrality in the membrane. Considering the long-lived proton dissociated state, the exchange of protons with the analyte should be much faster than the protons recombining with polymer 2. The dynamics of this process can be monitored via UV–vis spectroscopy providing a means to detect cations optically.

Scheme 2-1 Schematic Structures of the PAH Polymer in the Ion-Sensing Membrane[a]

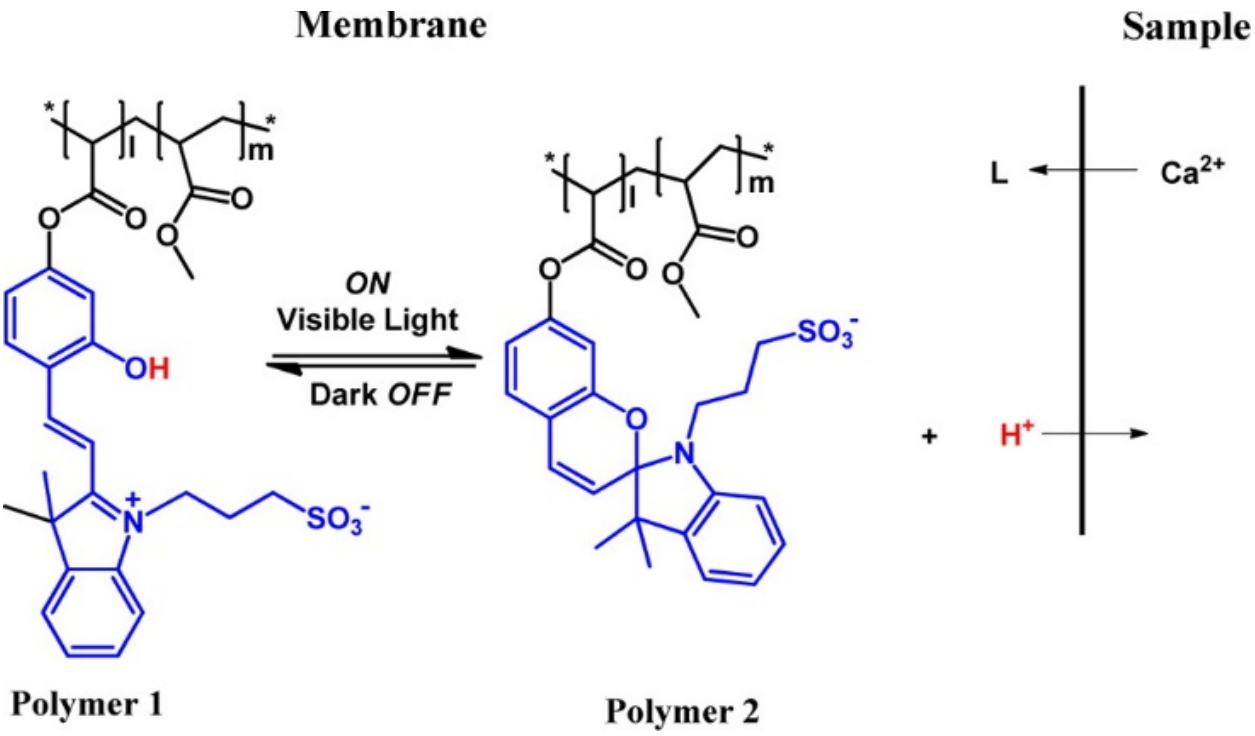

[a]L = Calcium Ionophore IV.

The sensing membrane used here was prepared with 9.74% (84.56 mmol/kg of PAH unit) of polymer 1, 8.48% (105.70 mmol/kg) of calcium ionophore IV, 27.26% of PVC, and 54.52% of o-NPOE. All components were dissolved in tetrahydrofuran, and the cocktail was spin coated onto glass slides to form the membranes. For measurements, 0.5 M tris(hydroxymethyl)aminomethane buffer at pH 7.40 (adjusted using 6.0 M HCl) was used. Figure 2-1 depicts the spectra of the ion-sensing membrane before irradiation (a), after 5 min of illumination at 470 nm (b), and finally after 35 min in the dark (c), while the sensing membrane was immersed in buffer solution.

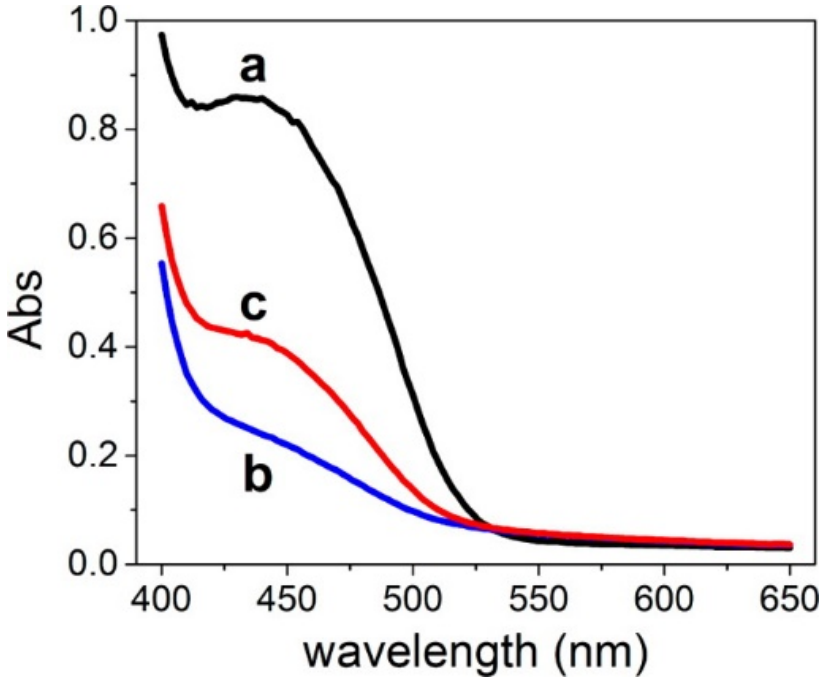

Figure 2-1 Absorbance spectra of ion-sensing membrane (a) before illumination, (b) after 5 min at 470 nm, and (c) after 35 min in the dark, in 0.5 M tris(hydroxymethyl)aminomethane buffer at pH 7.40.

The sensing membrane showed a change in absorbance at different concentrations of calcium ions. An increase in the calcium ion concentration in the sample solution favors the ion exchange between calcium ions and the photoreleased protons. Hence, more protons are released to the sample solution. Consequently, the formation of polymer 1 decreased, corresponding to a loss in absorbance (Figure 2-2A). A plot of the change in absorbance vs log of calcium ion activity is show in the Figure 2-2A inset. A blank experiment was performed where the sensing membrane was immersed in a buffer solution that did not contain calcium ions. The sensing membrane was illuminated for 5 min followed by 35 min in the dark. Ten subsequent runs were performed

showing barely any change in absorbance (Figure 2-2B). These results indicate that the sensor is stable over extended periods of illumination.

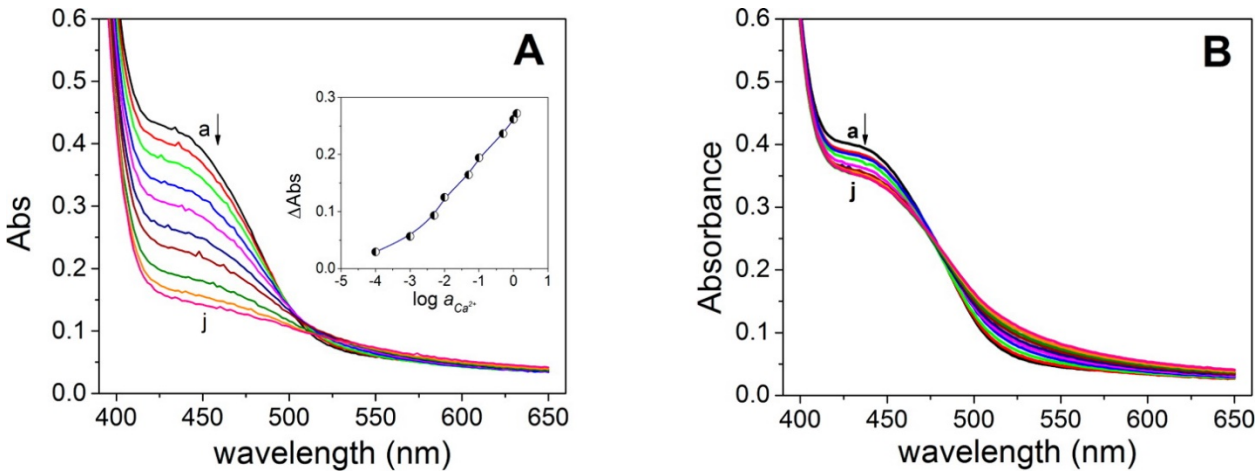

Figure 2-2 Absorbance spectra of ion-sensing membrane activated (A) after 35 min in the dark at different concentrations of calcium ions (a) 0.0, (b) 1.0×10^{-4}, (c) 1.0×10^{-3}, (d) 5.0×10^{-3}, (e) 1.0×10^{-2}, (f) 5.0×10^{-2}, (g) 1.0×10^{-1}, (h) 5.0×10^{-1}, (i) 1.0, and (j) 1.25 M. Inset in (A) shows the corresponding calibration curve for calcium ions. Conditions for the experiment were similar to Figure 2-1. (B) Blank experiment where ten subsequent runs were performed, after 5 min of illumination followed by 35 min in the dark when no calcium ions were present.

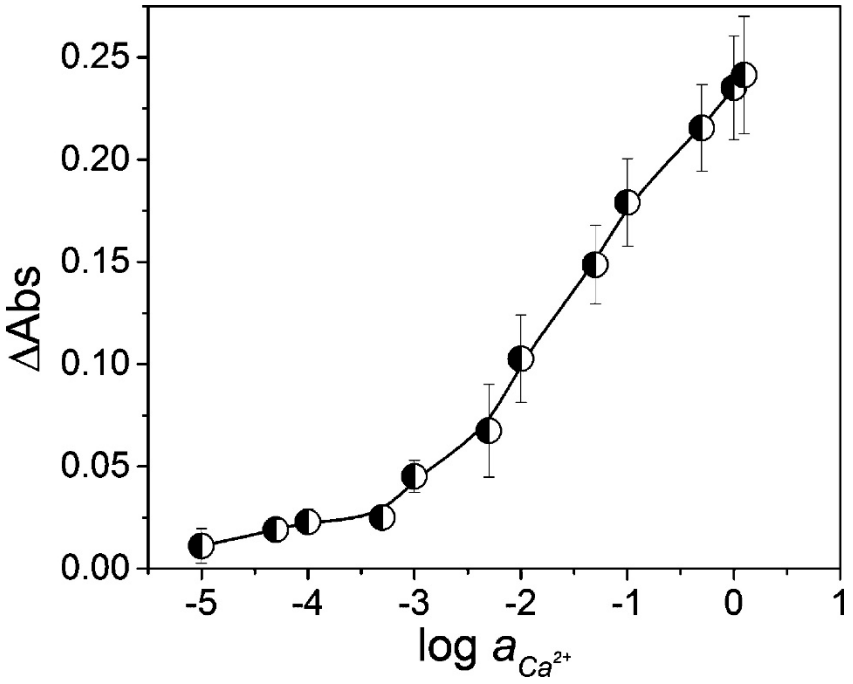

Figure 2-3 Calibration curve of ion-sensing membrane measured after 35 min upon activation for 3 different membranes. Conditions for the experiment are similar to Figure 2-1.

The reproducibility of the ion-sensing membrane response was evaluated by performing calibration curves with at least three different membranes, as can be seen in Figure 2-3. Concentrations in the range between 1.0×10^{-5} and 1.25 M Ca^{2+} were tested, and a detection limit of 5.0×10^{-4} M calcium ions was obtained. The response range of the photoactivated ion-sensing membrane presented here is similar to that reported in the literature based on the same ionophore[27,28] and is promising for applications requiring remote control. The change in absorbance for this sensor with an increase in Ca^{2+} concentration was evaluated after a 5 min activation at different times of the ion-exchange process (5, 10, 20, and 35 min), where the greatest

change was obtained at 35 min (see Appendix A, Figure A-1). For further experiments, 35 min was used.

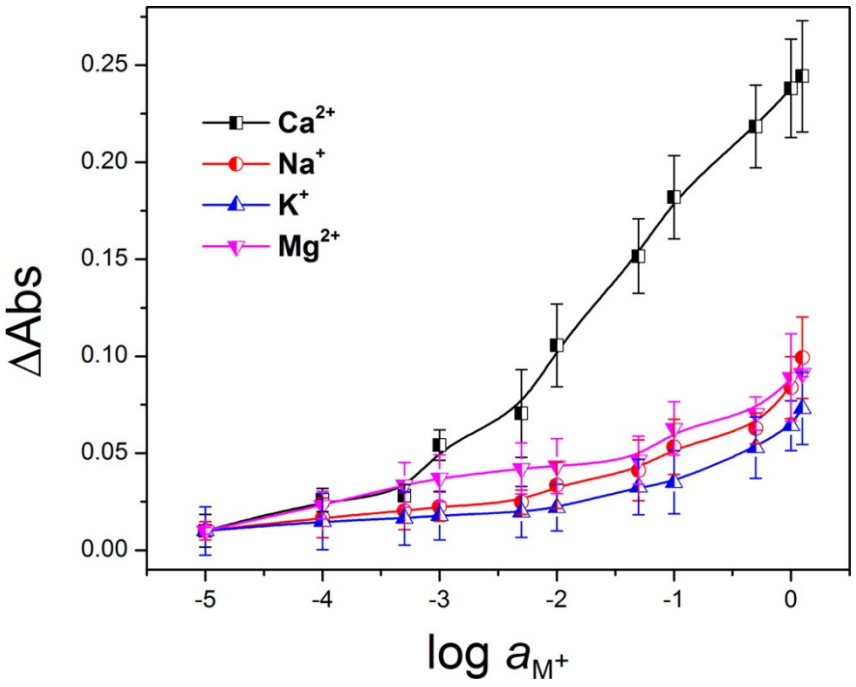

Figure 2-4 Selectivity for the ion-sensing membrane measured 35 min after activation. Conditions for the experiment are similar to Figure 2-1.

Two different matrices were tested for sensing: PVC/DOS and PVC/o-NPOE. While working with PVC/DOS, the sensing membrane did not discriminate against potassium ions. This was likely due to ion-pair formation of potassium ions with the sulfonate moiety present in polymer 2. The replacement of DOS by o-NPOE provided a polar medium to the membrane, due to its higher dielectric constant[3] disfavoring the formation of such ion-pairs between soft ions such as potassium and the sulfonate moiety. To further explore the selectivity of the ion-sensing membrane, different

ions were tested. Thus, Figure 2-4 shows the response of the calcium ion sensor after it was exposed to different concentrations of sodium, potassium, and magnesium ions in 0.5 M buffer solution for 35 min, which indicates a good selectivity with respect to the change in absorbance. When compared to traditional optodes using the same ionophore, the discrimination of interfering ions was found to be similar.[27]

2.4 Conclusion

For the first time, a visible light activated, lipophilic PAH polymer was incorporated into an ion-sensing membrane, which can be regenerated. A new dynamic sensing technique was also demonstrated for calcium ions based on phototriggered proton exchange. The importance of this sensor lies in the fact that the sensing membrane can be triggered only when desired by using visible light and needs no conditioning or ion-exchanger.

Work is in progress to improve the limits of detection and extend this sensing mechanism to other cations. It is anticipated that the PAH polymer will replace the pH sensitive dye used in traditional optodes. Such sensors will be especially useful for controlled sensing where the sensor can be turned ON/OFF merely by flipping a switch.

2.5 Acknowledgments

The authors acknowledge the College of Sciences and the Department of Chemistry at the University of Central Florida for financial support of this research. We also thank Dr. Liao (Florida Institute of Technology) for important discussions and advice on photoacids.

2.6 References

1 Morf, W. E.; Seiler, K.; Rusterholz, B.; Simon, W. *Anal. Chem*., **1990**, *62*, 738−742

2 Seiler, K.; Simon, W. *Anal. Chim. Acta* **1992**, *266*, 73−87.

3 Bakker, E.; Buhlmann, P.; Pretsch, E. *Chem. Rev*. **1997**, *97*, 3083−3132.

4 Hisamoto, H. *TrAC, Trends Anal. Chem*. **1999**, *18*, 513−524.

5 Tohda, K.; Yoshiyagawa, S.; Kataoka, M.; Odashima, K.; Umezawa, Y. *Anal. Chem*. **1997**, *69*, 3360−3369.

6 Evans, L.; Collins, G. E.; Shaffer, R. E. *Anal. Chem*. **1999**, *71*, 5322−5327.

7 Oosaki, S.; Hayasaki, H.; Sakurai, Y.; Yajima, S.; Kimura, K. *Chem. Commun*. **2005**, *41*, 5226−5227.

8 Radu, A.; Byrne, R.; Alhashimy, N.; Fusaro, M.; Scarmagnani, S.; Diamond, D. *J. Photochem. Photobiol., A* **2009**, *206*, 109−115.

9 Hakonen, A.; Hulth, S. *Talanta* **2010**, *80*, 1964−1969.

10 Mistlberger, G.; Crespo, G. A.; Xie, X.; Bakker, E. *Chem. Commun*. **2012**, *48*, 5662−5664.

11 Xie, X.; Mistlberger, G.; Bakker, E. *J. Am. Chem. Soc*. **2012**, *134*, 16929−16932.

12 Mistlberger, G.; Xie, X. J.; Pawlak, M.; Crespo, G. A.; Bakker, E. *Anal. Chem*. **2013**, *85*, 2983−2990.

13 Crivello, J. V. *J. Photopolym. Sci. Technol*. **2008**, *21*, 493−497.

14 Crivello, J. V. *J. Photopolym. Sci. Technol*. **2009**, *22*, 575−582.

15 Shizuka, H. *Acc. Chem. Res*. **1985**, *18*, 141−147.

16 Tolbert, L. M.; Solntsev, K. M. *Acc. Chem. Res*. **2002**, *35*, 19−27.

17 Nunes, R. M. D.; Pineiro, M.; Arnaut, L. G. *J. Am. Chem. Soc*., **2009**, *131*, 9456−9462.

18 Shvarev, A. *J. Am. Chem. Soc*. **2006**, *128*, 7138−7139.

19 Shi, Z.; Peng, P.; Strohecker, D.; Liao, Y. *J. Am. Chem. Soc*. **2011**, *133*, 14699−14703.

20 Johns, V. K.; Wang, Z.; Li, X.; Liao, Y. *J. Phys. Chem. A* **2013**, *117*, 13101−13104.

21 Luo, Y.; Wang, C. M.; Peng, P.; Hossain, M.; Jiang, T. L.; Fu, W.; Liao, Y.; Su, M. *J. Mater. Chem. B* **2013**, *1*, 997−1001.

22 Shi, Z.; Peng, P.; Johns, V. K.; Liao, Y. *Polym. Prepr*. **2012**, *53*, 125−126.

23 Johns, V. K.; Liao, Y. *Polym. Prepr*. **2012**, *53*, 255−256.

24 Heng, L. Y.; Hall, E. A. H. *Electroanalysis* **2000**, *12*, 178−186.

25 Qin, Y.; Peper, S.; Bakker, E. *Electroanalysis* **2002**, *14*, 1375−1381.

26 Muhammed, L., Ed. *Recent Advances in Plasticizers*; Intech: Rijeka, Croatia, 2012.

27 Bychkova, V.; Shvarev, A. *Anal. Chem*. **2009**, *81*, 2325−2331.

28 Crespo, G. A.; Bakker, E. *Analyst* **2012**, *137*, 4988−4994.

CHAPTER 3 CHARACTERIZING THERMODYNAMIC PROTON RE-CAPTURE PROCESS OF TWO DIFFERENT FUNCTIONALIZED METASTABLE-STATE PHOTOACID

3.1 Abstract

Herein, we present different functionalized meta-stable photoacids in ion-sensors to tune the equilibrium response time. As a proof of concept, two new meta-stable photoacids were synthesized, one contains an ether group and the other has an ester functional group. These functionalized meta-stable photoacids were elucidated in solution of ethanol and in ion-sensing films via pH and kinetic studies. In comparison from our previous work, the response time was reduced from hours to minutes by utilizing an ether functional group in the meta-stable photoacid.

3.2 Introduction

The last few decades have seen considerable progress in ion sensing electrodes and optodes.[1–3] Specifically in terms of improving the selectivity and detection limits at equilibrium and non-equilibrium conditions, as discussed by Bobacka et al.[4] Since ion-selective optodes provide "wireless" detection of ions, researchers have shown increased interest in developing these

sensors.[5–9] Optodes are made of a plasticized polymer (that serves as a matrix support) containing an ion-exchanger (that maintains electroneutrality), an ionophore (that is selective to the ion of interest), and chromoionophore or pH indicator (that is selective to a reference ion (H^+)).[2] The detection of the analyte depends on mass transfer equilibria, which is dictated by the activity of the analyte and the reference ion.[10–12] The changes in the optical property of the indicator relates to the activity of the ion of interest, and can be followed via absorbance and/or fluorescence spectroscopy.[13–15]

Most optodes are passive in nature which limits control over the ion-exchange process.[2,13] Whereas, an active optode would be ideal for ion detection applications done locally. One possible way to make an optode active is by using photoactive compounds. While different research groups have used photoacid generators[14] and spiropyrans (Sp)[16,17] to achieve this, we have used meta-stable photoacids (mPAHs).[18] A distinction must be made between photoacids (PAHs) and mPAHs. While both are reversible, PAHs release protons from an electronically excited state[19]; hence the proton recapture is too fast (in the order of nanoseconds to seconds) to be useful in diffusion mediated sensing. Alternatively, mPAHs photo- release protons from a meta-stable state.[20,21] This state is sufficiently long-lived (in the order of minutes to hours) for the ion-exchange process to take place.

In addition, mPAHs-based ion sensors can be remotely activated by visible light, do not suffer photo-fatigue[20,21], and enable reversibility of the sensor[18]. However, in order for those advantages to be realized, further studies are required. One of the major issues we encountered previously was

the fact that the proton re-association took hours to reach the equilibrium, consequently the detection was performed under non-equilibrium conditions.[18]

In order to achieve detection under equilibrium conditions, the photo-dissociated state of the mPAH should have a shorter lifetime (in the order of minutes). The stability of the photo-dissociated form of the mPAH is likely dictated by electronic effects. As the mPAH we used was covalently attached to the polymer backbone by an ester linkage,[18] we hypothesized that the electron withdrawing nature of the ester group at the meta position from the pyran oxygen could be extending the lifetime of the photo-dissociated state. We thus decided to study the effect of electron demand of the linker with respect to the mPAH to determine if the lifetime of the photo-dissociated state could be shortened.

Here, we present the synthesis of two mPAHs containing different functional groups, one has an ether group (PA-4Octadec) and the other has an ester group (PA-4Stearoyl). These functionalized mPAHs are characterized in solution and in the ion-sensing film. In addition, kinetic studies are presented to relate the effect of the functional group with the proton recapture process.

3.3 Experimental

3.3.1 Reagents

2,4-Dihydroxybenzaldehyde, stearoyl chloride, high molecular weight poly(vinyl chloride) (PVC), terakis(4-chlorophenyl)borate tetradodecylammonium salt (ETH 500), N,N-dicyclohexyl-N,N-

dioctadecyl-3-oxapentanediamide (calcium ionophore IV), triethylamine (Et_3N), 1,3-dichloro-1,1,3,3-tetramethyldisiloxane, and 2-nitrophenyl octyl ether (o-NPOE) were obtained from Sigma Aldrich, USA. Potassium iodide (KI), tris(hydroxymethyl) aminomethane (tris), ethanol (EtOH), acetonitrile (MeCN), hydrogen peroxide (H_2O_2), sulfuric acid (H_2SO_4), and hydrochloric acid (HCl) were obtained from Fischer Scientific, USA. Dichloromethane, ethyl acetate, hexane, and acetone were obtained from Macron, USA. Calcium chloride, 1-bromooctadecane, tetrahydrofuran (THF), and cyclohexanone were obtained from Acros, Belgium. Potassium carbonate anhydrous (K_2CO_3), and sodium sulfate anhydrous (Na_2SO_4) were obtained from Amresco, USA. Chloroform-D ($CDCl_3$) and dimethyl sulfoxide-D_6 (DMSO) were obtained from Cambridge Isotope Laboratories, Inc., USA.

3.3.2 Instruments

Absorption spectra were obtained using a UV-Visible spectrophotometer (Cary 50) from Varian, Australia. The light source for the photoreaction was a 470 nm LED array with 120 LEDs from Elixa, USA. NMR spectra were obtained with a NMR spectrometer (Avance III 400) of 400 MHz from Bruker, USA. The pH measurements were obtained with a pH meter (Orion Star A211) from Thermo Scientific, USA. The thickness of the ion-sensing films was measured using a profilometer (Tencor AlphaStep 500) from KLA Tencor, USA. DI water used to prepare solutions was purified by a water purification system with resistance of 18 MΩcm (PURELAB Ultra) from Siemens, USA. All experiments were carried out in the dark.

3.3.3 Synthesis

Scheme 3-1 shows the steps for the synthesis of the two new mPAHs.

3.3.3.1 Synthesis of 2-Hydroxy-4-(octadecyloxy)benzaldehyde) (1)

1.0 g (7.2 mmol) of 2,4-dihydroxybenzaldehyde, 1.0 g (7.2 mmol) of K_2CO_3, 0.072 g (0.42 mmol) of KI, and 3.0 mL of dry acetone were added to a round bottom flask and refluxed under N_2 for 30 min until the solution became cloudy and pink. Then, 2.4 g (7.2 mmol) of 1-bromooctadecane and 3.0 mL of dry acetone were added. The solution was refluxed overnight, quenched with water and filtered. The product was extracted in dichloromethane, dried with Na_2SO_4, and purified by column chromatography using 1 % ethyl acetate in hexane as the eluent. Yield (2.1 g, 74.8 %). H^1 NMR (400 MHz, $CDCl_3$), δ = 11.5 (s, 1H), 9.7 (s, 1H), 7.4 (m, 1H), 6.5 (m, 1H), 6.4 (m, 1H), 4.0 (t, 2H), 1.8 (m, 2H), 1.4 (m, 2H), 1.2 (m, 30H), 0.9 (m, 3H).

3.3.3.2 Synthesis of 2,3,3-Trimethyl-1-(3-sulfonatepropyl)-3H-indolium (2)

Compound 2 was synthesized according to the literature procedure.[21,22]

3.3.3.3 Synthesis of 4-Formyl-3-hydroxyphenyl stearate (3)

1.0 g (7.2 mmol) of 2,4-dihydroxybenzaldehyde, 1.4 mL (9.9 mmol) of dry Et_3N, 5.0 mL of dry acetone, and 25 mL of dry dichloromethane were added to a reaction flask under N_2. The reaction mixture was immersed in an ice-bath and stirred for 10 min. After that, 2.2 mL (6.6 mmol) of

stearoyl chloride was added. The mixture was slowly raised to room temperature and allowed to stir overnight, then quenched with water, washed with brine (saturated salt water) and dried with Na_2SO_4. The product was then chromatographed using 1 % ethyl acetate in hexane as the eluent. Yield (1.37 g, 47.1 %). ^{1}H NMR (400 MHz, $CDCl_3$), δ = 11.2 (s, 1H), 9.9 (s, 1H), 7.6 (m, 1H), 6.8 (m, 2H), 2.5 (t, 2H), 1.8 (m, 2H), 1.3 (m, 28H), 0.9 (m, 3H).

3.3.3.4 Synthesis of ((E)-3-(2-(2-Hydroxy-4-(octadecyloxy)styryl)-3,3-dimethyl-3H-indol-1-ium-1-yl)propane-1-sulfonate (PA-4Octadec)

Compound 1 (0.26 mmol) and 2 (0.26 mmol) were added into 2 mL EtOH. The mixture was allowed to reflux overnight under N_2. Orange solids were obtained on cooling, which were separated via filtration followed by washing the solids in cold EtOH, then 2 mL of dichloromethane followed by 10 mL of THF to provide the corresponding mPAH. Yield (0.095 g, 55.9 %). ^{1}H NMR (400 MHz, DMSO), δ = 11.2 (s, 1H), 8.4 (d, 1H, J = 16.1 Hz), 8.2 (d, 1H, J = 9.0 Hz), 7.9 (d, 1H, J = 7.9 Hz), 7.7 (d, 1H, J = 7.2 Hz), 7.6 (d, 1H, J = 16.2 Hz), 7.5 (m, 2H), 6.5–6.4 (m, 2H), 4.6 (t, 2H), 4.0 (t, 2H), 2.5 (t, 2H), 2.0 (m, 2H), 1.7 (s, 6H), 1.3–1.1 (m, 32H), 0.8 (m, 3H).

3.3.3.5 Synthesis of (E)-3-(2-(2-Hydroxy-4-(stearoyloxy)styryl)-3,3-dimethyl-3H-indol-1-ium-1-yl)propane-1-sulfonate (PA-4Stearoyl)

Compound 2 (0.26 mmol) and 3 (0.26 mmol) were added into 5 mL MeCN. The mixture was allowed to reflux overnight under N_2. Orange solids were obtained on cooling which were separated by filtration followed by washing the solids in copious amounts of hexane to provide the corresponding mPAH. Yield (0.050 g, 28.8 %). ^{1}H NMR (400 MHz, DMSO), δ = 11.4 (s, 1H), 8.5

(d, 1H, J = 16.3 Hz), 8.3 (d, 1H, J = 8.7 Hz), 8.0 (m, 1H), 7.9 (m, 2H), 7.6 (m, 2H), 6.8 (m, 2H), 4.8 (t, 2H), 2.6 (m, 4H), 2.2 (m, 2H), 1.8 (s, 6H), 1.6 (m, 2H), 1.2 (m, 28H), 0.8 (m, 3H).

Scheme 3-1 Steps for the synthesis of mPAHs (PA-4Octadec and PA-4Stearoyl).

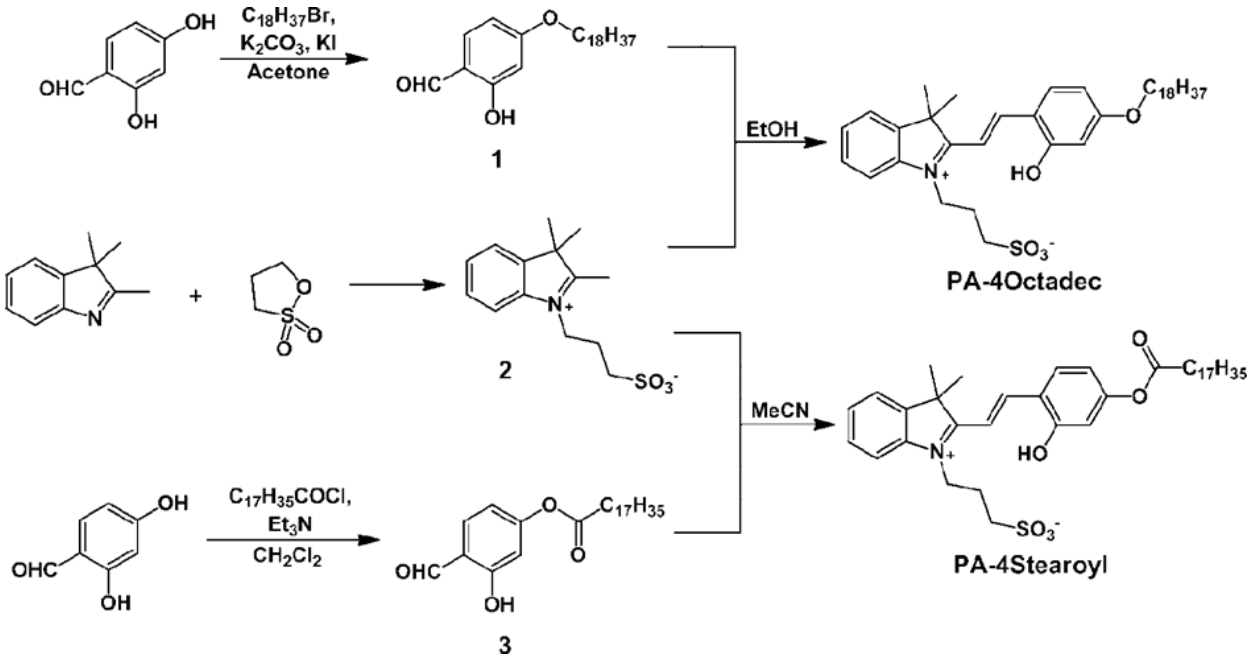

3.3.4 Preparation of Ion-Sensing Films

3.3.4.1 Silanization of Glass Slides

The silanization procedure is similar to the previously reported literature with few modifications.[23] The glass slides were previously cut to fit the cuvette, which were washed in piranha solution for 30 minutes at 90 °C (safety note: the piranha solution must be handled with caution). The glass slides were then thoroughly rinsed with deionized (DI) water and dried in a vacuum oven for 30

minutes. The clean glass slides were then silanized in a mixture of 1,3-dichloro-1,1,3,3-tetramethyldisiloxane and dichloromethane for 3 hours at 50 rpm on an orbital shaker. The silanized glass slides were thoroughly rinsed with isopropanol and DI water, then dried again in the vacuum oven, and stored in a vacuum desiccator until use.

3.3.4.2 Ion-Sensor Containing PA-4Octadec

The sensor contains 0.49 mg of PA-4Octadec (15.0 mmol/kg), 1.80 mg of calcium ionophore (45 mmol/kg), 0.86 mg of ETH 500 (15 mmol/kg), PVC (66.0 wt%), and o-NPOE (33 wt%). Cyclohexanone (800 µL) was added to dissolve all the components, and the mixture was vortexed for 30 minutes to obtain a homogeneous cocktail solution. Subsequently, 20 µL of cocktail solution was dropped onto silanized glass slides and stored in vacuum overnight. The thickness of the film formed was 9.07±0.22 µm.

3.3.4.3 Ion-Sensor Containing PA-4Stearoyl

The sensor contains 0.50 mg of PA-4Stearoyl (15 mmol/kg), 1.80 mg of calcium ionophore (45 mmol/kg), 0.86 mg of ETH 500 (15 mmol/kg), PVC (66 wt%), and o-NPOE (33 wt%). Cyclohexanone was used to dissolve all the components, and the following procedure was the same as in Section 3.3.4.2. The thickness of the film formed was 7.10±0.52 µm.

3.3.5 Characterization of mPAHs

3.3.5.1 pH Measurements

To measure the pH for both mPAHs, PA-4Octadec (1.04 mg) and PA-4Stearoyl (0.97 mg) were dissolved in a mixture of 90 % EtOH and 10 % DI water, separately. Prior to irradiation with visible light (470 nm), the pH of the solution was recorded. Subsequently, the dissolved mPAHs were irradiated for 2 minutes and the pH was registered. From the data acquired, the pKa's were calculated before irradiation for each mPAH.

3.3.5.2 Kinetics Measurements

Kinetics studies were performed by dissolving the mPAHs in EtOH (PA-4Octadec at the concentration of 21.6×10^{-6} M, and PA-4Stearoyl at 23.2×10^{-6} M) and irradiating for 2 minutes with visible light (470 nm). The rate of proton re-association was monitored by measuring the absorbance (of the reprotonated form) every 15 seconds for PA-4Octadec and every 15 minutes for PA-4Stearoyl, respectively. The molar absorptivities for both mPAHs in EtOH were calculated from the maximum absorbance obtained by acidifying the solution with 6.0 M HCl.

The above procedure was also used to determine the time it takes for proton re-association for each mPAH in the ion-sensing film using a 0.025 M tris buffer at pH 7.40 (adjusted by 6 M HCl).

All kinetic data were plotted as the maximum absorbance vs. time.

3.4 Results and Discussion

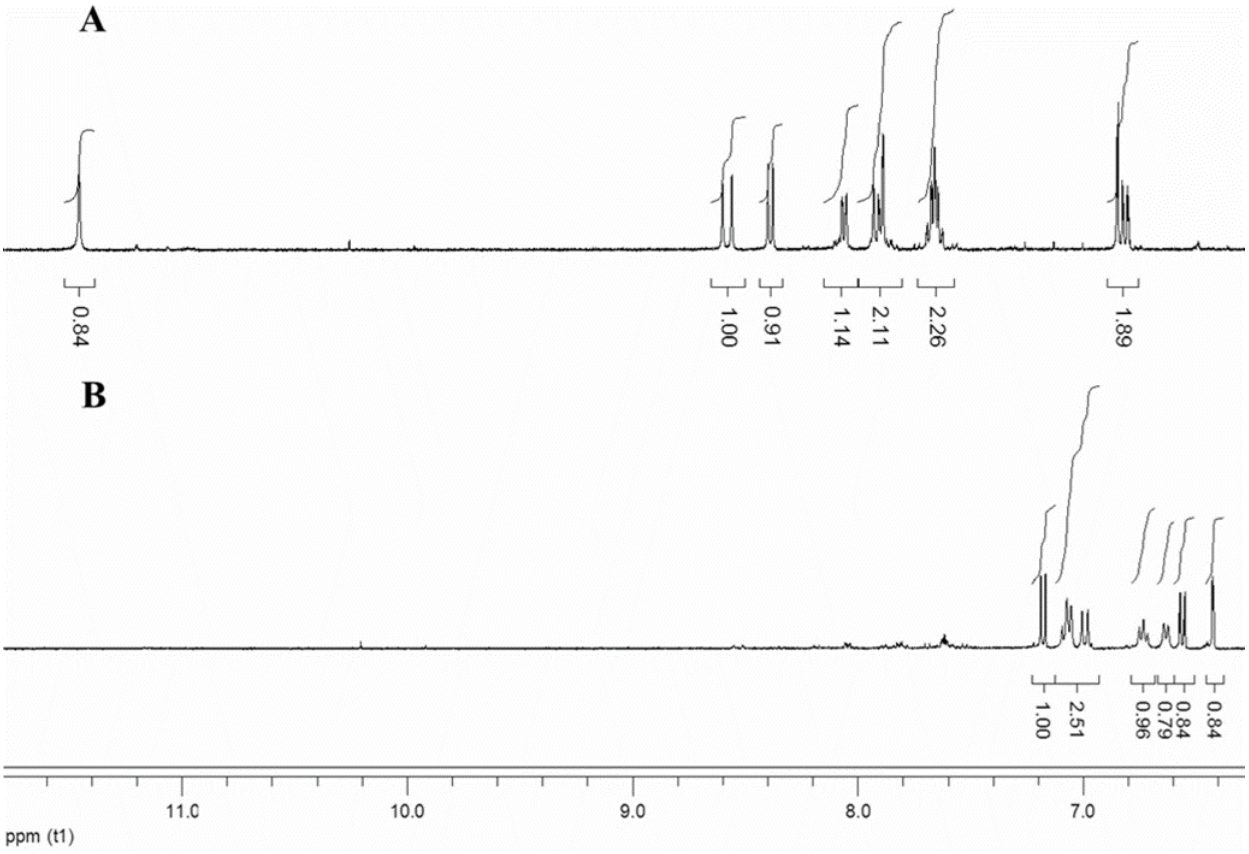

Figure 3-1 ^{1}H NMR of PA-4Stearoyl for (A) before irradiation, and (B) after 2 minutes irradiation (470 nm).

PA-4Octadec and PA-4Stearoyl were synthesized according to Scheme 3-1. PA-4Octadec was linked to a lipophilic alkyl chain via an ether functional group, whereas PA-4Stearoyl uses an ester as the linker. Initially, the mPAHs were studied by NMR spectroscopy to understand the photo-induced structural change and the effect of functional groups upon irradiation. Thus, spectra of PA-4Octadec in deuterated DMSO was collected before irradiation and after 2 min of irradiation.

The resulting spectral properties for both before and after irradiation showed no change. However, when PA-4Stearoyl was evaluated, a drastic change was observed (Figure 3-1A). Comparing the aromatic region of the spectra before and after irradiation showed the disappearance of the peak at 11.4 ppm (loss of the proton from the –OH group). In addition, the bridging hydrogens at 8.55 and 7.85 ppm disappeared and reappeared as multiplets between 7.19 to 6.43 ppm. This strong downfield shift is also indicative of the changes in structural configuration from a trans to a cis, which is further evidenced by a reduction of coupling constants from 16.3 Hz to 10.3 Hz. Moreover, the aromatic peaks shifted upfield after irradiation indicating a loss in conjugation. The spectrum (Figure 3-1B) after irradiation corresponds well with the structure of an anionic spiropyran.[20]

The stability of the spiropyran could be dictated by the electron density at the pyran oxygen which influences the proton recapture rate of the mPAHs after irradiation. The NMR study indicates that the PA-4Stearoyl photo-dissociates into a stable anionic spiropyran, while PA-4Octadec may or may not be photoactive. To determine whether the PA-4Octadec photo-dissociates, a pH study was conducted before and after irradiation.

The mPAHs (PA-4Octadec and PA-4Stearoyl) were dissolved in a solution of 90 % EtOH and 10 % DI water, showed pHs of 5.95±0.25 and 5.17±0.15, respectively. The corresponding pKa's were calculated to be 8.41±0.52 and 6.82±0.32, respectively. When the solutions were irradiated, the pH of the mPAHs dropped to 4.37±0.04 and 4.42±0.15 for PA-4Octadec and PA-4Stearoyl

respectively. This change in pH indicates that both mPAHs release their protons upon irradiation, thereby confirming photoactivity.

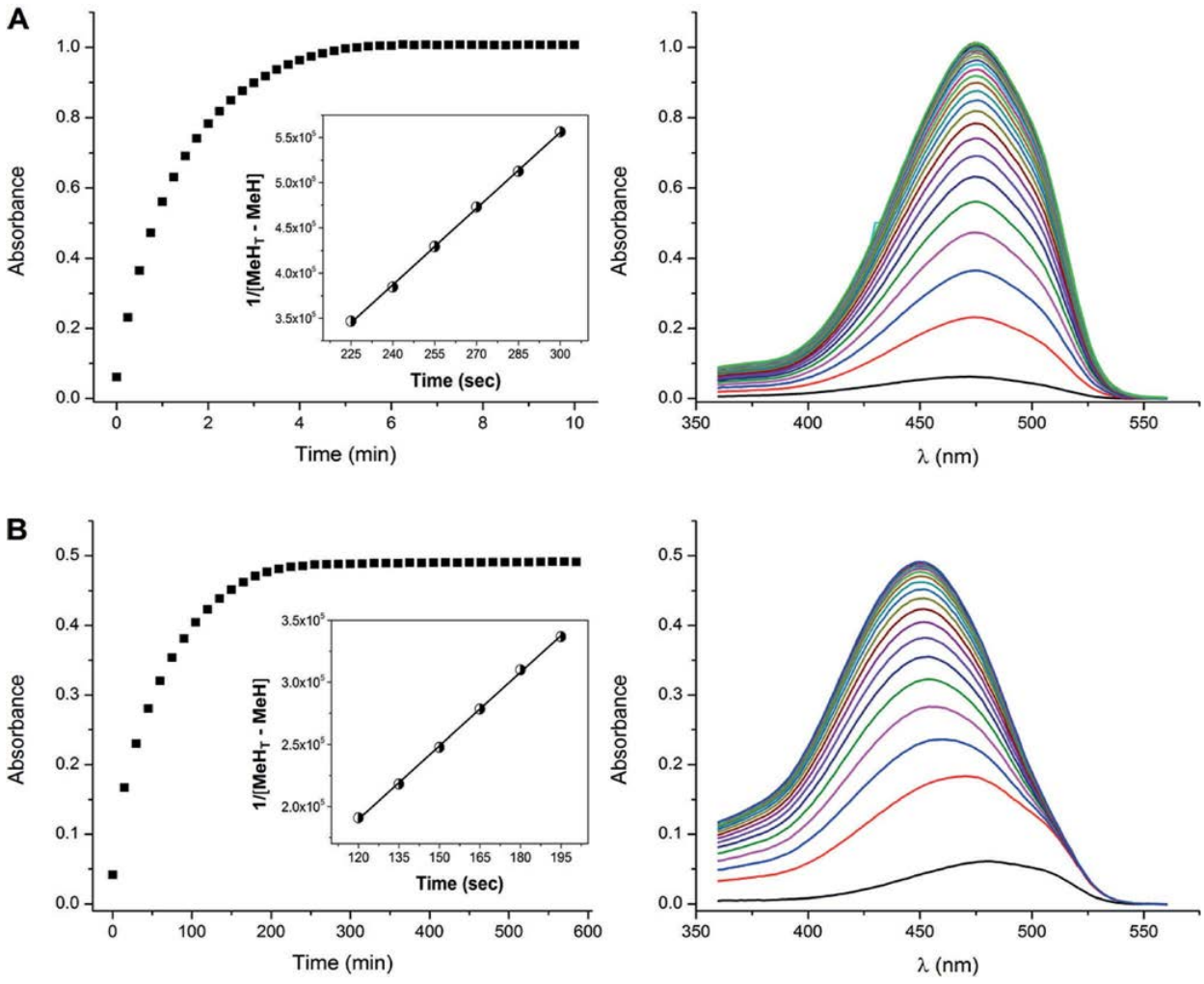

Figure 3-2 Kinetics of mPAHs in EtOH after 2 minutes of irradiation (470 nm) for (A) PA-4Octadec, and (B) PA-4Stearoyl. Left Figures are the response curve over time for both mPAHs obtained from its corresponding absorption spectra (right). (Inset: Plot of fitting the kinetic data in a second-order rate equation for both mPAHs)

Furthermore, kinetic studies were performed to understand the proton re-association rate of the mPAHs after irradiation. If the proton recapture process is the rate limiting step for the respective mPAHs, i.e. protonation of Sp^- ($Sp^- + H^+ \rightarrow MeH$) (MeH: protonated neutral merocyanine state; Sp^-: photo-dissociated anionic spiropyran state), by the majority of the protons in the solution produced from the high-acidity state MeH (i.e. $[H^+] = [Sp^-]$). Then the kinetics should follow a 2nd order rate equation[20]

$$\frac{d[MeH]}{dt} = k[Sp^-][H^+] = k[Sp^-]^2 \qquad [3.1]$$

If no other long-lived species are involved during this process, then $[Sp^-]=[MeH]_T-[MeH]$ ($[MeH]_T$ is the total concentration of mPAH), and Equation 3.1 can be intergrated to give Equation 3.2.[20]

$$\frac{1}{([MeH]_T-[MeH])} = kt + \frac{1}{[MeH]_T} \qquad [3.2]$$

Thus, the proton recapture process was monitored by UV-Vis spectroscopy after the mPAHs were irradiated for 2 min. The kinetics for both mPAHs in EtOH is shown in Figure 3-2, where the absorbance of PA-4Octadec (Figure 3-2A) and PA-4Stearoyl (Figure 3-2B) stabilized at 5 min and 225 min, respectively. This evidence indicates that the time of proton re-association is much faster for PA-4Octadec than for PA-4Stearoyl. This could be the reason why the NMR spectra for PA-4Octadec were similar before and after irradiation. The data provided from the kinetic experiment was fitted into Equation 3.2. And, as shown in the inset of Figure 3-2, the kinetics fits well into the 2nd order rate equation. The rate constant was calculated to be 2811.50 $M^{-1}s^{-1}$ with R^2 of

0.9996 for PA-4Octadec (Figure 3-2A Inset) and molar absorptivity of 41158.2 $M^{-1}cm^{-1}$. On the other hand, PA-4Stearoyl exhibited 1971.70 $M^{-1}s^{-1}$ as the rate constant with R^2 of 0.9994 (Figure 3-2B Inset) and molar absorptivity of 23567.16 $M^{-1}cm^{-1}$. The fact that the kinetic data fits well into Equation 3.2 indicates that the protonation of Sp^- is indeed involved during the rate-limiting step.

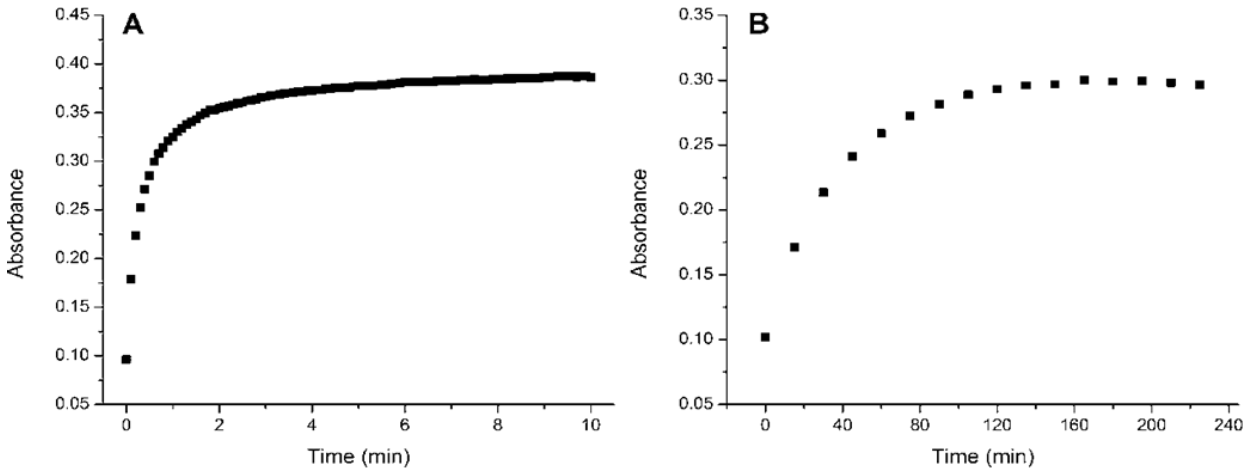

Figure 3-3 Kinetics of mPAHs in ion-sensing film after 2 minutes of irradiation (470 nm) in 0.025 M tris buffer solution at pH 7.40 for (A) PA-4Octadec (scans every 6 seconds), and (B) PA-4Stearoyl (scans every 15 minutes).

Likewise, the time for protons to re-associate for PA-4Octadec and PA-4Stearoyl in the ion-sensing film was evaluated. Figure 3-3 shows the change in absorbance arising from the protonation of Sp^- over time after the sensors were irradiated. The equilibrium response times were 8 min and 150 min for PA-4Octadec and PA-4Stearoyl in the ion-sensing film, respectively.

Scheme 3-2 Representation of the effect on the pyran oxygen due to the substituent groups. EWG: electron withdrawing group (Ester), EDG: electron donating group (Ether).

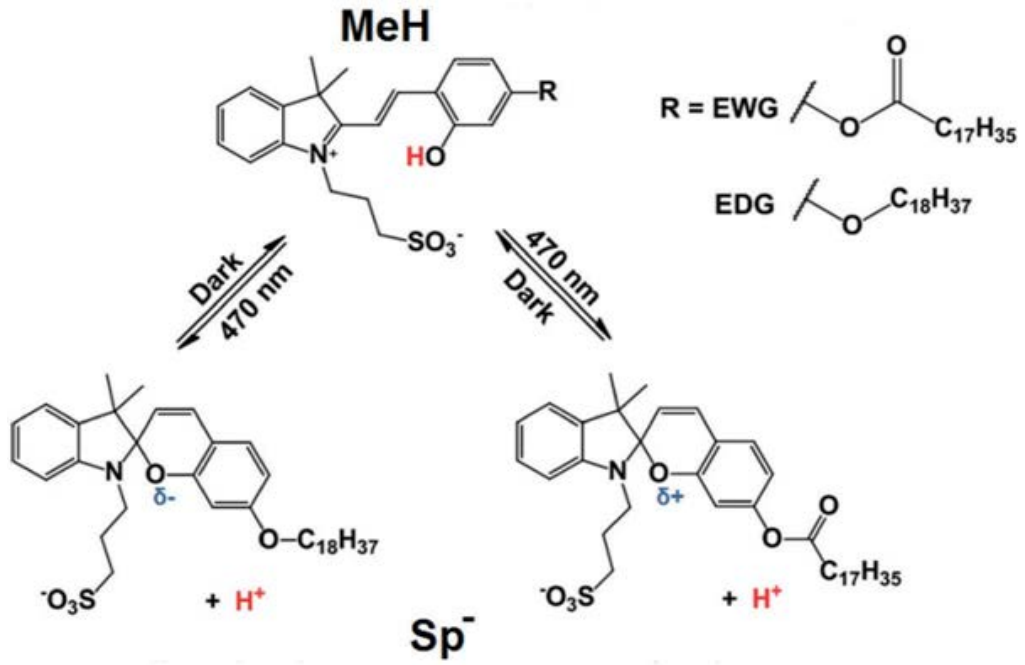

As mentioned before, the proton re-association time was reduced from hours to minutes by the use of an ether functional group (PA-4Octadec) in place of the ester group (PA-4Stearoyl). This is likely because PA-4Stearoyl in its Sp^- state is more stable after irradiation. The ester group withdraws electron density from the pyran oxygen (Scheme 3-2) and consequently reduces the tendency for the proton recapture by the pyran oxygen. On the other hand, PA-4Octadec is less stable in its deprotonated form because the ether group donates electron density to the pyran oxygen, hence speeding up the proton recapture process. Thus, PA-4Octadec has a short-lived photo-dissociated state. It is therefore clear that the lifetime of the photo-dissociated state is

dependent on the nature of the substituent (–R) meta to the pyran oxygen as represented in Scheme 3-2.

3.5 Conclusion

For the first time, we tuned the proton re-association rate of mPAHs by appropriate functionalization. When compared to our previous work[18], we were able to improve the response time from hours to minutes at pH 7.40. We envision that, by using mPAHs in ion-sensors, we can control the ion-exchange process that would ultimately lead to improved detection limits.

3.6 Acknowledgements

The authors acknowledge the College of Sciences and the Department of Chemistry at the University of Central Florida for financial support of this research.

3.7 References

1 H. Hisamoto, *TrAC, Trends Anal. Chem.* **1999**, *18*, 513-524.

2 E. Bakker, P. Buhlmann, E. Pretsch, *Chem. Rev.* **1997**, *97*, 3083-3132.

3 P. Buhlmann, E. Pretsch, E. Bakker, *Chem. Rev.* **1998**, *98*, 1593-1687.

4 J. Bobacka, A. Ivaska, A. Lewenstam, *Chem. Rev.* **2008**, *108*, 329- 351.

5 D. Diamond, S. Coyle, S. Scarmagnani, J. Hayes, *Chem. Rev*. **2008**, *108*, 652-679.

6 C. Xu, K. Wygladacz, R. Retter, M. Bell, E. Bakker, *Anal. Chem*. **2007**, *79*, 9505-9512.

7 K. Watanabe, E. Nakagawa, H. Yamada, H. Hisamoto, K. Suzuki, *Anal. Chem*. **1993**, *65*, 2704-2710.

8 V. Bychkova, A. Shvarev, *Anal. Chem*. **2009**, *81*, 2325-2331.

9 I. H. A. Badr, R. D. Johnson, M. J. Madou, L. G. Bachas, *Anal. Chem*. **2002**, *74*, 5569-5575.

10 K. Seiler, W. Simon, *Anal. Chim. Acta* **1992**, *266*, 73-87.

11 E. Bakker, W. Simon, *Anal. Chem*. **1992**, *64*, 1805-1812.

12 E. Antico, M. Lerchi, B. Rusterholz, N. Achermann, M. Badertscher, M. Vaiente, E. Pretsch, *Anal. Chim. Acta* **1999**, *388*, 327-338.

13 W. E. Morf, K. Seiler, B. Rusterholz, W. Simon, *Anal. Chem*. **1990**, *62*, 738-742.

14 A. Shvarev, *J. Am. Chem. Soc*. **2006**, *128*, 7138-7139.

15. Y. Ge, J. Zhu, W. Zhao, Y. Qin, *Sens. Actuators B, Chem*. **2012**, *166*, 480- 484.

16. G. Mistlberger, G. A. Crespo, X. Xie, E. Bakker, *Chem. Commun*. **2012**, *48*, 5662- 5664.

17. G. Mistlberger, X. Xie, M. Pawlak, G. A. Crespo, E. Bakker, *Anal. Chem*. **2013**, *85*, 2983-2990.

18 V. K. Johns, P. K. Patel, S. Hassett, P. Calvo-Marzal, Y. Qin, K. Y. Chumbimuni-Torres, *Anal. Chem*. **2014**, *86*, 6184-6187.

19 H. Shizuka, *Acc. Chem. Res*.**1985**, *18*, 141-147.

20 V. K. Johns, Z. Wang, X. Li, Y. Liao, *J. Phys. Chem. A* **2013**, *117*, 13101-13104.

21 Z. Shi, P. Peng, D. Strohecker, Y. Liao, *J. Am. Chem. Soc*. **2011**, *133*, 14699-14703.

22 S. J. Mason, J. L. Hake, J. Nairne, W. J. Cummins, S. Balasu- bramanian, *J. Org. Chem*. **2005**, *70*, 2939-2949.

23 K. Y. Chumbimuni-Torres, R. E. Coronda, A. M. Mfuh, C. Castro-Guerrero, M. F. Silva, G. R. Negrete, R. Bizios, C. D. Gracia, *RSC. Adv*. **2011**, *1*, 706-714.

CHAPTER 4 VISIBLE-LIGHT ACTIVATED METASTABLE-STATE PHOTOACID IN ION-SELECTIVE OPTODE SENSORS FOR SODIUM AND CALCIUM IONS: EXPERIMENTAL AND THEORETICAL APPROACH

Reproduced from P. K. Patel, K. Y. Chumbimuni-Torres, "Visible light-induced ion-selective optodes based on a metastable photoacid for cation detection.", *Analyst*, **2016**, *141*, 85-89 with permission of The Royal Society of Chemistry.

4.1 Abstract

A new platform of ion-selective optodes is presented here to detect cations under thermodynamic equilibrium via ratiometric analysis. This novel platform utilizes a 'one of a kind' visible light-induced metastable photoacid as a reference ion indicator to achieve activatable and controllable sensors. These ion-selective optodes were studied in terms of their stability, sensitivity, selectivity, and theoretical aspects.

4.2 Introduction

Ion selective optodes (ISOs) have been extensively studied to monitor different cations for biomedical and environmental applications.[1–11] In recent years, there has been considerable interest to study ISOs that are activatable, reversible and controllable for their use in ion sensing applications that require localized detection of free ions without perturbing their surroundings.[12–15] Attempts have been made to convert the traditional passive mode ISOs into active mode by the

use of photoactive compounds such as spiropyrans and photoacid generators.[16–19] However, the use of spiropyrans in an ISO requires UV light to activate the sensor, which can result in cellular damage when applied in biomedical applications.[20] In addition, UV light photodegrades the active compound in the ISO, shortening the sensor's lifetime.[13–17] Moreover, photoacid generators in an ISO undergo photolysis, making the sensor irreversible.[18,19] To overcome photodegradation and irreversibility for such ISOs, we propose to use a 'one of a kind' visible light activatable and controllable ISO based on a metastable photoacid (mPAH) to detect cations under equilibrium conditions by ratiometric analysis.

Scheme 4-1 Cation-exchange process of ISOs that utilize a (A) neutral basic indicator, and a (B) neutral acidic indicator. (In: neutral basic indicator; L: cation selective ionophore; R^-: anionic additive; InH: neutral acidic indicator).

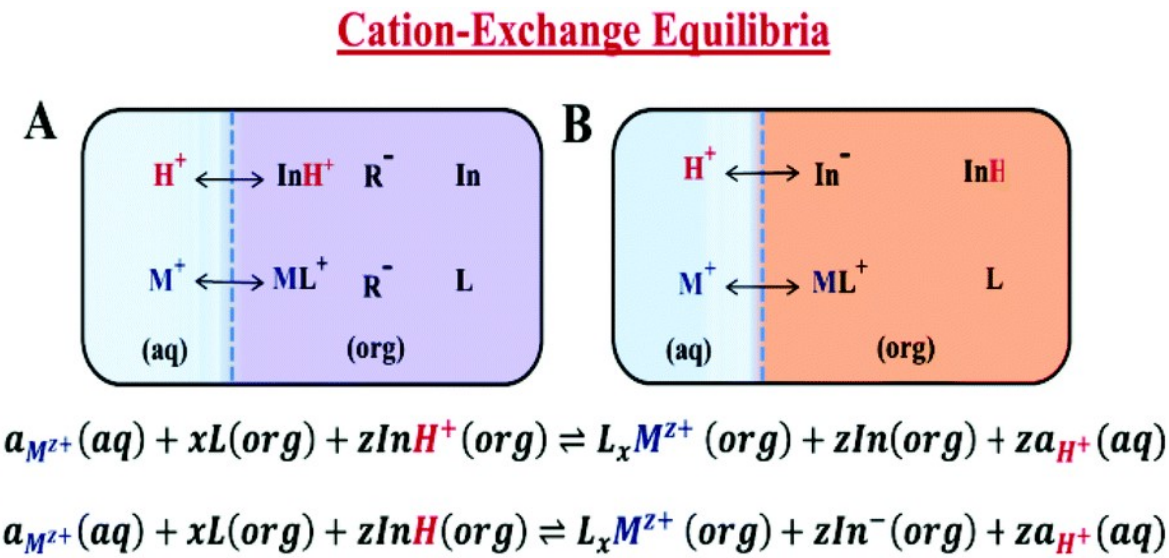

$$A)\ a_{M^{z+}}(aq) + xL(org) + zInH^{+}(org) \rightleftharpoons L_xM^{z+}(org) + zIn(org) + za_{H^{+}}(aq)$$

$$B)\ a_{M^{z+}}(aq) + xL(org) + zInH(org) \rightleftharpoons L_xM^{z+}(org) + zIn^{-}(org) + za_{H^{+}}(aq)$$

A typical ISO consists of a neutral basic indicator (In) that is selective to a reference ion (H^+), an ionophore (L) that is selective to the cation of interest, and anionic additives (R^-) that maintain electroneutrality in the plasticized polymer matrix (Scheme 4-1A).[21–23] The response mechanism of these ISOs is dictated by mass transfer equilibria (cation-exchange process) between an organic (ISO) and an aqueous phase.[24,25] Consequently, the detection of the cation of interest, after achieving thermodynamic equilibrium, is made by measuring the changes in the indicators' optical properties, either by absorption or fluorescence spectroscopy.[26] Nevertheless, prior to cation detection, these ISOs need an external source of protons for the cation-exchange process to proceed, resulting in a response mechanism with multiple steps. In contrast, the proposed tricyanofuran based mPAH (CF_3PhTCF-PAH) acts as a neutral acidic indicator (InH), providing protons for the cation-exchange process. Considering that mPAH is a photoactive compound, it photodissociates its proton upon irradiation and thermally undergoes proton reassociation with a dissociated state that is sufficiently long-lived,[27,28] thus eliminating the need for an external source of protons, while the dissociated state of the mPAH acts as an anionic additive to maintain electroneutrality within the ISO as shown in Scheme 4-1B.[22] Hence, an ISO based on the proposed mPAH exhibits a one-step response mechanism.

We have recently shown that merocyanine based mPAH linked to an acrylate polymer backbone can be utilized in an ISO to detect calcium ions.[29] This merocyanine based mPAH is a neutrally charged acidic indicator which exhibits a longer equilibrium response time (in the order of hours). Consequently, the detection of calcium ions was performed under non-equilibrium conditions.[29] Moreover, we have shown that by modifying the merocyanine based mPAH with an appropriate

functional group (electron donating group), the equilibrium response time can be shortened to the order of minutes.[30] However, the charged nature of the merocyanine based mPAH was optimal only with a polar plasticizer, such as 2-nitrophenyl octyl ether (o-NPOE), to reduce ion-pair formation that affects selectivity.[29] o-NPOE absorbs under 400 nm, interfering with the absorbance peak of the deprotonated state merocyanine based mPAH, and inhibited ratiometric analysis. In contrast, the non-charged CF_3PhTCF-PAH has shown ideal compatibility with a non-polar plasticizer, such as bis(2-ethylhexyl)sebacate (DOS) which does not interfere optically, allowing ratiometric analysis to further increase the sensor sensitivity and signal reproducibility.[31]

4.3 Results and Discussion

Scheme 4-2 Photoresponsive behaviour of CF_3PhTCF-PAH when incorporated in an ISO.

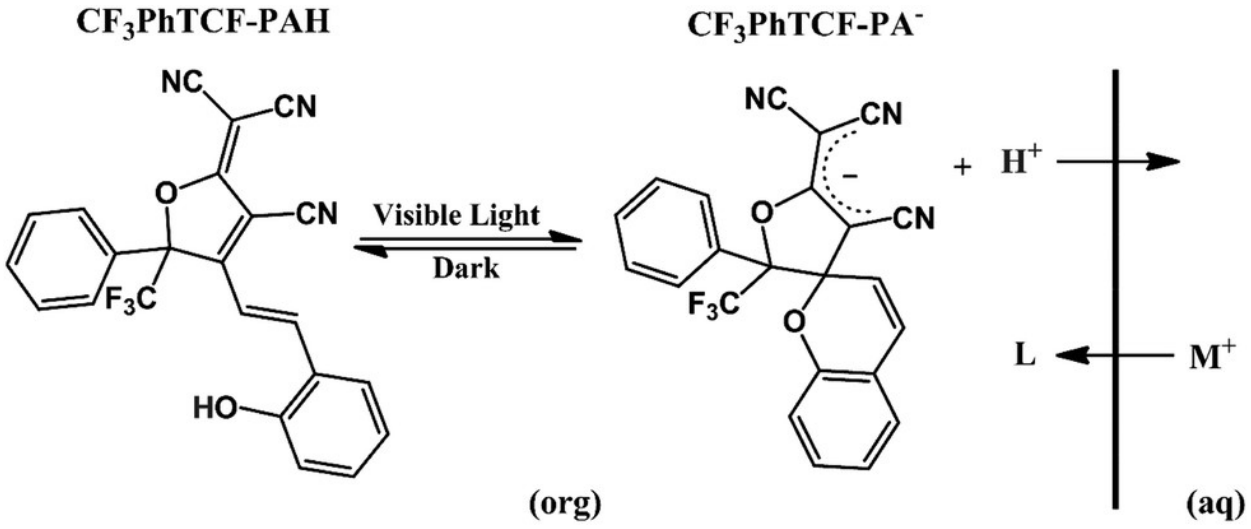

As shown in Scheme 4-2, it is expected that CF_3PhTCF-PAH within the ISO would undergo oxidative photoreaction under visible light irradiation, resulting in a stable carbanion state (CF_3PhTCF-PA^-) of the mPAH along with its photodissociated proton.[32] Likewise, the photodissociated protons would be exchanged when exposed to cations of interest, as the CF_3PhTCF-PA^- state is sufficiently long-lived to allow for the diffusion mediated cation-exchange process.

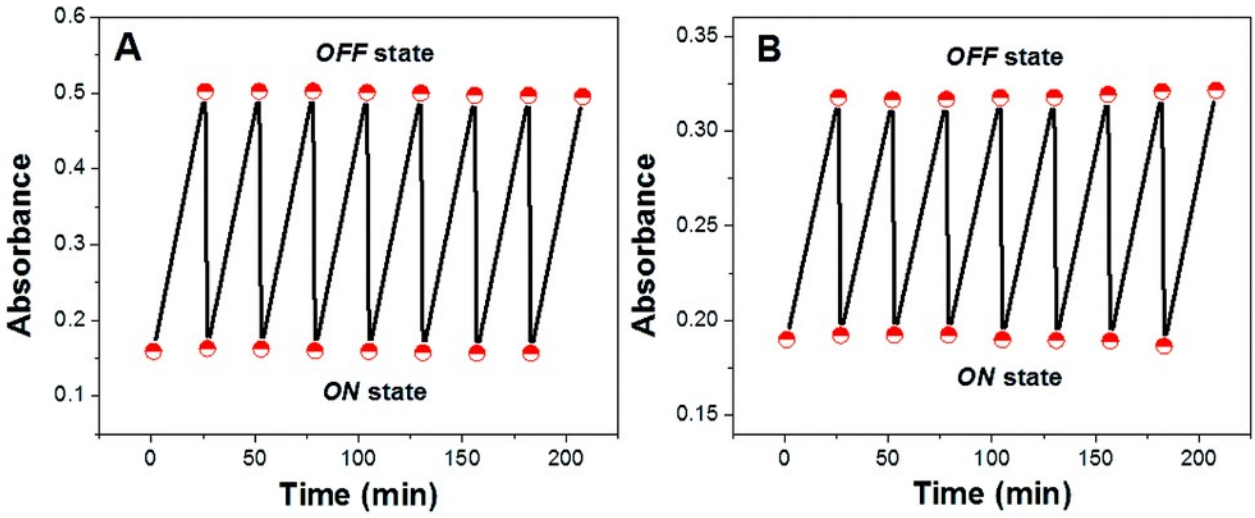

Figure 4-1 Stability of CF_3PhTCF-PAH in ISOs for (A) calcium sensor in 0.5 M formate buffer at pH 4.5, and (B) sodium sensor in 0.3 M magnesium acetate buffer at pH 5.5. Absorbance was recorded at 470 nm. (ON state: after 1 minute irradiation with 470 nm; OFF state: after 25 minutes in the dark).

CF_3PhTCF-PAH was synthesized according to a literature procedure.[32–34] The calcium and sodium ISOs proposed here contain CF_3PhTCF-PAH (7.5 mmol kg^{-1}), and calcium ionophore IV (22.5

mmol kg^{-1}) or sodium ionophore X (7.5 mmol kg^{-1}) within poly(vinyl chloride) (33 wt%) and DOS (66 wt%).

At first, these ISOs were exposed to their respective buffer solutions without any cation of interest. As shown in Figure 4-1, the ISOs based on CF_3PhTCF-PAH were stable over repeated activation cycles between the ON (deprotonated form) and OFF states (protonated form) without any loss of the absorbance signal, indicating no observable photodegradation.

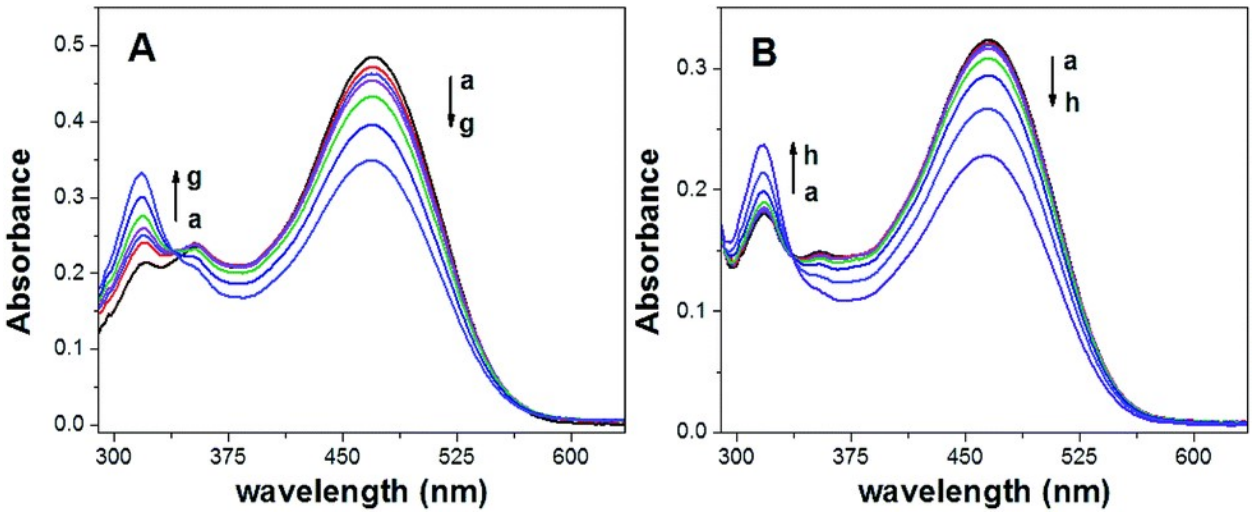

Figure 4-2 Absorption spectra of ISOs for 25 minutes in the dark after activation for different concentrations of (A) calcium ions in 0.5 M formate buffer at pH 4.5; concentrations (a) 0, (b) 1.0×10^{-8}, (c) 1.0×10^{-7}, (d) 1.0×10^{-6}, (e) 1.0×10^{-5}, (f) 1.0×10^{-4}, and (g) 1.0×10^{-3} M, and (B) sodium ions in 0.3 M magnesium acetate buffer at pH 5.5; concentrations (a) 0, (b) 1.0×10^{-6}, (c) 1.0×10^{-5}, (d) 1.0×10^{-4}, (e) 1.0×10^{-3}, (f) 1.0×10^{-2}, (g) 1.0×10^{-1}, and (h) 1.0 M.

Figure 4-2 shows the absorption spectra of the ISOs based on CF_3PhTCF-PAH towards different concentrations of calcium (Figure 4-2A) and sodium (Figure 4-2B) ions at thermodynamic equilibrium (25 minutes in the dark) once the ISOs were activated by visible light (470 nm) for 1 minute. From both absorption spectra, it is observed that as the concentration of the cation of interest increases, there is a gradual decrease in the CF_3PhTCF-PAH peak (470 nm) and a gradual increase in the CF_3PhTCF-PA^- peak (318 nm). These absorbance changes allow for ratiometric analysis (protonated and deprotonated absorbance peaks of the CF_3PhTCF-PAH) to indirectly correlate the activity of the cation of interest.

The experimental data obtained were then compared to the theoretical response function. The theoretical response function (eqn [4.1]), in terms of the activity of protons and the cation of interest, was generated from the ion-exchange equilibria (Scheme 4-1B). This was derived by utilizing mass balance (eqn [4-2] and eqn [4-3]), charge balance (eqn [4-4]), degree of deprotonation using the ratio of absorbance at 470 nm and 318 nm (eqn [4-5]), and the ion-exchange equilibrium constant (eqn [4-6])) equations. This is analogous to that of traditional ISO theory which was established in the early 1990s.[21–23]

Theoretical response function for cation:

$$a_{M^{z+}} = (K_{exch})^{-1}\left(\frac{(1-\alpha)a_{H^+}}{\alpha}\right)^{z}\frac{[InH]_T(1-\alpha)}{z\left([L]_T-\frac{x}{z}[InH]_T(1-\alpha)\right)^{x}} \qquad [4.1]$$

Mass balance equations:

$$[InH]_T = [InH] + [In]^- \quad [4.2]$$

$$[L]_T = [L] + x[L_x M^{z+}] \quad [4.3]$$

Charge balance equation:

$$[In^-] = z[L_x M^{z+}] \quad [4.4]$$

Degree of deprotonation (α):

$$\alpha = \frac{[InH]}{[InH]_T} = \frac{A - A_D}{A_P - A_D} \quad [4.5]$$

Cation-exchange equilibrium constant (Kexch) for the neutral acidic indicator:

$$K_{exch} = \left(\frac{[In^-]a_{H^+}}{[InH]}\right)^z \frac{[L_x M^{z+}]}{a_{M^{z+}}[L]^x} \quad [4.6]$$

The subscript "T" indicates the total concentration of CF_3PhTCF-PAH ($[InH]_T$) and the ionophore ($[L]_T$). The activity of the cation of interest and the proton is denoted as a_{Mz+} and a_{H+}. Also, "x" and "z" denote the value of the ionophore chelating with the cation of interest and charge of the cation of interest, respectively. The ratio of absorbance for CF_3PhTCF-PAH is denoted as A, the protonated state of CF_3PhTCF-PAH in 1 M hydrochloric acid as A_P, and the deprotonated state of CF_3PhTCF-PAH in 1 M sodium hydroxide as A_D; for 25 minutes in the dark after activation.

As shown in Figure 4-3, the experimental data present a strong correlation with the theoretical response curve. From the resulting cation response curves, the experimental limit of detection

(LOD) for calcium and sodium ions was 2.6×10^{-6} M and 2.3×10^{-3} M, respectively. These values were obtained by intersecting two extrapolated segments of the response curve as indicated in the literature.[35] Furthermore, the cation-exchange constant (log K_{exch}) for calcium and sodium ISOs was -9.3 ± 0.3 and -5.3 ± 0.1, respectively. The ionophore–cation complex ratio for calcium ISO was 3 to 1 and for sodium ISOs was 1 to 1.[36,37]

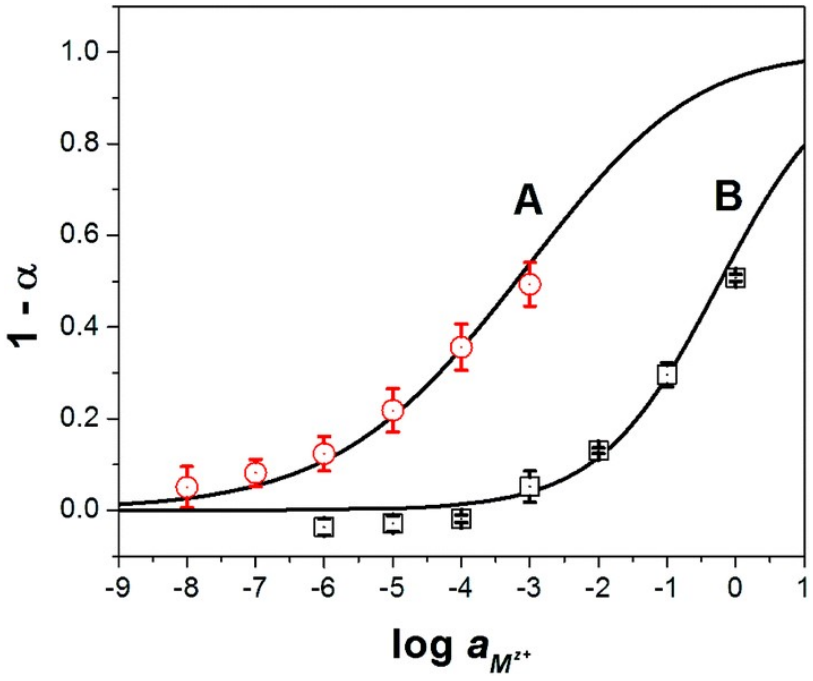

Figure 4-3 Experimental (and) and theoretical (lines) responses of ISOs based on CF_3PhTCF-PAH for the detection of (A) calcium, and (B) sodium ions for 25 minutes in the dark after activation (n = 3).

It was hypothesized that ISOs which contain no anionic additive, cannot maintain constant ionic strength within the ISO.[23] As a result, the cation-exchange constant cannot be retained, due to each

change in the activity of protons and the activity of the cation of interest.[23] However, the changes in the ionic strength within the ISO based on CF_3PhTCF-PAH, containing no additional anionic additive, were negligible as observed in the kinetic data for different concentrations of sodium ions (Figure 4-4), where stable responses over time were obtained at thermodynamic equilibrium. It is noteworthy that the interactions between the negatively and positively charged components for such an ISO do occur, after a certain threshold ($1 - \alpha > 0.5$), as the ionic strength within the ISO changes drastically. Accordingly, higher concentrations of cations are not shown in Fig. 3 because the thermodynamic equilibrium was not maintained, and thus the upper detection limit was 6.3×10^{-4} M and 0.6 M for calcium and sodium ions, respectively (at $\alpha = 0.5$).

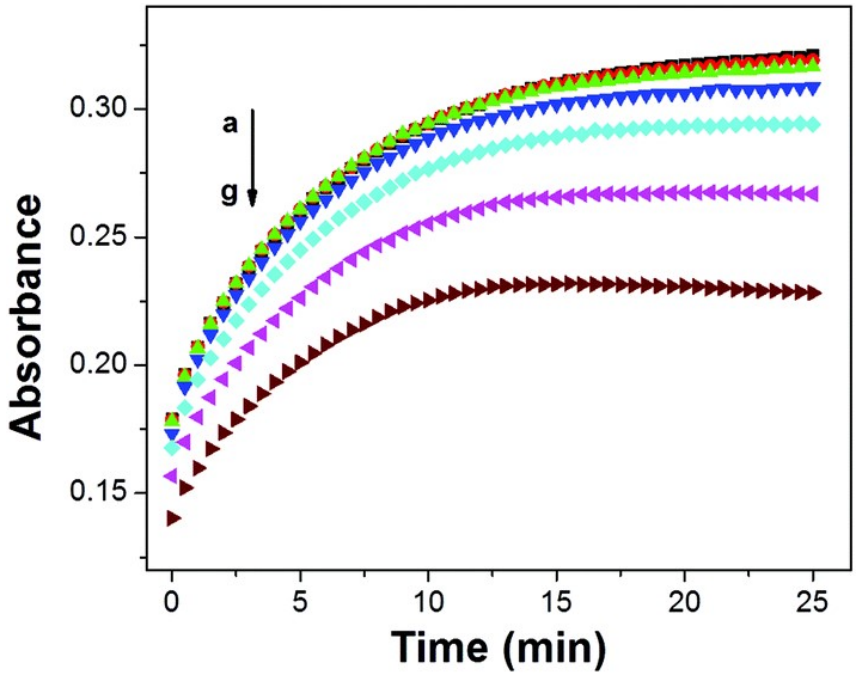

Figure 4-4 Kinetic study for ISOs based on CF_3PhTCF-PAH at different concentrations of sodium ions in 0.3 M magnesium acetate buffer at pH 5.5. Scans every 30 second after activation; concentrations (a) 1.0×10^{-6}, (b) 1.0×10^{-5}, (c) 1.0×10^{-4}, (d) 1.0×10^{-3}, (e) 1.0×10^{-2}, (f) 1.0×10^{-1}, and (g) 1.0 M.

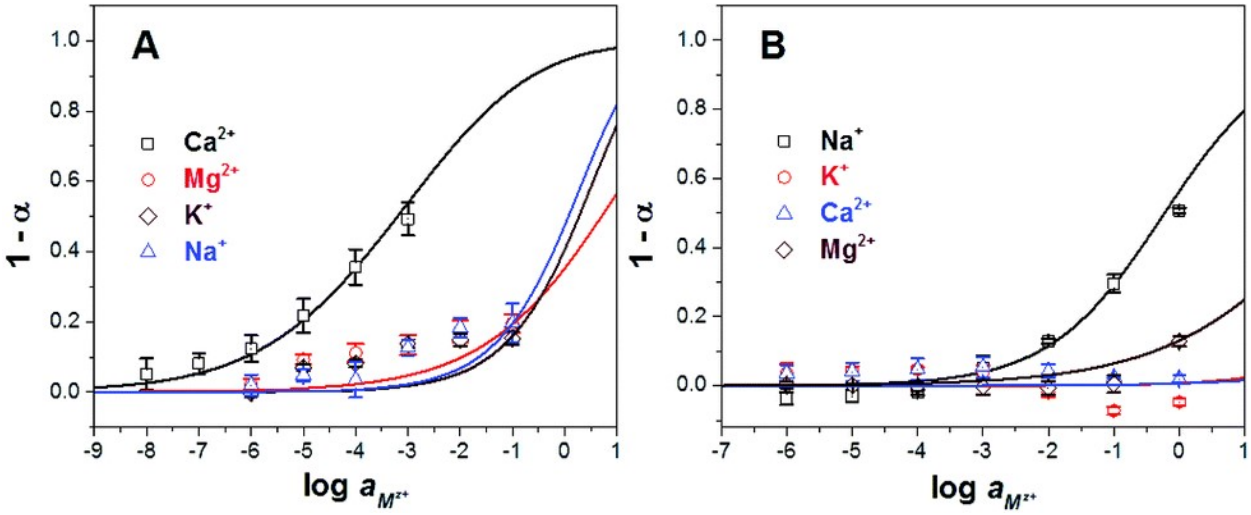

Figure 4-5 Selectivity response for (A) calcium (buffer: 0.5 M formate at pH 4.5), and (B) sodium (buffer: 0.3 M magnesium acetate at pH 5.5) ISOs towards interfering cations for 25 minutes in the dark after activation (n = 3).

Furthermore, these ISOs based on CF_3PhTCF-PAH were studied in terms of selectivity towards interfering cations (J) by a separate solution method.[25,38] As shown in Figure 4-5, all interfering ions were highly discriminated for both ISOs, calcium (Figure 4-5A) and sodium (Figure 4-5B). Thus, the selectivity coefficient values for the calcium ISO towards magnesium, sodium and potassium ions were −3.8, −3.1 and −3.3, respectively. When compared to other ISOs, containing the same ionophore and spiropyran as the reference indicators, the selectivity coefficients were −2.9 (magnesium ion), −6.6 (sodium ion) and −8.9 (potassium ion).[16] The log $K_{M,J}$ values for the sodium ISO towards potassium, calcium and magnesium ions were −4.5, −6.6 and −2.7, respectively. These values are comparable to the selectivity coefficient of sodium against the potassium ion (−2.4), calcium ion (−4.0) and magnesium ion (−4.1) containing spiropyran as a

reference indicator.[16] The selectivity coefficient (log $K_{M,J}$) values were calculated using eqn [4.7], and is analogous to that of ISO theory at $\alpha = 0.5$.[23]

Selectivity coefficient for interfering cations:

$$K_{MJ}^{opt} = \frac{K_{exch}^{J}}{K_{exch}^{M}} \left[\frac{(1-\alpha)a_{H^+}}{\alpha}\right]^{z-w} \frac{w\left([L]_T - \frac{p}{w}[InH]_T(1-\alpha)\right)^{w}}{z\left([L]_T - \frac{x}{z}[InH]_T(1-\alpha)\right)^{x}} \quad [4.7]$$

The high discrimination observed may be due to the proton affinity towards CF_3PhTCF-PA^- (deprotonated form) to be greater than the binding energy of interfering cations by the respective ionophores. Consequently, these ISOs inhibit the competitive behaviour between the interfering cations and protons during the cation-exchange process, even at high concentrations. As a result, an ISO based on CF_3PhTCF-PAH may also be utilized for practical purposes which demands negligible interactions towards interfering cations.

4.4 Conclusion

In conclusion, this novel visible light activatable and controllable ISO based on CF_3PhTCF-PAH that does not exhibit photodegradation, showed good stability, selectivity and reproducibility. Furthermore, the responses of these ISOs towards calcium and sodium ions were standardized following the cation-exchange equilibria. Similarly, other cations can be detected using this platform by interchanging the ionophore within the polymer matrix. Also, we aim to optimize this type of ISO in terms of size reduction and sensitivity. Likewise, we expect that this novel mPAH

(CF_3PhTCF-PAH) may act as a substitute to neutral basic indicators for their use in cation sensing applications that provide control using visible light as needed.

4.5 Acknowledgements

The authors acknowledge the Colleges of Sciences and the Department of Chemistry at the University of Central Florida (USA) for financial support for this research. We also acknowledge Dr Yi Liao (Florida Institute of Technology, USA) to provide tricyanofuran based metastable photoacids for preliminary studies, Dr Eric Bakker (University of Geneva, Switzerland) and Dr Philippe Buhlmann (University of Minnesota, USA) for advice on ion-selective optode theory.

4.6 References

1 W. E. Morf, K. Seiler, B. Rusterholz and W. Simon, *Anal. Chem*., **1990**, *62*, 738.

2 K. Wang, K. Seiler, W. E. Morf, U. E. Spichiger, W. Simon, E. Lindner and E. Pungor, *Anal. Sci*., **1990**, *6*, 715.

3 K. Seiler, K. Wang, E. Bakker, W. E. Morf, B. Rusterholz, U. E. Spichiger and W. Simon, *Clin. Chem*., **1991**, *37*, 1350.

4 M. Lerchi, E. Bakker, B. Rusterholz and W. Simon, *Anal. Chem*., **1992**, *64*, 1534.

5 H. Hisamoto, N. Miyashita, K. Watanabe, E. Nakagawa, N. Yamamoto and K. Suzuki, *Sens. Actuators, B*, **1995**, *29*, 378.

6 M. Lerchi, F. Orsini, Z. Cimerman, E. Pretsch, D. A. Chowdhury and S. Kamata, *Anal. Chem.*, **1996**, *68*, 3210.

7 M. R. Shortreed, S. Dourado and R. Kopelman, *Sens. Actuators, B*, **1997**, *38*, 8.

8 J. M. Dubach, D. I. Harjes and H. A. Clark, *J. Am. Chem. Soc.*, **2007**, *129*, 8418.

9 B. Kuswandi, Nuriman, H. H. Dam, D. N. Reinhoudt and W. Verboom, *Anal. Chim. Acta*, **2007**, *591*, 208.

10 A. A. Ensafi and M. Fouladgar, *Sens. Actuators, B*, **2009**, *136*, 326.

11 M. T. Bamsey, A. Berinstain and M. A. Dixon, *Sens. Actuators, B*, **2014**, *190*, 61.

12 G. Mistlberger, G. A. Crespo, X. J. Xie and E. Bakker, *Chem. Commun.*, **2012**, *48*, 5662.

13 X. J. Xie, G. Mistlberger and E. Bakker, *J. Am. Chem. Soc.*, **2012**, *134*, 16929.

14 X. J. Xie, G. Mistlberger and E. Bakker, *Anal. Chem.*, **2013**, *85*, 9932.

15 X. J. Xie and E. Bakker, *ACS Appl. Mater. Interfaces*, **2014**, *6*, 2666.

16 G. Mistlberger, X. J. Xie, M. Pawlak, G. A. Crespo and E. Bakker, *Anal. Chem.*, **2013**, *85*, 2983.

17 G. Mistlberger, M. Pawlak, E. Bakker and I. Klimant, *Chem. Commun.*, **2015**, *51*, 4172.

18 A. Shvarev, *J. Am. Chem. Soc*., **2006**, *128*, 7138.

19 X. J. Xie, G. Mistlberger and E. Bakker, *Sens. Actuators, B*, **2014**, *204*, 807.

20 V. Adler, A. Schaffer, J. Kim, L. Dolan and Z. Ronai, *J. Biol. Chem*., **1995**, *270*, 26071–26077.

21 K. Seiler and W. Simon, *Sens. Actuators, B*, **1992**, *6*, 295.

22 K. Seiler and W. Simon, *Anal. Chim. Acta*, **1992**, *266*, 73.

23 E. Bakker and W. Simon, *Anal. Chem*., **1992**, *64*, 1805.

24 X. J. Xie and E. Bakker, *Anal. Bioanal. Chem*., **2015**, *407*, 3899.

25 E. Bakker, P. Buhlmann and E. Pretsch, *Chem. Rev*., **1997**, *97*, 3083.

26 P. Buhlmann, E. Pretsch and E. Bakker, *Chem. Rev*., **1998**, *98*, 1593.

27 Z. Shi, P. Peng, D. Strohecker and Y. Liao, *J. Am. Chem. Soc*., **2011**, *133*, 14699.

28 V. K. Johns, Z. Z. Wang, X. X. Li and Y. Liao, *J. Phys. Chem. A*, **2013**, *117*, 13101.

29 V. K. Johns, P. K. Patel, S. Hassett, P. Calvo-Marzal, Y. Qin and K. Y. Chumbimuni-Torres, *Anal. Chem*., **2014**, *86*, 6184.

30 P. K. Patel, V. K. Johns, D. M. Mills, J. E. Boone, P. Calvo- Marzal and K. Y. Chumbimuni-Torres, *Electroanalysis*, **2015**, *27*, 677.

31 S. Peper, I. Tsagkatakis and E. Bakker, *Anal. Chim. Acta*, **2001**, *442*, 25.

32 V. K. Johns, P. Peng, J. DeJesus, Z. Z. Wang and Y. Liao, *Chem. – Eur. J.*, **2014**, *20*, 689.

33 M. Q. He, T. M. Leslie and J. A. Sinicropi, *Chem. Mater*., **2002**, *14*, 2393.

34 S. Liu, M. A. Haller, H. Ma, L. R. Dalton, S. H. Jang and A. K. Y. Jen, *Adv. Mater*., **2003**, *15*, 603.

35 E. Bakker, M. Willer and E. Pretsch, *Anal. Chim. Acta*, **1993**, *282*, 265–271.

36 P. Gehrig, B. Rusterholz and W. Simon, *Chimia*, **1989**, *43*, 377.

37 D. Diamond, G. Svehla, E. M. Seward and M. A. Mckervey, *Anal. Chim. Acta*, **1988**, *204*, 223.

38 Y. Umezawa, P. Buhlmann, K. Umezawa, K. Tohda and S. Amemiya, *Pure Appl. Chem*., **2000**, *72*, 1851.

CHAPTER 5 SWITCHING FLUORESCENCE AND ACIDITY BY VISIBLE-LIGHT ACTIVATED METASTABLE-STATE PHOTOACID AND BODIPY IN SOLUTION

Reproduced from P. K. Patel, J. E. Arias, R. S. Gongora, F. E. Hernandez, A. Moncomble, S. Aloïse, K. Y. Chumbimuni-Torres, "Visible light-triggered fluorescence and pH modulation using metastable-state photoacids and BODIPY.", *Physical Chemistry Chemical Physics,* **2018**, *20,* 26804-26808 with permission from the PCCP Owner Societies.

5.1 Abstract

Small changes in the pH gradient play a critical role in numerous biological and chemical pathways. Systems capable of monitoring and regulating these changes with high sensitivity and minimum photo-fatigue are in demand. Herein, we propose a visible light-triggered molecular system that allows for reversible regulation of acidity and fluorescence. This robust bi-functional system opens a new horizon towards novel studies that rely on small changes in acid-mediated controlled processes with high sensitivity. The two photosensitive compounds employed, a metastable-state photoacid (mPAH) and a boron-dipyrromethene (BODIPY) derivative, allow for consistent modulation of both fluorescence (based on the working principle of the inner filter effect) and pH (around a magnitude) over multiple cycles.

5.2 Introduction

Organic photochromic molecules such as spiropyrans, azobenzenes or diarylethenes are compounds that undergo reversible structural changes when exposed to light.[1–3] The physicochemical changes associated with the structural transformations of these compounds include variations in their optical properties, dipole moment, and/or conductivity.[4–8] As so, pH sensitive photochromic compounds are attractive for applications concerning proton-transfer processes. Traditionally, spiropyrans have been used for this purpose.[9] Nonetheless, these molecules require acidification using an external source of protons while activated with UV light to photoisomerize them from the spiropyran form (SP) to the merocyanine form (MC). The protonated merocyanine species obtained by this procedure (MCH^+) is then sensitive to visible light (Scheme 5-1A). In practice, these conditions could prove challenging in terms of bio-applicability and robustness. To circumvent these obstacles, a new class of visible light-triggered molecular switches called metastable-state photoacids (mPAHs) has been proposed.[10]

In contrast to classical super photoacids,[11] this new class of visible light-triggered mPAHs also allows for a large pH change with high efficiency and good reversibility. These novel mPAHs are designed by linking an electron-accepting (EA) moiety and a weakly acidic nucleophilic moiety (NuH) with a double bond (Scheme 5-1B).[10] Under irradiation, the trans–cis photoisomerization, followed by a nucleophilic reaction between the two moieties, results in an efficient proton release. In the dark, the metastable-state relaxes to the initial conformation within a few seconds to hours, thus making it essential to study proton-transfer processes due to the long-lived nature of the metastable state.[12–16] Due to their acidity-modulating capabilities, mPAHs have found applications

in hydrogels,[17] ion-selective optodes,[18,19] polymerization reactions,[20] photo-activated ion-channels,[21] and waste management systems.[22]

Scheme 5-1 (A) Photochromic equilibrium of spiropyran and external acidification to produce light triggered proton releasing merocyanine. (B) General scheme for mPAHs. (C) Acido-basic and photochromic equilibria between Mer-mPAH (protonated-open form), Mer-mPA$^-$ (conjugate basic-open form) and SP-mPA$^-$ (conjugate basic-closed form).

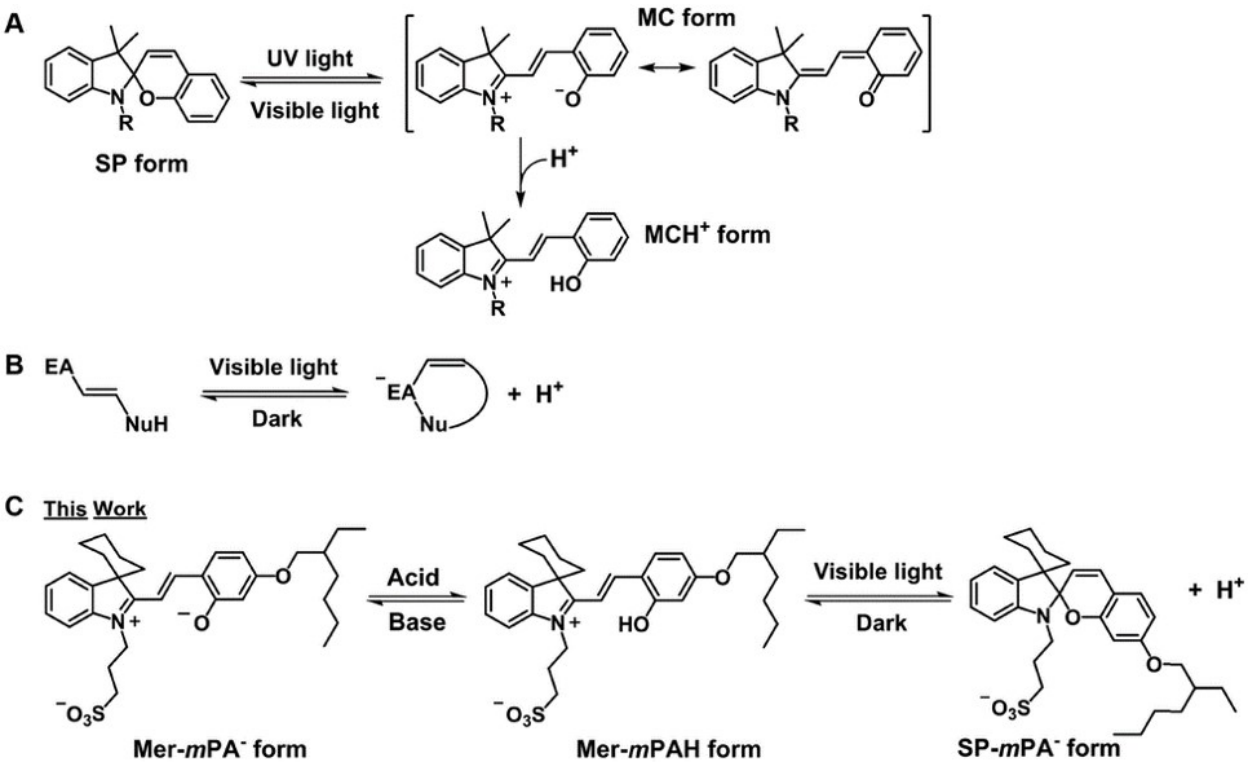

Recently, a new class of multi-stimulus-responsive fluorescent molecular switches based on mPAHs has been shown.[23] The authors provided a unique approach to covalently link a UV light activated fluorophore to the mPAH moiety. As mentioned before, the need of a UV light source to

induce fluorescence may likely compromise the robustness of the photonic device and its use in biological applications.

Herein, we present a simple and robust pH and fluorescence modulating system that can be activated with visible light. This system is composed of a high quantum yield pH insensitive fluorophore (a boron-dipyrromethene (BODIPY) derivative)[24–26] and a novel merocyanine-type mPAH (Mer-mPAH; Scheme 5-1C) acting as a molecular switch. By utilizing the concept of the inner filter effect,[27] both the absorption and emission of BODIPY are modulated by the state of Mer-mPAH. The approach of using the inner filter effect has found success in improving pH-dependent fluorescence sensitivity for other systems.[28,29] Nonetheless, these systems do not exploit the benefits of mPAHs.

5.3 Synthesis

A lipophilic Mer-mPAH was synthesized according to the pioneering work of Shi et al. with few modifications to make the product more stable and compatible with organic solvents (Scheme C-1 in Appendix C).[10]

5.4 Acido-basic equilibrium

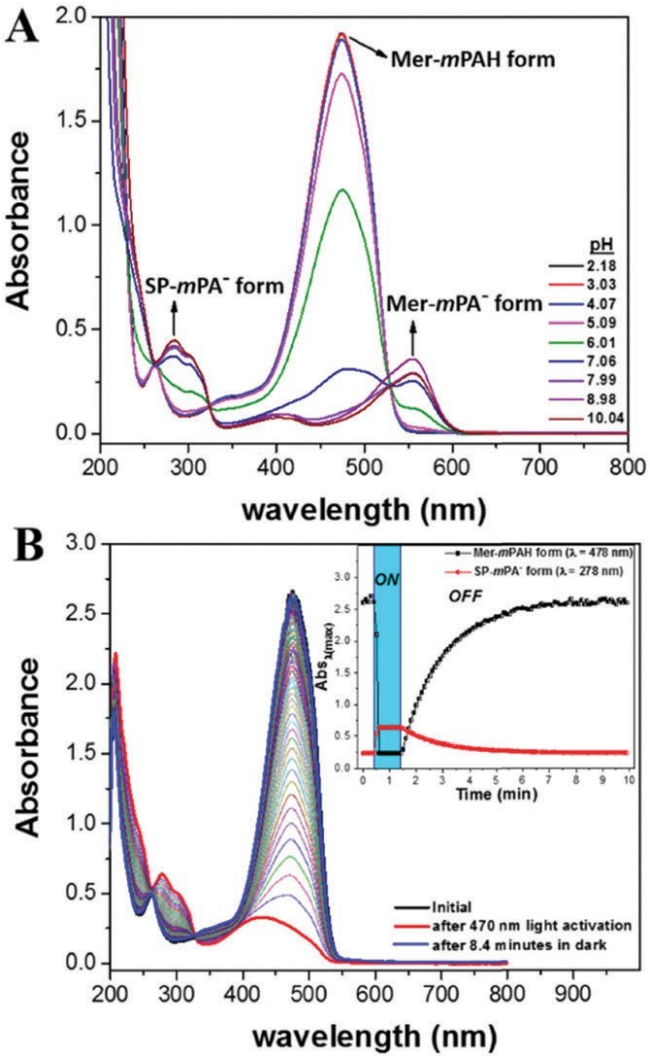

Figure 5-1 (A) pH dependent absorption spectra of Mer-mPAH (50 µM) in 0.1 M of different buffers in co-solvent (ethanol/water – 50/50) system. (B) Time-dependent absorbance spectra of Mer-mPAH (65 µM) in pure ethanol recorded every 0.1 minute after 470 nm light irradiation (ON) and in the dark (OFF). Inset: Changes in major absorption peaks between protonated and deprotonated forms of Mer-mPAH with respect to time.

First, the acido-basic equilibrium of Mer-mPAH (50 μM) was investigated by acquiring absorption spectra in 0.1 M Britton–Robinson (pH 2 to 7), 0.1 M Tris–HCl (pH 8 to 9) and 0.1 M Glycine–NaOH (pH 10) buffers. Different buffers were used due to solubility issues at high pH in the co-solvent (ethanol/water – 50/50) system. This experiment was performed to identify the spectral signatures of three acido-basic species (Scheme 5-1C). As shown in Figure 5-1A, a strong absorption band with a peak at 474 nm was predominant in acidic media (pH 2.18) with a distinct yellow colour. This intense and broad spectral feature was assigned to the unique protonated species Mer-mPAH. TD-DFT computations (Section C.3 in Appendix C) on optimized geometries (Figure C-7 in Appendix C) confirmed this statement. Although the theoretical transition energy seemed to be slightly overestimated (0.22 eV), the general shape of the absorption band was well reproduced (Figure C-8A in Appendix C).

When the pH was increased, the absorption band peak of the protonated-open form decreased, and the two absorption band peaks at 284 nm and 556 nm increased (colour of the solution turned to light pink). These two absorption bands correspond to the two different conjugate basic forms of Mer-mPAH. The red shifted peak centered at 556 nm corresponds to the conjugate basic open-form (Mer-mPA$^-$), due to the electronic enhancement by the resonance of Mer-mPAH. The blue shifted peak centered at 284 nm is assigned to the conjugate basic-closed form (SP-mPA$^-$), given that the resonance is broken at the chiral sp^3 carbon center. Theoretical calculations allowed confirming the identity of the two species that give rise to the peaks in basic media (Figure C-8B and C in Appendix C). The red-shift that occurs upon deprotonation is well reproduced for Mer-

mPA$^-$ (experimental: 0.39 eV, theoretical: 0.31 eV) and the shape of the absorption spectra of SP-mPA$^-$ is well reproduced.

With complete rationalization of acido-basic species, the thermodynamic acidity constant of Mer-mPAH was then estimated to be 6.15 by following a literature protocol (Section C.4 in Appendix C).[30]

5.5 Photochromism

Next, the visible light-triggered photochromic behaviour of Mer-mPAH (65 μM) was examined in pure ethanol solution. It is evident from Figure 5-1B that in ethanol solution, the starting material is exclusively in its protonated-open form with a strong absorption band peak at 478 nm. Upon irradiation with visible light (470 nm), the yellow coloured solution turns colourless within a few seconds. This is the result due to the drastic decrease in the protonated-open form and reaching a photo-stationary state (Figure 5-1B, inset, blue region). Only the conjugate basic SP-mPA$^-$ form was observed, as attested by the increase of the 278 nm absorption band (analogous to the 284 nm band reported before) and the lack of the 556 nm shoulder. When irradiation of visible light was ceased, the peak at 478 nm appeared again, and the solution recovered its yellow colour. The exponential time constant for this recovery kinetic is 1.56 ± 0.01 minutes, which is indicative of the fast thermal back reaction via carbon–oxygen bond breaking followed by unfolding merocyanine isomerization with proton assistance.[16] Using the ground state structures obtained theoretically, Mer-mPAH was found to be more stable than SP-mPA$^-$ (Section C.3 in Appendix C). Accordingly, the changes in Gibbs free energy between the photo-stationary (SP-mPA$^-$ form)

and ground (Mer-mPAH form) states were 87.8 kJ mol^{-1} in ethanol and 83.0 kJ mol^{-1} in aqueous solutions. To the best of our knowledge, this is the first theoretical report on the thermodynamics of mPAH. For comparison, based on theoretical thermodynamics reported for spiropyrans, the changes in Gibbs free energy between the photo-stationary (MC form, see Scheme 5-1A) and ground (SP form, see Scheme 5-1A) states are also positive values.[31–36] Likewise, due to the more stable nature of Mer-mPAH, this difference in energy may likely assist the thermodynamic reverse process in darkness.

To corroborate that protons have been released from the Mer-mPAH by visible light, pH measurements under irradiation were performed (Fig. C-10 in Appendix C). A 65 μM Mer-mPAH solution in ethanol/water (90/10) yielded an initial pH of 5.5. When visible light was switched ON, the pH of the solution decreased to 4.3, with a 1.20 ± 0.02 change. This is an important performance compared to previously reported mPAHs.[10,12–15] These observations confirmed that the Mer-mPAH has the ability to concomitantly release its protons while converting to its conjugate basic form using visible light. Likewise, when the visible light was switched OFF, the pH increased to its initial state, confirming the thermodynamic reversibility of the process. Moreover, a consistent magnitude of pH change can be modulated over multiple cycles with no observable photo-degradation.

5.6 Visible light-triggered pH/fluorescence bi-molecular system

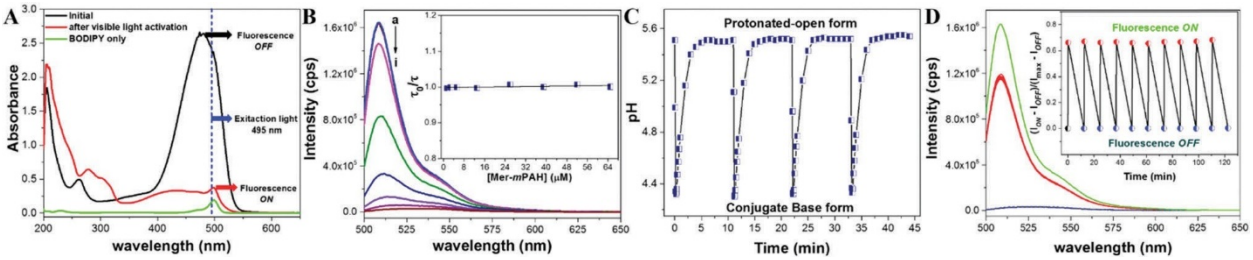

Figure 5-2 (A) Absorption spectra for the optimized chromophore mixture (2.6 μM of BODIPY with 65 μM of Mer-mPAH) in pure ethanol without (black curve) and under visible light irradiation (red curve). Arrows indicate possible fluorescence from BODIPY (inner filter effect illustration). (B) Emission spectra (excitation at 495 nm) for BODIPY (2.6 μM) in pure ethanol with increasing Mer-mPAH concentration (a - i: 0, 1.3, 2.6, 5.2, 13, 26, 39, 52, 65 μM). Inset: Stern–Volmer plot for the ratio of fluorescence lifetime decays, where ‘‘τ_0’’ and ‘‘τ’’ represent the lifetimes of BODIPY only and the mixture, respectively. (C) pH modulation by 470 nm light for an ethanol/water (90/10) solution containing the chromophore mixture (2.6 μM of BODIPY with 65 μM Mer-mPAH) with respect to time. (D) Fluorescence modulation for the optimized chromophore mixture in pure ethanol: green curve refers to BODIPY only emission (I_{max}); black curve refers prior to visible light irradiation; red curve refers after 0.25 minute of visible light irradiation (I_{ON}); and blue dashed curve refers after 10 minutes in the dark (I_{OFF}). Inset: Repeatability cycles.

The objective of this study was to obtain an efficient visible light-triggered BODIPY fluorescence in parallel to pH modulation using Mer-mPAH through the well-known inner-filter effect.[27] To

better understand the visible light-triggering of fluorescence in the chromophore mixture, we measured the absorption spectra for a blend of BODIPY (2.6 μM) and Mer-mPAH (65 μM) (Figure 5-2A). In the dark, Mer-mPAH absorption is predominant, thus avoiding the BODIPY molecules to absorb the excitation light (495 nm) and consequently resulting in negligible fluorescence (Mer-mPAH is poorly fluorescent, Figure C-11 in Appendix C). In this state, the fluorescence of BODIPY is OFF. Reversely, when the blend was exposed to visible radiation, Mer-mPAH converts to its conjugate basic forms with reduced absorbance in the visible region, thus allowing the BODIPY molecules to absorb the excitation light. In this state, the fluorescence of BODIPY is ON.

As a matter of fact, the key points to design such a system are (i) a good overlap between Mer-mPAH and BODIPY absorption bands and (ii) significant differences between extinction coefficients between acidic and basic species of Mer-mPAH. Consequently, we decided to investigate the best choice of concentrations for both molecules in the blend. Photochemical parameters of BODIPY are well known,[24–26] and for ethanol solution, the absorption maximum is typically observed at approximately 500 nm (Figure C-12A in Appendix C). After testing different BODIPY concentrations in ethanol (excitation at 495 nm), we found that 2.6 μM yields a maximum emission intensity within the linear dynamic range at 509 nm (Fig. C-12B, inset, in Appendix C). Furthermore, as shown in Fig. 2B, ~99% of BODIPY (2.6 μM) emission was inhibited when 25 equivalents of Mer-mPAH (65 μM) were used. In fact, the optimized choice of concentrations was contemplated by the differences in molar extinction coefficients of BODIPY

(98040 $M^{-1}cm^{-1}$) and Mer-mPAH (40138 $M^{-1}cm^{-1}$) (Figure C-13 in Appendix C). Therefore, excess Mer-mPAH was required to maximize fluorescence inhibition.

To explore possible dynamic quenching of BODIPY fluorescence by Mer-mPAH, and to validate that the inner filter effect is the only responsible criterion for fluorescence inhibition, fluorescence lifetime measurements were performed for BODIPY (2.6 μM) with different concentrations of Mer-mPAH in ethanol solution (Figure 5-2B, inset; and Figure C-14, Table C-1 in Appendix C). The results showed no observable differences, which indicates that the fluorescence inhibition is intrinsically governed by the inner filter effect.[27]

With the optimized concentrations of the chromophore mixture (BODIPY – 2.6 μM and Mer-mPAH – 65 μM), the repetitive modulation of pH and fluorescence was investigated. Like the pH modulation study shown earlier for Mer-mPAH using visible light, this chromophore mixture in ethanol/water (90/10) solution displayed an identical pH change of 1.20 ± 0.01 over multiple cycles (Figure 5-2C). Moreover, this chromophore mixture in ethanol solution exhibits similar photochromic response when monitored by absorption with an exponential time constant for the recovery kinetic of 1.41 ± 0.01 minutes (Fig. C-15 in Appendix C). No observable changes were observed for solution containing BODIPY only. Finally, upon examination of fluorescence switching for this chromophore mixture in ethanol solution, ~67% of emission after visible light irradiation was observed (Figure 5-2D) compared to the emission of BODIPY only. This is due to a part of excitation light (495 nm) being absorbed by the remaining protonated-open form of Mer-mPAH after irradiation with visible light. This outcome underlines the fact that for future

development and the design of a mPAH, one must consider a strong absorption overlap between the initial form of mPAH and the fluorophore for the best inner filter effect. Likewise, upon visible light irradiation of mPAH, the inner filter effect will be eliminated. Thereby, allowing the fluorophore to absorb excitation light and emit as fluorescence. Moreover, the observed emission intensity was completely inhibited to its initial state after 10 minutes in the dark. Likewise, no photo-degradation was observed while performing fluorescence switching of this chromophore mixture by visible light over multiple times for more than two hours (Figure 5-2D, inset). With these cumulative results, Mer-mPAH has demonstrated its ability to modulate both pH and fluorescence by incorporating BODIPY in solution.

5.7 Conclusions

We have shown a novel visible light-triggered bimolecular system capable of simultaneously modulating pH and fluorescence. This system exhibits good photostability, and consistent pH and fluorescence changes over multiple cycles. This controllable system is expected to find applications in the study of pH dependent enzymes, pH sensitive drug tracking and release near cancerous sites, and improvement of the sensitivity of light stimulated sensing platforms for ions.

The fluorescence modulation shown in the Mer-mPAH and BODIPY blend is the result of the inner filter effect. However, the switching of fluorescence is not as effective as the dynamic quenching mechanism.[27] A better understanding of this family of chromophores and further investigation of ultrafast mechanisms in these systems are still necessary for more emissive mPAHs. This possibility is currently being explored in our laboratory.

5.8 Acknowledgements

The authors gratefully acknowledge the College of Sciences and the Department of Chemistry at the University of Central Florida for financial support, and the University of Central Florida Stokes Advanced Research Computing Center for providing computing time. The authors thank Eduardo Romero from the University of Central Florida for insightful discussion on the theoretical component of this work.

5.9 References

1 F. Ercole, T. P. Davis and R. A. Evans, *Polym. Chem*., *2010*, *1*, 37.

2 F. M. Raymo and M. J. Tomasulo, *J. Phys. Chem. A*, **2005**, *109*, 7343.

3 M. Natali and S. Giordani, *Chem. Soc. Rev*., **2012**, *41*, 4010.

4 G. Callierotti, A. Bianco, C. Castiglioni, C. Bertarelli and G. Zerbi, *J. Phys. Chem. A*, **2008**, *112*, 7473.

5 F. L. E. Jakobsson, P. Marsal, S. Braun, M. Fahlman, M. Berggren, J. Cornil and X. Crispin, *J. Phys. Chem. C*, **2009**, *113*, 18396.

6 P. Toman, W. Bartkowiak, S. Nešpůrek, J. Sworakowski and R. Zaleśny, *Chem. Phys.*, **2005**, *316*, 267.

7 T. Tsujioka and M. Irie, *J. Photochem. Photobiol., C*, **2010**, *11*, 1.

8 M. Irie, T. Fukaminato, K. Matsuda and S. Kobatake, *Chem. Rev*., **2014**, *114*, 12174.

9 L. Kong, H. L. Wong, A. Y. Y. Tam, W. H. Lam, L. Wu and V. W. W. Yam, *ACS Appl. Mater. Interfaces*, **2014**, *6*, 1550.

10 Z. Shi, P. Peng, D. Strohecker and Y. Liao, *J. Am. Chem. Soc*., **2011**, 133, 14699.

11 L. M. Tolbert and K. M. Solntsev, *Acc. Chem. Res*., **2002**, *35*, 19.

12 V. K. Johns, Z. Wang, X. Li and Y. Liao, *J. Phys. Chem. A*, **2013**, *117*, 13101.

13 N. Abeyrathna and Y. Liao, *J. Am. Chem. Soc*., 2015, *137*, 11282.

14 Z. Wang, W. K. Johns and Y. Liao, *Chem. – Eur. J.*, **2014**, *20*, 14637.

15 P. K. Patel, V. K. Johns, D. M. Mills, J. E. Boone, P. Calvo-Marzal and K. Y. Chumbimuni-Torres, *Electroanalysis*, **2015**, *27*, 677.

16 Y. Liao, *Acc. Chem. Res.*, **2017**, *50*, 1956–1964.

17 F. Trausel, F. Versluis, C. Maity, J. M. Poolman, M. Lovrak, J. H. van Esch and R. Eelkema, *Acc. Chem. Res*., **2016**, *49*, 1440.

18 V. K. Johns, P. K. Patel, S. Hassett, P. Calvo-Marzal, Y. Qin and K. Y. Chumbimuni-Torres, *Anal. Chem*., **2014**, *86*, 6184.

19 P. K. Patel and K. Y. Chumbimuni-Torres, *Analyst*, **2016**, *141*, 85.

20 C. Fu, J. Xu and C. Boyer, *Chem. Commun*., **2016**, *52*, 7126.

21 O. S. Shafaat, J. R. Winkler, H. B. Gray and D. A. Dougherty, *ChemBioChem*, **2016**, *17*, 1323.

22 L. A. Tatum, J. T. Foy and I. Aprahamian, *J. Am. Chem. Soc*., **2014**, *136*, 17438.

23 Q. Yu, X. Su, T. Zhang, Y. Zhang, M. Li, Y. Liu and S. X.-A. Zhang, *J. Mater. Chem. C*, **2018**, *6*, 2113.

24 N. Boens, V. Leen and W. Dehaen, *Chem. Soc. Rev*., **2012**, *41*, 1130.

25 A. C. Benniston and G. Copley, *Phys. Chem. Chem. Phys*., **2009**, *11*, 4124.

26 A. Loudet and K. Burgress, *Chem. Rev*., **2007**, *107*, 4891.

27 J. R. Lakowicz, *Principles of Fluorescence Spectroscopy*, Springer, New York, 2006.

28 G. Gabor and D. R. Walt, *Anal. Chem*., **1991**, *63*, 793.

29 H. He, H. Li, G. Mohr, B. Kovacs, T. Werner and O. S. Wolfbeis, *Anal. Chem*., **1993**, *65*, 123.

30 E. Bakker, M. Lerchi, T. Rosatzin, B. Rusterholz and W. Simon, *Anal. Chim. Acta*, **1993**, *278*, 211.

31 N. P. Ernsting, J. Chen, D. Jacquemin and W. R. Browne, *Pure Appl. Chem.*, **1990**, *62*, 6423.

32 V. I. Minkin, *Chem. Rev.*, **2004**, *104*, 2751.

33 J. Liu and K. Morokuma, *J. Am. Chem. Soc*., **2013**, *135*, 10693.

34 S. Prager, I. Burghardt and A. J. Drew, *J. Phys. Chem. A*, **2014**, *118*, 1339.

35 M. Savarese, U. Raucci, P. A. Netti, C. Adamo, N. Rega and I. Ciofini, *Theor. Chem. Acc*., **2016**, *135*, 211.

36 L. Kortekaas, J. Chen, D. Jacquemin and W. R. Browne, *J. Phys. Chem. B*, **2018**, *122*, 6423.

APPENDIX A: SUPPORTING INFORMATION OF CHAPTER 2

A.1 Materials

Calcium Ionophore IV (ETH 5234), poly (vinyl chloride) high molecular weight (PVC), o-nitrophenyl octyl ether (o-NPOE), bis(2-ethylhexyl) sebacate (DOS) and tetrahydrofuran (THF) were provided from Sigma Aldrich (St. Louis, MO). Calcium, potassium sodium, magnesium, and cadmium chlorides, tris(hydroxymethyl)aminomethane and hydrochloric acid were purchased from Fisher Chemicals (Fair Lawn, NJ).

A.2 Instrumentation

A 470 nm LED array with 56 10,000 mcd LEDs (Elixa, Ltd.) was used for irradiation. A UV-Vis spectrophotometer (Cary 50 Bio UV/Visible) from Varian, Australia; a spin coater (WS-650MZ-23NPP) from Laurell North Wales, PA; and a deionized water laboratory purification system (PURELAB Ultra) from Siemens, Orlando, FL.

A.3 Preparation of sensing membranes

The ion-sensing optode membrane contains 9.74% (84.56 mmol/kg of photoacid unit) of polymer 1, 8.48% (105.70 mmol/kg) of calcium ionophore IV, 27.26% PVC and 54.52% o-NPOE. THF was added and the mixture was vigorously shaken for 30 minutes to dissolve all the components. Subsequently, a 20 µL of the cocktail was added onto clean glass slides and spin coated for 2 minutes at 600 rpm to form a thin optode membrane for UV-Vis analysis. The glass slides were previously cut to fit the cuvette, cleaned in an ethanol bath while being scrubbed with cotton swabs and dried under mild heat using a heat gun.

A.4 UV-Vis spectrophotometer measurements

UV-Vis measurements were done in 0.5 M Tris(hydroxymethyl)aminomethane solution at pH 7.40 (pH was adjusted using 6.0 M HCl). Calibration curve was performed using different concentrations of calcium chloride solutions in the range of 1.0×10^{-5} to 1.25 M. First, a baseline was corrected using glass slide in buffer solution. Prior to irradiation, the sensing membrane was scanned in the buffer to obtain the absorbance maxima. Immediately, the sensing membrane was irradiated for 5 minutes at 470 nm to turn the system ON, and subsequently scanned. Then the sensing membrane was kept in dark for 35 minutes and scanned, the resulting spectra was referred as in the dark. The last two steps were repeated subsequently with increasing calcium concentrations. The absorbance registered was plotted against the log of the activity of calcium ions. Figure A-1 shows the change in absorbance for different concentrations of calcium ions after 5 min activation at different times of ion-exchange process (5, 10, 20 and 35 min).

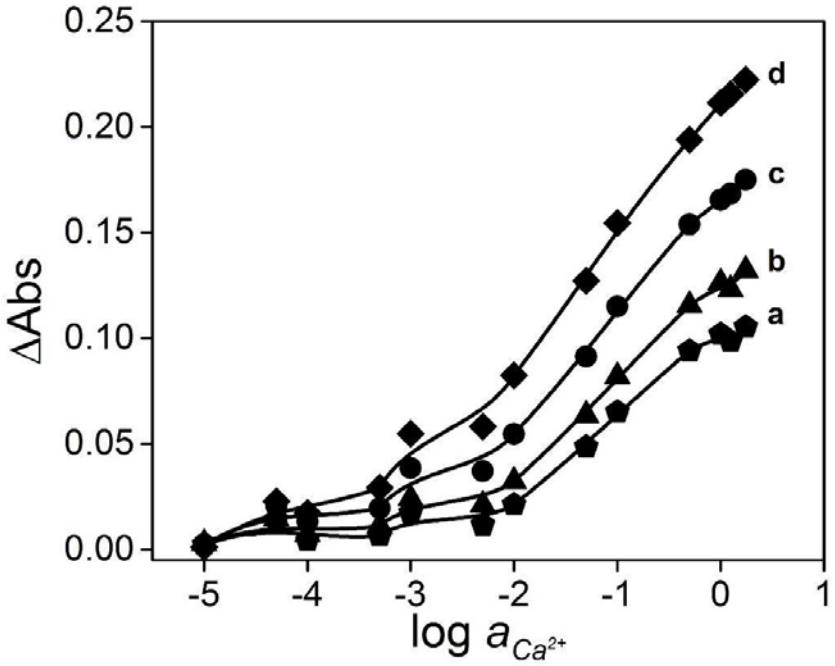

Figure A-1 Absorbance response of calcium-sensing optode membrane activated at 5 min and allowed for different ion-exchange times at a) 5, b) 10, c) 20 and d) 35 minutes in the dark at concentrations of calcium ions ranging from 1.0 x 10^{-5} to 1.25 M. In 0.5 M of tris(hydroxymethyl)aminomethane buffer at pH 7.40.

A.5 Selectivity measurements

For selectivity measurements a similar process was followed as described above. First, the signal was obtained in the buffer solution and then in the corresponding analyte (Ca^{2+}, Na^{+}, K^{+} and Mg^{2+}) at different concentrations.

APPENDIX B: SUPPLEMENTARY INFORMATION OF CHAPTER 4

Reproduced from P. K. Patel, K. Y. Chumbimuni-Torres, "Visible light-induced ion-selective optodes based on a metastable photoacid for cation detection.", *Analyst*, **2016**, *141*, 85-89 with permission of The Royal Society of Chemistry.

B.1 Experimental Methods

B.1.1. Reagents

N,N-Dicyclohexyl-N′,N′-dioctadecyl-3-oxapentanediamide (Calcium ionophore IV), 4-tert-butylcalix[4]arene-tetraacetic acid tetraethyl ester (Sodium Ionophore X), high molecular weight poly(vinyl chloride) (PVC), bis(2-ethylhexyl) sebacate (DOS), tetrahydrofuran (THF), sodium chloride, potassium chloride, calcium chloride, magnesium chloride, magnesium acetate tetrahydrate and sodium hydroxide were purchased from Sigma Aldrich, USA. Formic acid, hydrochloric acid and glacial acetic acid were purchased from Fisher Scientific, USA. Potassium hydroxide was purchased from Amresco, USA. Tricyanofuran based metastable photoacid (CF_3PhTCF-PAH) was synthesized according to literature procedures.[1-3]

B.1.2 Instrumentation

The absorbance measurements were performed using a UV-Vis spectrophotometer (Cary 50 Bio UV/Visible) from Varian, Australia. The source of visible light irradiation was a 470 nm LED array with 120 LEDs from Elixa, USA. The thickness of the cation-selective optode membranes was measured using a profilometer (Tencor AlphaStep 500) from KLA Tencor, USA. Deionized

water used to prepare solutions for analysis was purified by a water purification system with resistance of 18 MΩcm (PURELAB Ultra) from Siemens, USA. The pH of the solutions was obtained with a pH meter (Orion Start A211) from Thermo Scientific, USA. All experiments were carried out in the dark.

B.1.3 Preparation of Cation-selective optodes

The calcium and sodium ion-selective optodes contains CF_3PhTCF-PAH (7.5 mmol/kg), calcium ionophore IV (22.5 mmol/kg) and sodium ionophore X (7.5 mmol/kg), respectively, PVC (33 wt%), and DOS (66 wt%). These components were dissolved in THF (0.8 mL) and shaken until the solution was homogenous. Subsequently, 20 μL of the cocktail solution was added onto clean silanized glass slides.[4] The resultant ISO membranes were dried first in air for 1 hour (in the dark) and then stored in vacuum until use. The membrane thicknesses were between 35 – 45 μm.

B.1.4 Response measurements

The absorbance measurements were performed in 0.5 M formate buffer at pH 4.5 (pH was adjusted with 2.0 M KOH) for calcium-selective optode and 0.3 M magnesium acetate buffer at pH 5.5 (pH was adjusted with dilute acetic acid) for sodium-selective optode. First, a baseline was corrected using a clean silanized glass slide in buffer solution. Prior to irradiation, the cation-selective optode membrane was scanned in the buffer. Immediately, the sensing membrane was turned ON by irradiating with 470 nm visible light for 1 minute and subsequently scanned. Then, the sensing

membrane was kept in dark for 25 minutes (OFF state) and scanned. Afterwards, the buffer solution was changed and the last two steps were repeated four more times.

The response for both cation-selective optode membranes towards its cation of interest and the kinetic experiment for sodium-selective optode membrane were performed similarly as mentioned above. First, the response (ON and OFF state) of the cation sensing membrane was obtained in buffer solution. Then, the last two steps were repeated with increasing cation concentrations (calcium chloride: 1.0×10^{-8} M to 1.0×10^{-3} M, and sodium chloride: 1.0×10^{-6} M to 1.0 M) in their respective buffer. This experiment was performed in triplicates. However, for the kinetic experiment, the response of the CF_3PhTCF-PAH was obtained by scanning the sensing membrane every 30 seconds for 25 minutes after 1 minute irradiation (470 nm).

B.1.5 Selectivity measurements

These measurements were performed similarly as mentioned above in triplicates. The interfering cations used were magnesium, sodium and potassium for calcium-selective optode, and potassium, calcium and magnesium for sodium-selective optode.

B.2 Supplementary References

1. V. K. Johns, P. Peng, J. DeJesus, Z. Z. Wang, Y. Liao, *Chem.-Eur. J.*, **2014**, *20*, 689.

2. M. Q. He, T. M. Leslie, J. A. Sinicropi, *Chem. Mater.*, **2002**, *14*, 2393.

3. S. Liu, M. A. Haller, H. Ma, L. R. Dalton, S. H. Jang, A. K. Y. Jen, *Adv. Mater*., **2003**, *15*, 603.

4. P. K. Patel, V. K. Johns, D. M. Mills, J. E. Boone, P. Calvo-Marzal, K. Y. Chumbimuni-Torres, *Electroanalysis*, **2015**, *27*, 677.

APPENDIX C: SUPPLEMENTARY INFORMATION OF CHAPTER 5

Reproduced from P. K. Patel, J. E. Arias, R. S. Gongora, F. E. Hernandez, A. Moncomble, S. Aloïse, K. Y. Chumbimuni-Torres, "Visible light-triggered fluorescence and pH modulation using metastable-state photoacids and BODIPY.", *Physical Chemistry Chemical Physics*, **2018**, *20*, 26804-26808 with permission from the PCCP Owner Societies.

C.1 Experimental Section

C.1.1 Materials and Instrumentation

Acetone, dichloromethane (DCM), hexanes, ethyl acetate, methanol, ethanol, glacial acetic acid, hydrochloric acid (HCl), sodium hydroxide (NaOH) and sodium bicarbonate were purchased from Fisher, USA. Benzoyl chloride, 2,4-dimethylpyrrole, boron trifluoroetherate, glycine, acetonitrile, and 2-ethylhexyl bromide were purchased from Acros, USA. 2,4-dihydroxybenzaldehyde and cyclohexyl methyl ketone were purchased from Alfa Aesar, USA. Phenyl hydrazine hydrochloride was purchased from TCI, USA. Potassium carbonate (K_2CO_3), tris(hydroxymethyl)aminomethane (Tris) and sodium sulfate were purchased from Amresco, USA. Potassium iodide (KI), sodium chloride (NaCl), boric acid, phosphoric acid, 1,3-propanesultone and triethylamine were purchased from Sigma-Aldrich, USA. Deuterated NMR solvents were purchased from Cambridge Isotope Laboratories, Inc., USA. BODIPY was synthesized according to literature procedure.[1]

^{1}H and ^{13}C NMR spectroscopy were carried out with NMR spectrometer (Avance III 400) from Bruker, USA. Absorbance based experiments were performed using a UV-Vis spectrophotometer (Cary 50 Bio UV/Visible) from Varian, Australia. The source of visible light activation was a 470

nm 120 LED array (maximum average power of 1800 mW) from Elixa, USA. Deionized water used to prepare solutions for pH studies was purified by a water purification system with resistance of 18 MΩcm (Milli-Q Academic) from EMD Millipore Corporation, USA. The pH of the solutions was obtained with a pH meter (Orion Start A211) from Thermo Scientific, USA. Steady-state fluorescence experiments were performed using a spectrofluorometer (FluoroMax-4 Spectrofluorometer) from Horiba Scientific, USA. Time-resolved fluorescence (lifetime decay profiles) studies were performed using a spectrofluorometer (FLS980 Spectrometer) equipped with a 470 nm ± 10 nm picosecond pulsed diode laser as the excitation source (EPL – 470 with a maximum average power of 5 mW) from Edinburgh Instruments, UK. The excitation wavelength of diode laser (EPL – 470) was 470 nm ($\Delta\lambda$ = 1 nm), pulse duration was 92 ps, pulse spacing was fixed at 200 ps, and pulse repetition rate was 5 MHz. The emission wavelength selected was 509 nm ($\Delta\lambda$ = 1 nm) based on the steady-state fluorescence experiment. The fluorescence lifetime decay profiles were recorded until 2000 peak counts were reached for all ethanolic solutions (see Figure C-14 and Table C-1 for concentrations used) at room temperature. The decay profiles were corrected with background (instrument response function) and processed to determine the lifetime values obtained by global analysis (reconvolution) fitting using FAST Version 3.4.2. Software (Edinburgh Instruments, UK). All experiments were carried out in the dark unless mentioned otherwise.

C.1.2 Synthesis

Scheme C-1 Synthetic route used to prepare Mer-mPAH.

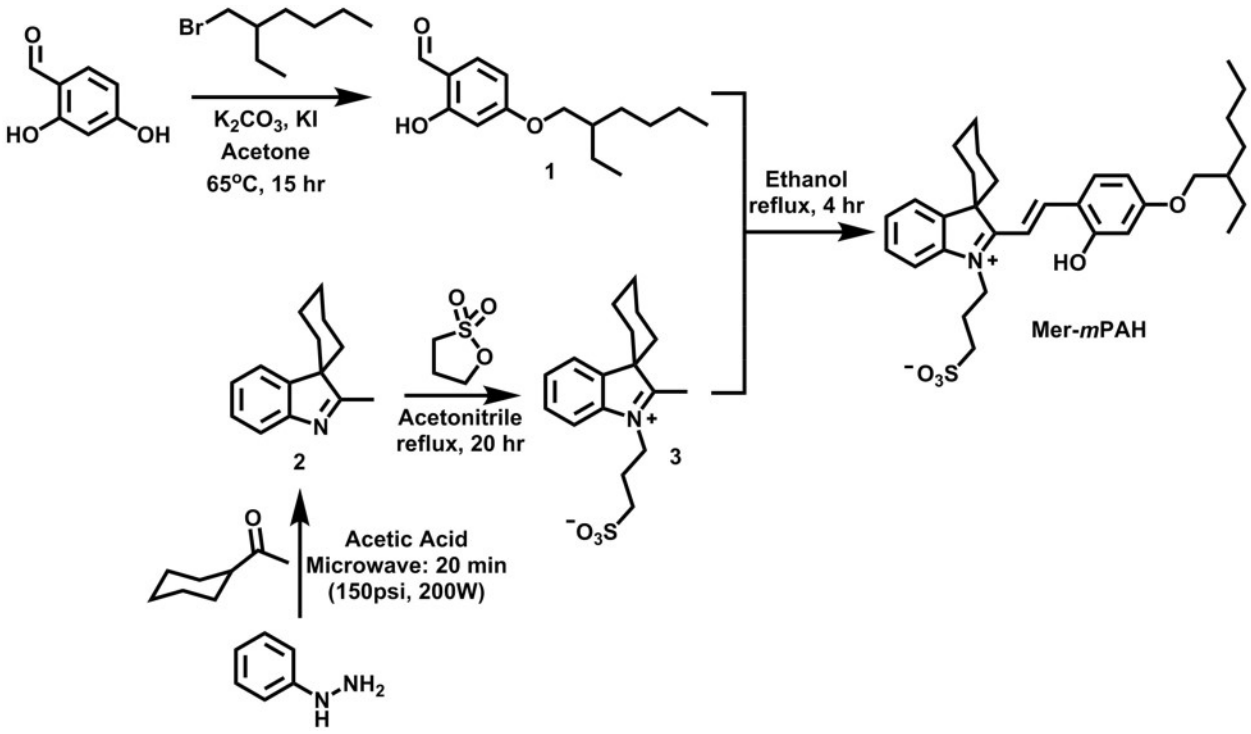

2-hydroxy-4-(2-ethylhexoxy)benzaldehyde (1): The synthesis of 1 was modified following literature procedure.[2] In a 50 mL two-neck flask, equipped with a stir bar and a reflux condenser, was charged with K_2CO_3 (0.506 g, 3.656 mmol) followed by flame drying and purging with nitrogen gas (three times) the equipment setup. Under nitrogen gas, 2,4-dihydroxybenzaldehyde (1.000 g, 7.240 mmol) and dry acetone (8 mL) were added to the reaction flask, followed by raising the temperature to 65°C. After 20 minutes, a solution of KI (10%) and 2-ethylhexyl bromide (2.438 g, 7.312 mmol) in dry acetone (12 mL) was added dropwise to the reaction flask. After 15 hours, the reaction mixture was concentrated in vacuo, and excess 2-ethyl hexyl bromide was removed by distillation. The remaining organic residue was dissolved in minimal DCM and neutralized with

0.1 M HCl. The acid washes were extracted with DCM. Then, the organic phase was washed with brine (saturated NaCl), separated and passed through a drying column. After concentrating the organics in vacuo, the crude was purified by column chromatography (silica) in hexanes and eluted in 50% ethyl acetate in hexanes to afford a colorless oil. Yield (49%). ^{1}H NMR (400 MHz, $CDCl_3$): δ (ppm) = 11.48 (s, 1H), 9.70 (s, 1H), 7.42-7.40 (d, J = 8.67 Hz, 1H), 6.55-6.52 (dd, J = 2.32 Hz, J = 8.66 Hz, 1H), 6.42 (d, J = 2.29 Hz, 1H), 3.90-3.89 (d, J = 5.83 Hz, 2H), 1.77-1.71 (m, 1H), 1.53-1.30 (m, 10H), 0.95-0.91 (m, 6H). ^{13}C NMR (400 MHz, $CDCl_3$): δ (ppm) = 194.24, 166.69, 164.53, 135.14, 114.98, 108.80, 101.07, 71.05, 39.13, 30.40, 29.00, 23.77, 22.99, 11.04.

2'-methylspiro[cyclohexane-1,3'-[3H]indole] (2): The synthesis of 2 was modified following literature procedure.[3] In a 30 mL microwave reaction flask, equipped with a stir bar, was charged with cyclohexyl methyl ketone (1.003 g , 7.949 mmol) and glacial acetic acid (13.93 mL). This reaction mixture was sonicated for few minutes before adding phenyl hydrazine hydrochloride (1.138 g, 7.870 mmol). After 20 mins of microwave irradiation (150 psi, 200W), glacial acetic acid was removed in vacuo to result an orange residue. This residue was dissolved in DCM and neutralized with sodium bicarbonate. The organic phase was separated and washed three times with brine. Then, the organic phase was collected, dried with anhydrous sodium sulfate and the DCM was removed in vacuo to afford a red brown oil. Yield (77%). ^{1}H NMR (400 MHz, $CDCl_3$): δ (ppm) = 7.71-7.69 (d, J = 7.36 Hz, 1H), 7.56-7.54 (d, J = 7.54 Hz, 1H), 7.34-7.30 (td, J = 7.57 Hz, J = 15.21 Hz 1H), 7.17-7.13 (td, J = 7.48 Hz, J = 14.98Hz, 1H), 2.27 (s, 3H), 1.98-1.73 (m, 8H), 1.31-1.26 (m, 2H). ^{13}C NMR (400 MHz, $CDCl_3$): δ (ppm) = 187.65, 154.12, 144.48, 127.39, 124.14, 124.13, 120.00, 57.77, 31.06, 25.21, 21.51, 16.02.

2’-methyl-1’-(3-sulfopropyl)spiro[cyclohexane-1,3’-[3H]indolium] inner salt (3): The synthesis of 3 was modified following literature procedure.[4] In a 125 mL round bottom flask equipped with a stir bar, 2 (1.10 g, 5.517 mmol) dissolved in acetonitrile (55 mL) was added under nitrogen gas. Then, 1,3-propanesultone (0.741 g, 6.068 mmol) was added dropwise over a period of 30 minutes to the reaction mixture at room temperature under nitrogen gas. Afterwards, the reaction mixture was refluxed under nitrogen gas for 20 hours. Acetonitrile was then removed under vacuo and the crude was purified by column chromatography (silica) using 7% (v/v) methanol in DCM to remove unreacted 1,3-propanesultone. Both purple and brown fractions were combined and concentrated under vacuo, and used without further purification. NMR spectra could not be obtained. Crude yield (60 %).

Mer-mPAH: The synthesis of Mer-mPAH was modified following literature procedure.[5] In a 125 mL round bottom flask, crude 3 (0.200 g, 0.622 mmol) was dissolved in anhydrous ethanol (25 mL). Prior to immediate addition of 1 (0.267 g, 0.684 mmol) to the reaction mixture, it was first placed under high vacuum overnight. After addition, the reaction mixture was heated to reflux under nitrogen for 4 hours. Ethanol was removed in vacuo, and the residue was purified by column chromatography (silica, washed with 1% acetic acid in mobile phase) using 6% (v/v) methanol in DCM. All orange and pink fractions were collected and washed with aqueous 1.0 M HCl and extracted with DCM. The organic phase was separated and dried using anhydrous sodium sulfate. The clear reddish orange organic solution was concentrated in vacuo to afford a red solid. Yield (20%). ^{1}H NMR (400 MHz, DMSO-d_6): δ (ppm) = 11.34 (br. s, 1H), 8.76- 8.72 (d, J = 16.16 Hz, 1H), 8.32-8.29 (d, J = 9.61 Hz, 1H), 8.13-8.11 (d, J = 7.43 Hz, 1H), 8.02-8.00 (d, J = 8.07 Hz, 1H),

7.66-7.60 (m, 2H), 7.53-7.49 (t, J = 7.48 Hz, J = 15.00 Hz, 1H), 6.59 (m, 2H), 4.78-4.74 (br. t, J = 7.36 Hz, J = 14.99 Hz, 2H), 3.95-3.93 (d, J = 5.46 Hz, 2H), 2.69-2.66 (br. t, J = 5.95 Hz, J = 12.15 Hz, 2H), 2.22-1.88 (m, 10H), 1.69-1.64 (m, 3H), 1.33-1.24 (m, 6H), 0.90-0.87 (m = 8H). ^{13}C NMR (400 MHz, DMSO-d_6): δ (ppm) = 165.77, 161.66, 148.25, 141.74, 141.35, 128.89, 127.43, 125.46, 115.04, 114.80, 108.64, 106.97, 101.07, 70.56, 55.53, 47.31, 44.91, 38.37, 34.26, 29.72, 28.31, 24.27, 24.20, 23.12, 22.40, 20.60, 13.85, 10.79

C.2 ^{1}H and ^{13}C NMR spectra for 1, 2 and Mer-mPAH

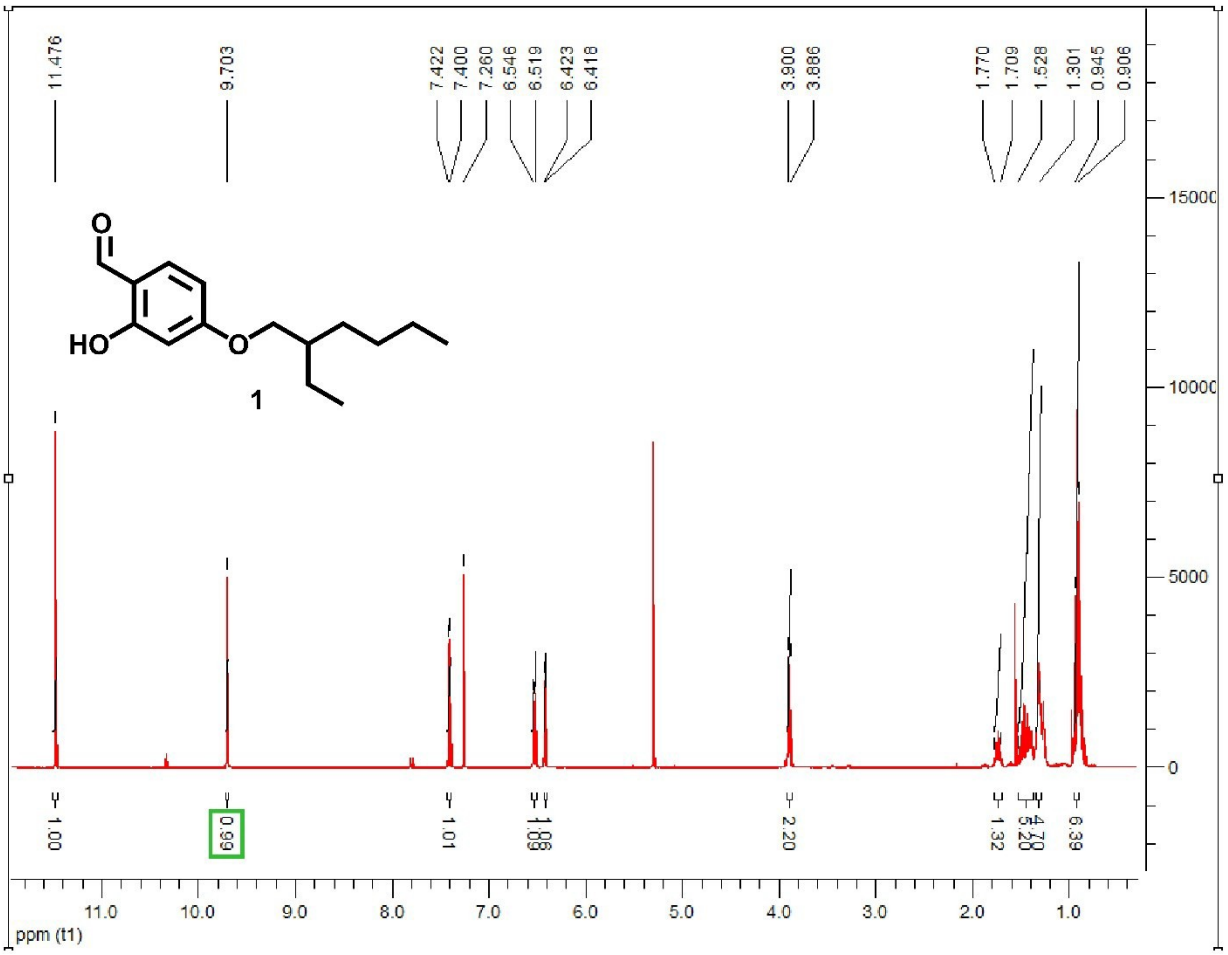

Figure C-1 ^{1}H NMR spectra of 1.

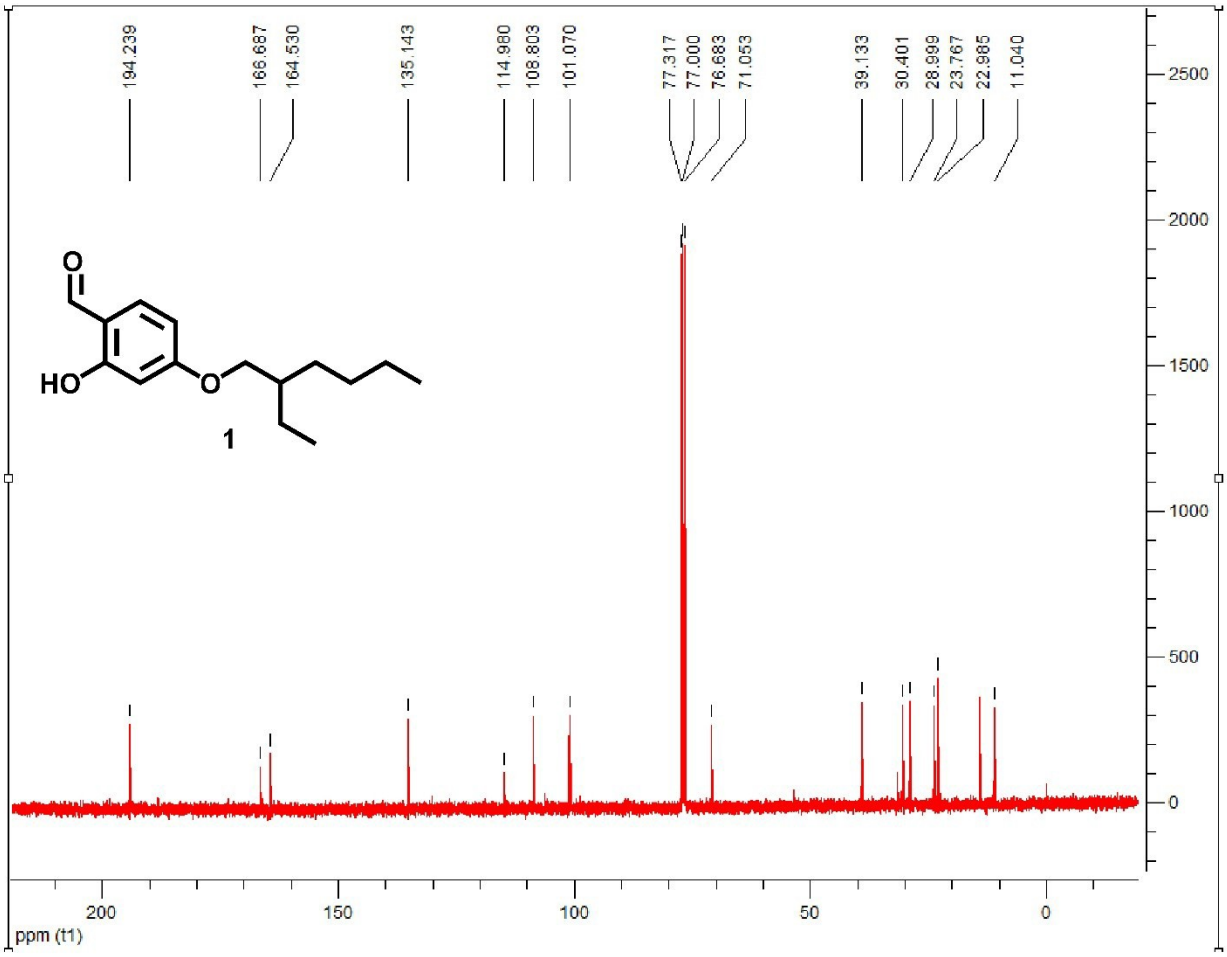

Figure C-2 ^{13}C NMR spectra of 1.

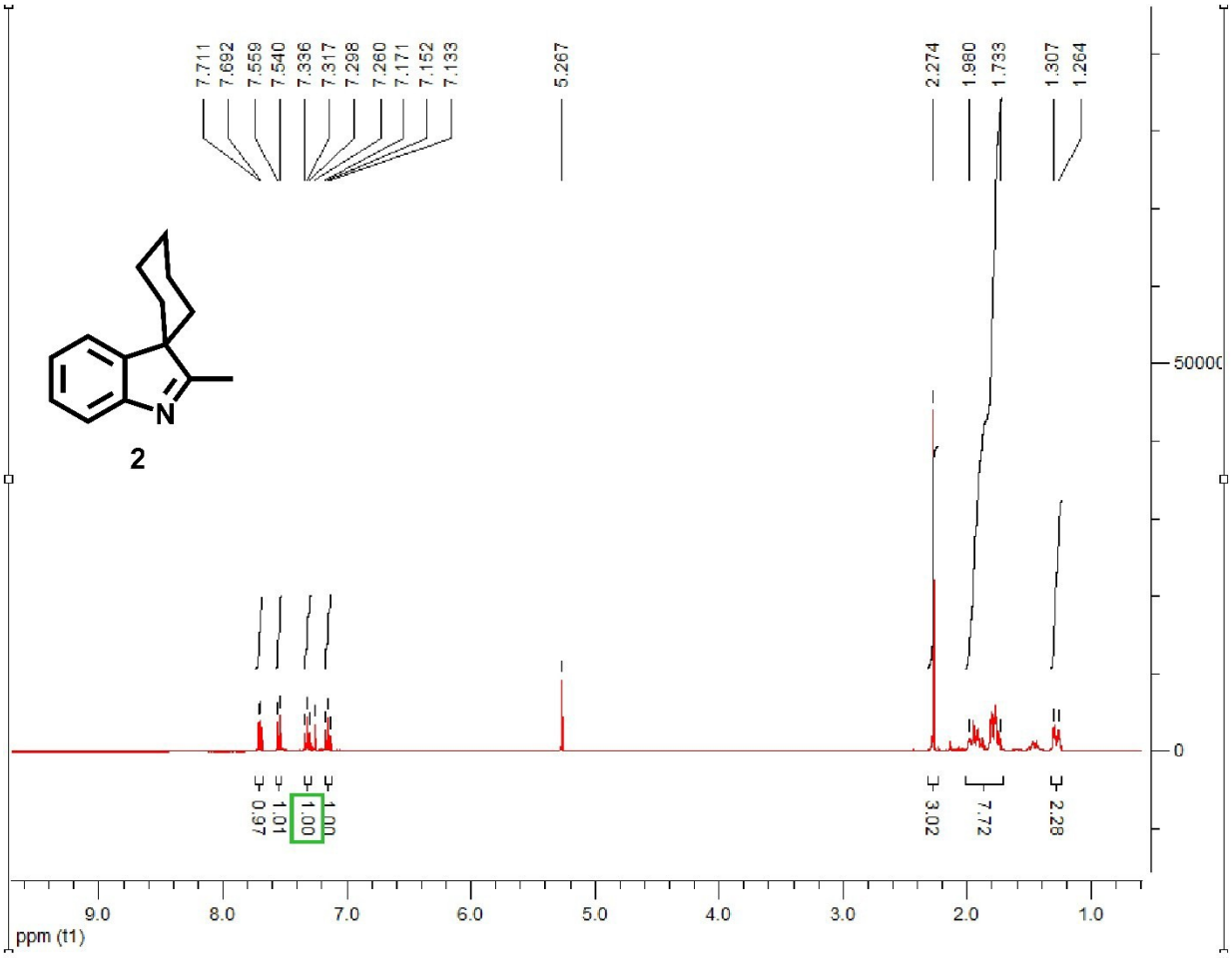

Figure C-3 ^{1}H NMR spectra of 2.

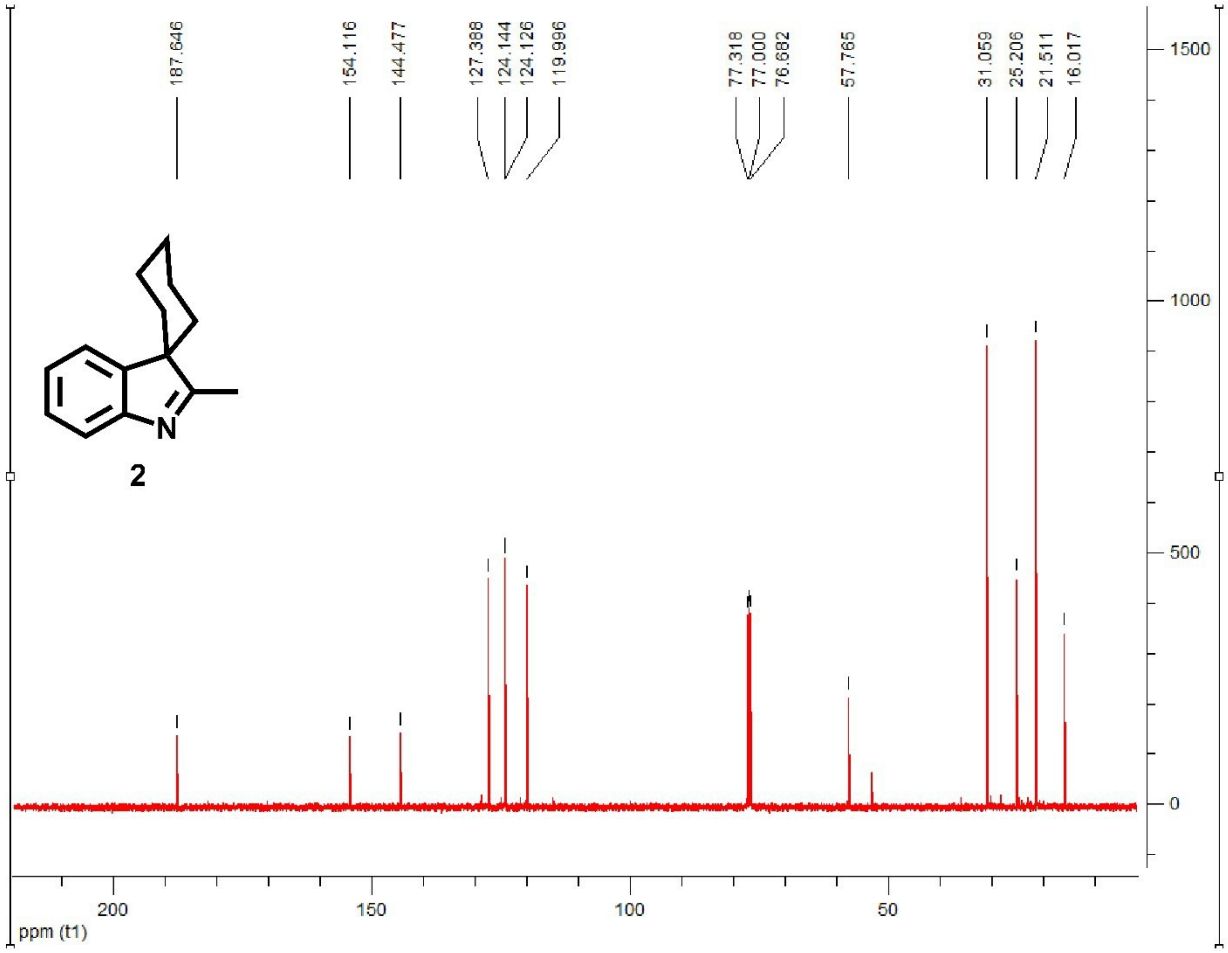

Figure C-4 ^{13}C NMR spectra of 2.

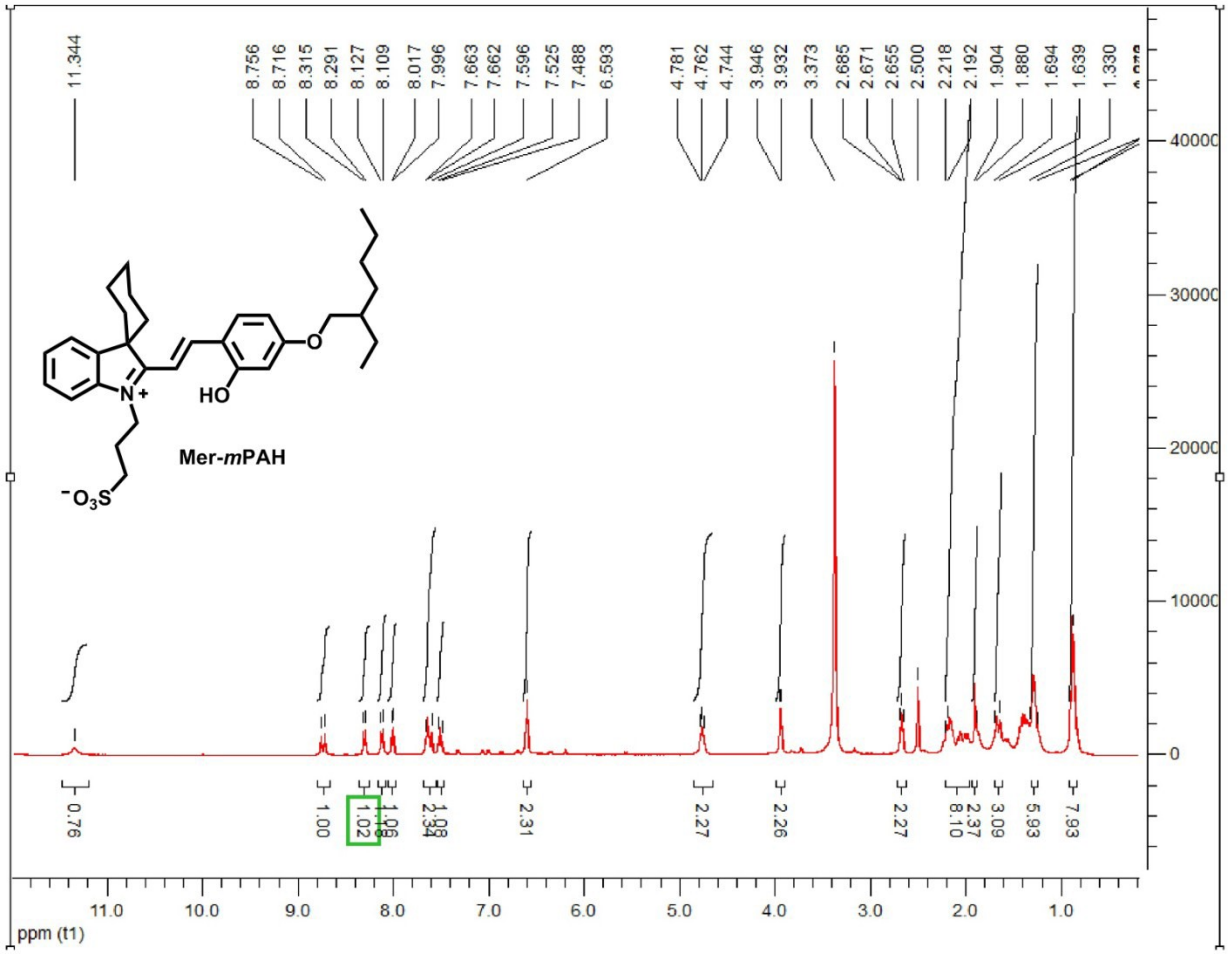

Figure C-5 ^{1}H NMR spectra of Mer-mPAH.

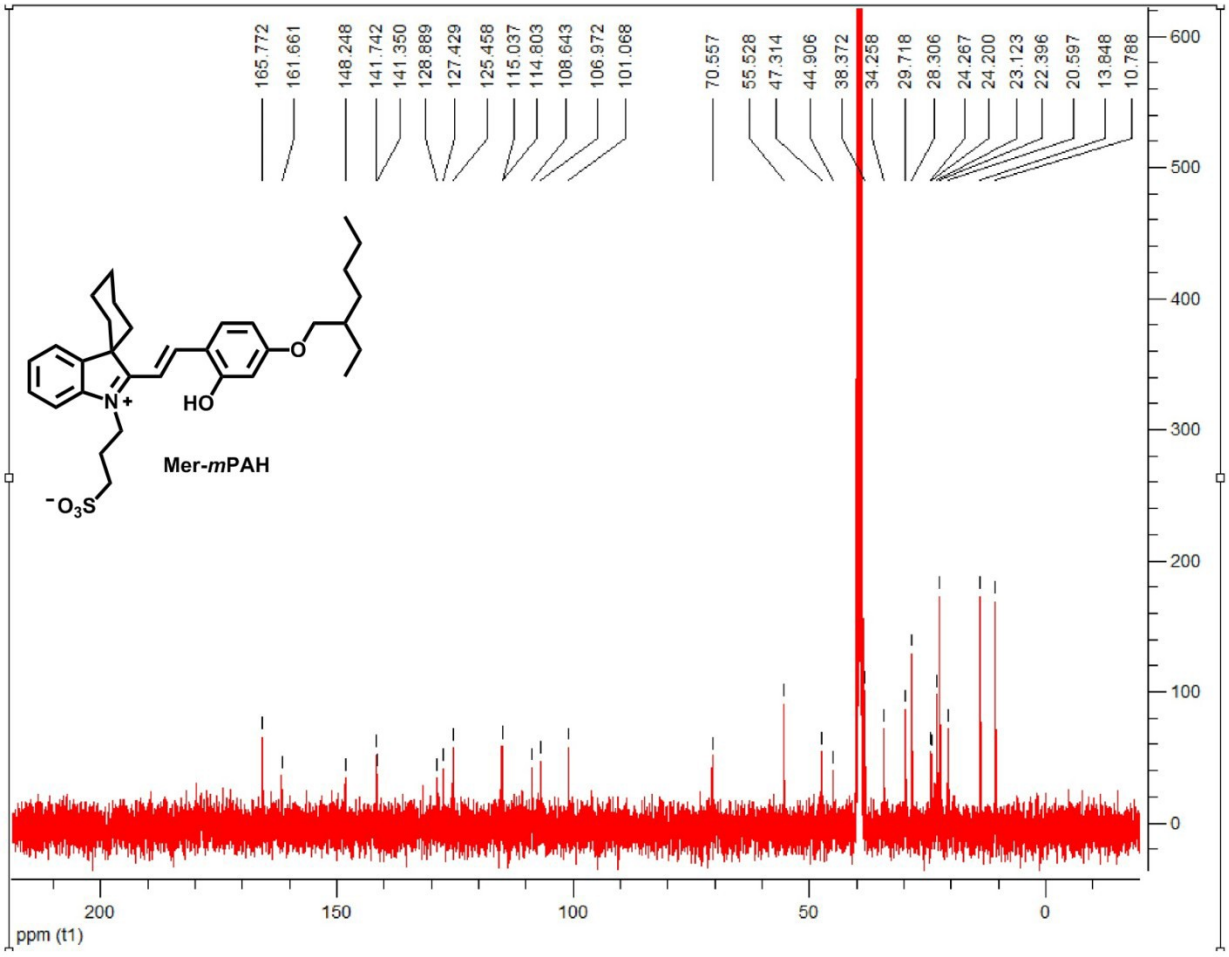

Figure C-6 ^{13}C NMR spectra of Mer-mPAH.

C.3 DFT/TD-DFT calculations

All calculations were performed using the Gaussian 09 package.[6] The visualizations were obtained using the Avogadro 1.2.0n software.[7] All calculations including the geometry optimizations, the frequency calculations, and the time-dependent single point energy calculations were carried out with the B3LYP global hybrid functional using the 6-311++G (2d,p) basis set.[8] Ethanol was accounted as an implicit solvent using the IEFPCM solvation model.[9]

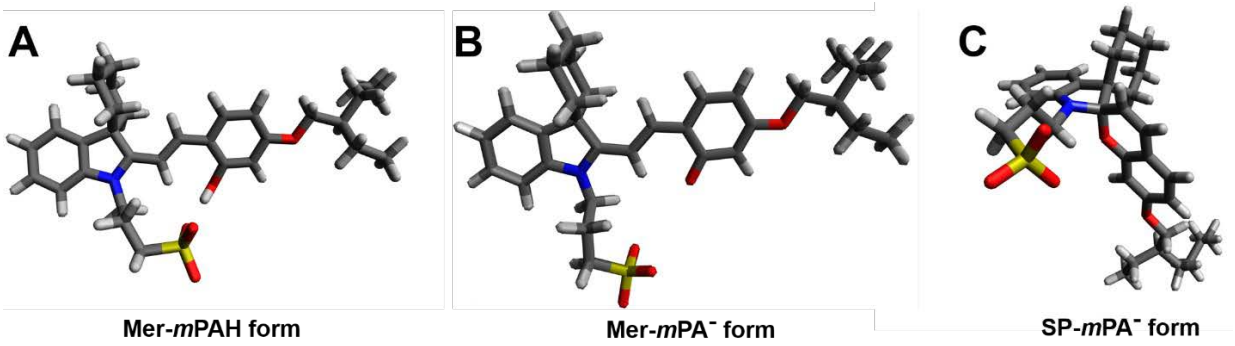

Figure C-7 Optimized geometries for ground state structure of (A) Mer-mPAH, (B) Mer-mPA$^-$, and (C) SP-mPA$^-$ forms.

C.3.1 Gibbs-free energy calculations

The Zero-Point Energy (ZPE) corresponds to the energy of a system where the molecular vibrations that persist at 0K are taken into consideration.[10] To obtain the Gibbs-free energies of mPAH in its different states, we performed frequency calculations on the optimized structures of

Mer-mPAH, Mer-mPA$^-$, and SP-mPA$^-$. Then, the energy of the system in its different states was computed as follows:

$$\Delta G_{Mer-mPAH} = ZPE_{Mer-mPAH} = -5446010.5\ kJ/mol \quad [C.1]$$

$$\Delta G_{Mer-mPA^-} = ZPE_{Mer-mPA^-} + \Delta G_{Solvated\ H^+} = \left(-5444831.6\frac{kJ}{mol}\right) + \left(-1104.5\frac{kJ}{mol}\right) = -5445936.1\ kJ/mol \quad [C.2]$$

$$\Delta G_{SP-mPA^-} = ZPE_{SP-mPA^-} + \Delta G_{Solvated\ H^+} = \left(-5444818.3\frac{kJ}{mol}\right) + \left(-1104.5\frac{kJ}{mol}\right) = -54445922.761\ kJ/mol \quad [C.3]$$

All the ΔG were normalized to ΔG Mer-mPAH as follows:

$$Normalized\ \Delta G_{Mer-mPAH} = \Delta G_{Mer-mPAH} - \Delta G_{Mer-mPAH} = 0\ kJ/mol \quad [C.4]$$

$$Normalized\ \Delta G_{Mer-mPA^-} = \Delta G_{Mer-mPA^-} - \Delta G_{Mer-mPAH} = 74.4\ kJ/mol \quad [C.5]$$

$$Normalized\ \Delta G_{SP-mPA^-} = \Delta G_{SP-mPA^-} - \Delta G_{Mer-mPAH} = 87.8\ kJ/mol \quad [C.6]$$

Note that the energy of a solvated proton must be added to the Mer-mPA$^-$ and SP-mPA$^-$ forms in order to make all the Gibbs free energies comparable. The value for the Gibbs free energy for a solvated proton in aqueous media was obtained from Tissander et al seminal work on solvated ions.[11] Unfortunately, there is no paper that follows Tissander et al procedure on calculating the Gibbs free energy of a solvated proton in ethanol via cluster calculations. Nonetheless, Markovic et al provide Gibbs free energy calculations for a solvated proton in ethanol (and many other

solvents) using accurate calculations.[12] Although their work does not feature a fully comprehensive solvation model for the proton, it does go on to show that the Gibbs free energies for solvated protons are not so far in water and in ethanol (-1055.8 kJ/mol and -1064.9 kJ/mol, respectively). Hence, we choose to approximate the solvation Gibbs free energy for a proton in ethanol, or in an ethanol-water mixture, by the highly accurate reported value by Tissander et al. It is important to recognize that the predicted energy for the Mer-mPA$^-$ might have a significant error, since the model does not seem to be able to fully account for its electronic structure (refer to Figure C-8B).

For completion, we repeated the same process for an aqueous solution. All structures were optimized with B3LYP/6-311++G(2d,p) accounting for water as a solvent using the IEFPCM model. A frequency calculation using those same parameters was performed to obtain the ZPE-corrected Gibbs-free energies. The energy of the system (in water) in its different states was computed as follows:

$$\Delta G_{Mer-mPAH} = ZPE_{Mer-mPAH} = -5446016.3\ kJ/mol \quad [C.1]$$

$$\Delta G_{Mer-mPA^-} = ZPE_{Mer-mPA^-} + \Delta G_{Solvated\ H^+} = \left(-5444833.3\frac{kJ}{mol}\right) + \left(-1104.5\frac{kJ}{mol}\right) = -5445937.8\ kJ/mol \quad [C.2]$$

$$\Delta G_{SP-mPA^-} = ZPE_{SP-mPA^-} + \Delta G_{Solvated\ H^+} = \left(-5444828.8\frac{kJ}{mol}\right) + \left(-1104.5\frac{kJ}{mol}\right) = -5445933.3\ kJ/mol \quad [C.3]$$

All the ΔG were normalized to ΔG Mer-mPAH as follows:

$$Normalized\ \Delta G_{Mer-mPAH} = \Delta G_{Mer-mPAH} - \Delta G_{Mer-mPAH} = 0\ kJ/mol \quad [C.4]$$

$$Normalized\ \Delta G_{Mer-mPA^-} = \Delta G_{Mer-mPA^-} - \Delta G_{Mer-mPAH} = 78.5\ kJ/mol \quad [C.5]$$

$$Normalized\ \Delta G_{SP-mPA^-} = \Delta G_{SP-mPA^-} - \Delta G_{Mer-mPAH} = 83.0\ kJ/mol \quad [C.6]$$

C.3.2 Correlation between experimental and theoretical absorbance spectra

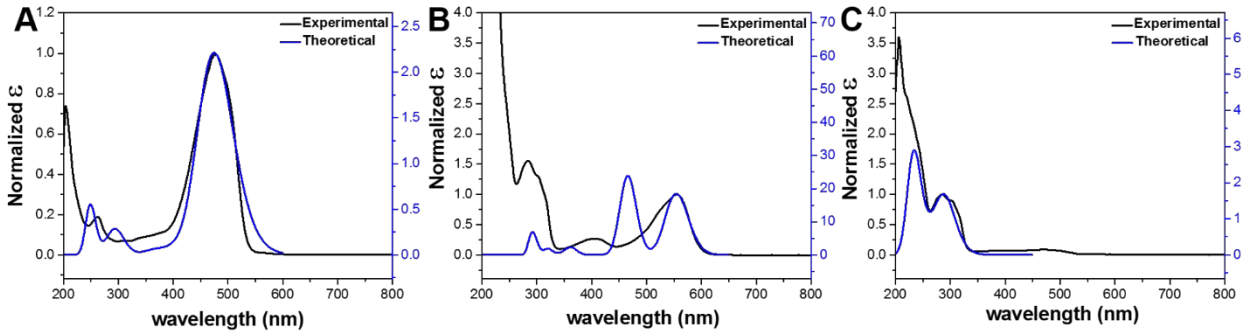

Figure C-8 Overlap of the normalized experimental absorption spectra (black line) and the shifter computed spectra (blue line; more details provided below) for (A) Mer-mPAH, (B) Mer-mPA$^-$, and (C) SP-mPA$^-$ forms.

The first 40 excited states for Mer-mPAH, Mer-mPA$^-$, and SP-mPA$^-$ forms were calculated using time-dependent DFT on the previously optimized structures. The scales for the theoretical Mer-mPA$^-$ spectra seem disproportionate because there is a significant population of the mPAH in its SP-mPA$^-$ conformer (evidenced by the peak at 287 nm in the Mer-mPA$^-$ experimental spectra). If the experimental spectra contained solely Mer-mPA$^-$, the scales would be in better agreement. For example, refer to the spectra of the SP-mPA$^-$. The experimental spectrum shows no mPAH in its

Mer-mPA$^-$ conformer (peak at 554 nm) and a negligible amount of mPAH in its Mer-mPAH conformer (peak at 474 nm). As a result, the scales of the theoretical and experimental spectra are much closer.

The spectra in Figure C-8A were normalized to the peak corresponding to the Mer-mPAH form in the experimental spectrum in 100% ethanol. The theoretical spectra required a shift of -0.221 eV to match the experimental first electronic transition (from 437.91 nm to 474.91 nm). A FWMH of 0.21 eV was required to provide the best possible overlap.

The spectra in Figure C-8B were normalized to the peak corresponding to the Mer-mPA$^-$ form in the experimental spectrum in ethanol/water (50/50). The theoretical spectra required a shift of -0.282 eV to match the experimental first electronic transition (from 492.21 nm to 554.21 nm). A FWMH of 0.10 eV was required to provide the best possible overlap.

The spectra in Figure C-8C were normalized to the lowest energy electronic transition of the experimental spectrum in 100% ethanol. The theoretical spectra for SP-mPA$^-$ required a shift of 0.178 eV to match the experimental first electronic transition (from 300.24 nm to 287.23 nm). A FWMH of 0.33 eV was required to provide the best possible overlap.

The overlaps are good except in the case of Mer-mPA$^-$ form (Figure C-8B), where the transition corresponding to a shoulder in the experimental spectra is predicted to be at a considerable distance from the transition of lowest energy. As a result, the theoretical spectrum creates a new peak instead of a shoulder. This could be linked to the FWMH that is quite small in this case. A larger

FWMH should merge these two peaks and lead to a better agreement. The inversion of the relative intensities of the two lowest transitions could also be an artifact due to a too crude model (B3LYP/6-311++G (2d,p)) or to the use of ethanol as the only solvent. Further investigations are required to give more insight on these issues.

C.4 Determination of thermodynamic acidity constant

The ground state acidity constant (pKa) of metastable-state photoacid (mPAH) is determined by the following thermodynamic reaction provided below.

$$mPAH \underset{\text{Acid}}{\overset{\text{Base}}{\rightleftharpoons}} mPA^- + H^+$$

Likewise, Henderson-Hasselbalch equation [C.7] was correlated with degree of protonation [C.8]. Accordingly, mass-balance equation [C.9] was used to modify Equation [C.7] to [C.10].

Henderson-Hasselbalch equation based of mPAH equilibrium reaction:

$$pH = pK_a + log\frac{[In^-]}{[InH]} \qquad [C.7]$$

Degree of protonation, "α":

$$\alpha = \frac{[mPAH]}{[mPAH]_T} = \frac{A - A_D}{A_P - A_D} \qquad [C.8]$$

Degree of protonation is defined as the ratio of acidic-open form mPAH, where subscript "T" signifies total concentration of mPAH. Likewise, the concentrations of acidic-open form mPAH can be related to absorbance as denoted by "A". The symbols "AD" and "AP" represents absorbance values of acidic-open form mPAH absorption peak when it is fully deprotonated and fully protonated.

Mass-balance equation:

$$[mPAH]_T = [mPAH] + [mPA^-] \quad \text{[C.9]}$$

Modified Henderson-Hasselbalch equation:

$$pH = pK_a + log\left[\frac{(1-\alpha)}{\alpha}\right] \quad \text{[C.10]}$$

This theoretical equation was derived by rearranging [C.7] by incorporation of both [C.8] and [C.9], and was used to fit the experimental for estimating the pKa of Mer-mPAH.

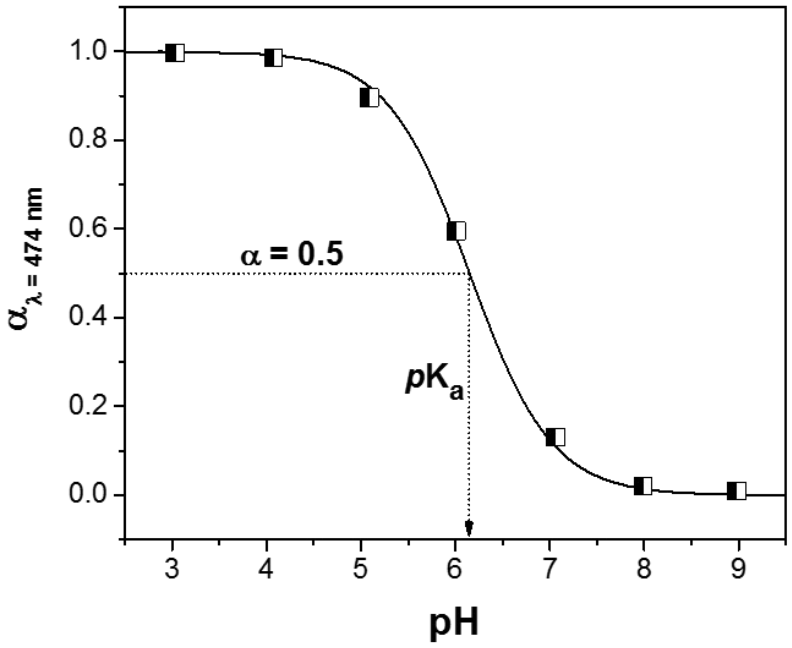

Figure C-9 Correlation between theoretical fitting and the obtained experimental data to estimate the thermodynamic acidity constant.

C.5 Additional Figures and Table

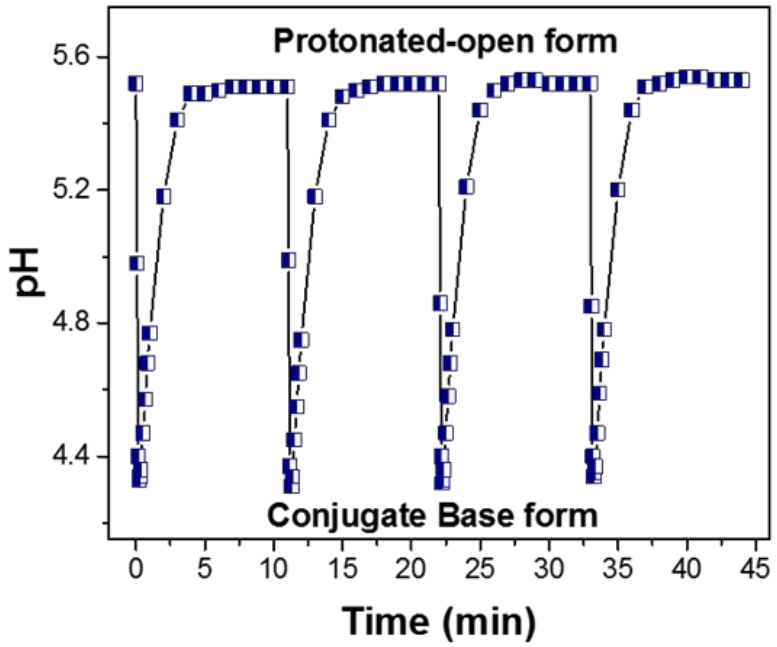

Figure C-10 Modulation of pH by 470 nm light over multiple cycles with respect to time for an ethanol/water (90/10) solution containing 65 µM of Mer-mPAH.

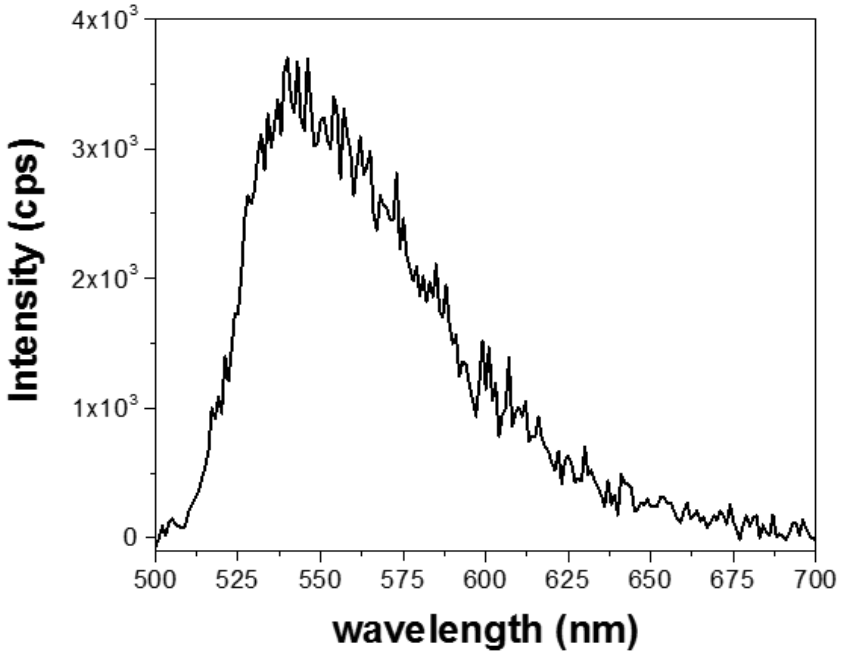

Figure C-11 Emission spectra for ethanol solution containing Mer-mPAH (6.50×10^{-5} M) only. Excitation wavelength 478 nm was used.

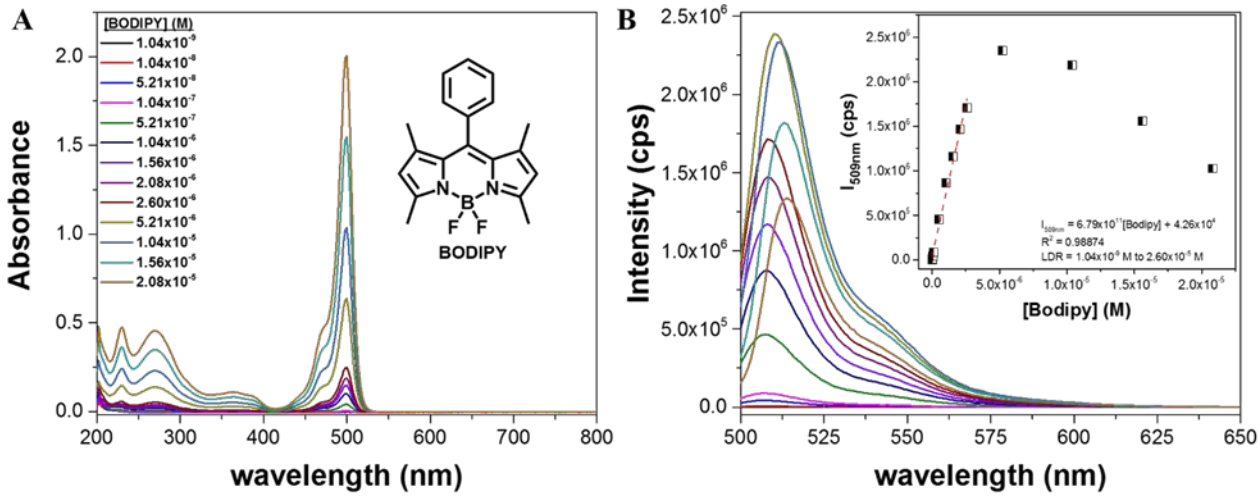

Figure C-12 Optical characteristics for different concentrations of BODIPY in ethanol. A) Absorbance spectra. B) Emission spectra (excitation wavelength was 495 nm) with calibration plot to illustrate self-quenching behaviour (Inset).

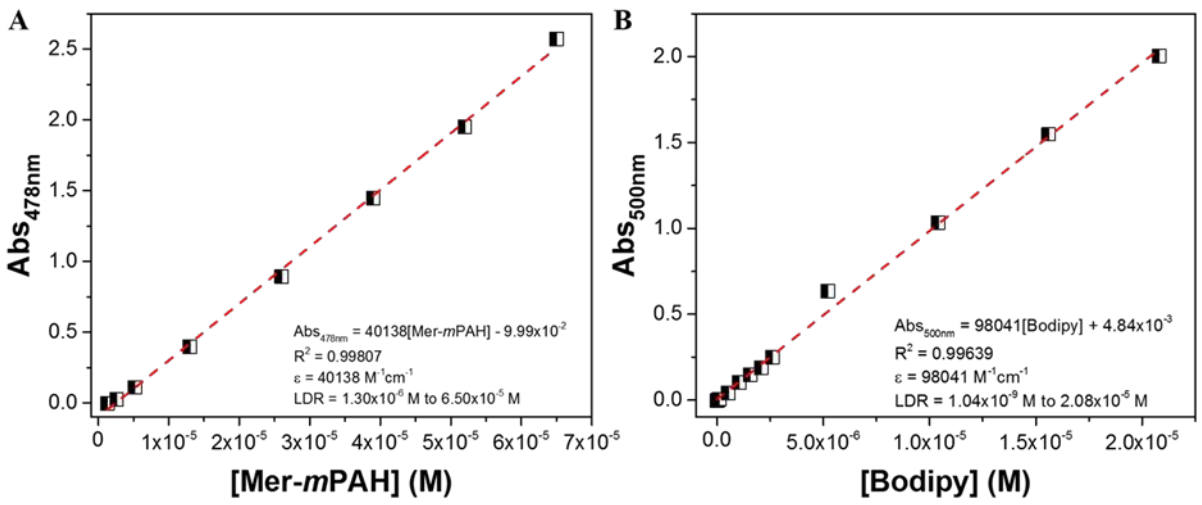

Figure C-13 Absorbance-based calibration plot for ethanol solutions containing different concentrations of A) Mer-mPAH (1.30×10^{-6} M, 2.60×10^{-6} M, 5.21×10^{-6} M, 1.30×10^{-5} M, 2.60×10^{-5} M, 3.90×10^{-5} M, 5.20×10^{-5} M and 6.50×10^{-5} M), and B) BODIPY (1.04×10^{-9} M, 1.04×10^{-8} M, 5.21×10^{-8} M, 1.04×10^{-7} M, 5.21×10^{-7} M, 1.04×10^{-6} M, 1.04×10^{-6} M, 1.56×10^{-6} M, 2.08×10^{-6} M, 2.60×10^{-6} M, 5.21×10^{-6} M, 1.04×10^{-5} M, 1.56×10^{-5} M and 2.08×10^{-5} M).

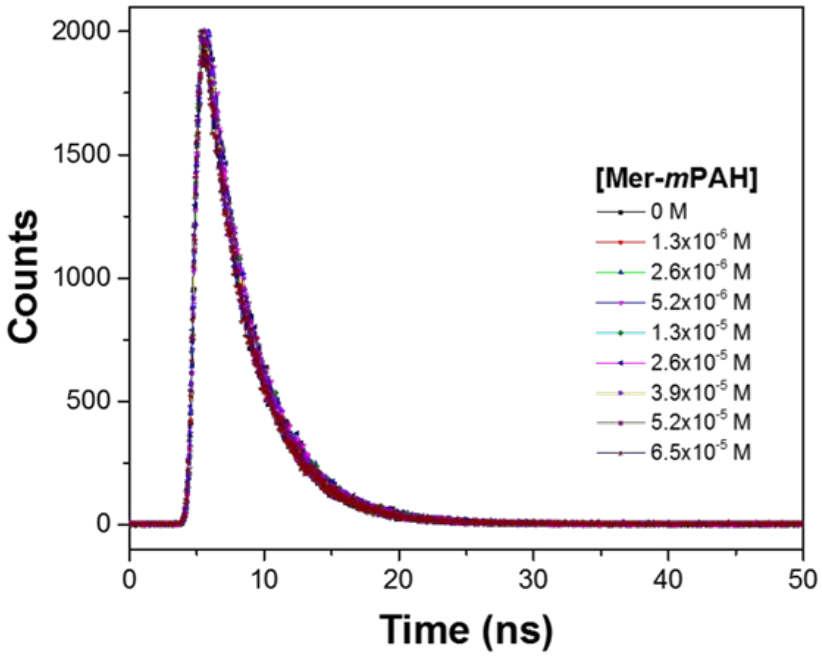

Figure C-14 Lifetime decay profiles for ethanol solutions containing fixed concentration of BODIPY (2.60×10^{-6} M) with different concentrations of Mer-mPAH.

Table C-1 Lifetime decay data for different concentration of Mer-mPAH with fixed concentration of BODIPY.

[Mer-*m*PAH] + 2.6×10^{-6} M BODIPY	τ (ns)
0 M	3.317 [a]
1.3×10^{-6} M	3.328
2.6×10^{-6} M	3.321
5.2×10^{-6} M	3.320
1.3×10^{-5} M	3.326
2.6×10^{-5} M	3.294
3.9×10^{-5} M	3.316
5.2×10^{-5} M	3.295
6.5×10^{-5} M	3.315

[a] τ_0

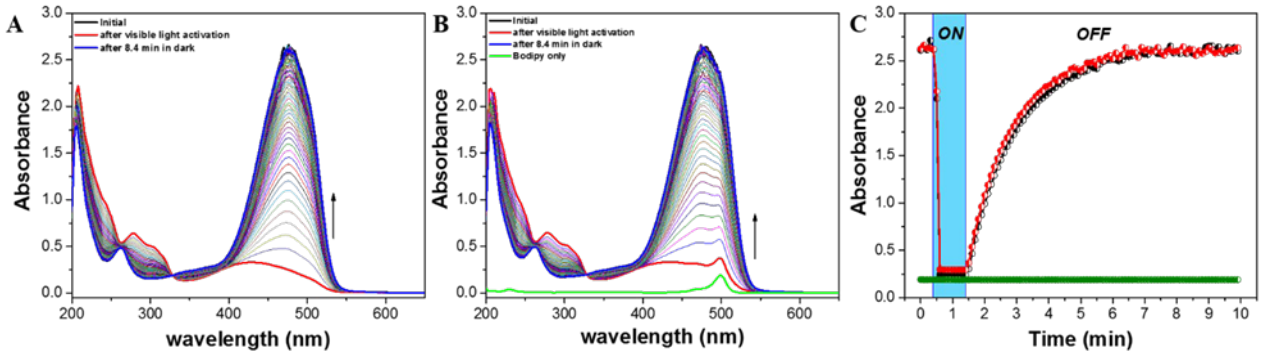

Figure C-15 Absorbance-based experiments for ethanol solution containing A) 6.50×10^{-5} M of Mer-mPAH, B) 6.50×10^{-5} M of Mer-mPAH with 2.60×10^{-6} M of BODIPY (in green: absorbance spectra of 2.60×10^{-6} M of BODIPY), and C) Kinetic plots for a solution of 6.50×10^{-5} M Mer-mPAH only (in black, λ_{abs} = 478 nm), 2.60×10^{-6} M BODIPY with 6.50×10^{-5} M Mer-mPAH (in red, λ_{abs} = 478 nm), and 2.60×10^{-6} M BODIPY only (in green, λ_{abs} = 500 nm) (ON region signifies visible light activation by 470 nm light, while the OFF region signifies in the dark).

C.1 References

1. Y. Chen, J. Zhao, H. Guo, L. Xie, *J. Org. Chem.*, **2012**, *77*, 2192.

2. C. R. Bhattacharjee, G. Das, P. Mondal, *J. Coord. Chem.*, **2011**, *64*, 3273.

3. E. A. Owens, N. Bruschi, J. G. Tawney, M. Henary, *Dyes Pigm.*, **2015**, *113*, 27.

4. A. Alagumalai, M. K. Munavvar Fairoos, P. Vellimalai, M. C. Sil, J. Nithyanandhan, *ACS Appl. Mater. Interfaces*, **2016**, *8*, 35353.

5. Z. Shi, P. Peng, D. Strohecker, Y. Liao, *J. Am. Chem. Soc*., **2011**, *133*, 14699.

6. M. J. Frisch, G. W. Trucks, H. B. Schlegel, G. E. Scuseria, M. A. Robb, J. R. Cheeseman, G. Scalmani, V. Barone, B. Mennucci, G. A. Petersson, H. Nakatsuji, M. Caricato, X. Li, H. P. Hratchian, A. F. Izmaylov, J. Bloino, G. Zheng, J. L. Sonnenberg, M. Hada, M. Ehara, K. Toyota, R. Fukuda, J. Hasegawa, M. Ishida, T. Nakajima, Y. Honda, O. Kitao, H. Nakai, T. Vreven, J. A. Montgomery Jr., J. E. Peralta, F. Ogliaro, M. Bearpark, J. J. Heyd, E. Brothers, K. N. Kudin, V. N. Staroverov, T. Keith, R. Kobayashi, J. Normand, K. Raghavachari, A. Rendell, J. C. Burant, S. S. Iyengar, J. Tomasi, M. Cossi, N. Rega, J. M. Millam, M. Klene, J. Knox, J. B. Cross, V. Bakken, C. Adamo, J. Jaramillo, R. Gomperts, R. E. Stratmann, O. Yazyev, A. J. Austin, R. Cammi, C. Pomelli, J. W. Ochterski, R. L. Martin, K. Morokuma, V. G. Zakrzewski, G. A. Voth, P. Salvador, J. J. Dannenberg, S. Dapprich, A. D. Daniels, O. Farkas, J. B. Foresman, J. V. Ortiz, J. Cioslowski, D. J. Fox, *Gaussian, Inc.*, Wallingford CT, **2013**.

7. M. D. Hanwell, D. E. Curtis, D. C. Lonie, T. Vandermeersch, E. Zurek, G. R. Hutchison, *J. Cheminf.*, **2012**, *4*, 17.

8. A. D. Becke, *J. Chem. Phys*., 1993, 98, 1372.

9. M. Cossi, G. Scalmani, N. Rega, V. Barone, *J. Chem. Phys*., 2002, 117, 45.

10. J. B. Foresman, A. E. Frisch, *Exploring Chemistry with Electronic Structure Methods*, Gaussian Inc., Pittsburgh PA, **1993**.

11. M. D. Tissander, K. A. Cowen, W. Y. Feng, E. Gundlach, M. H. Cohen, A. D. Earhart, J. V. Coe, T. R. Tuttle, *J. Phys. Chem. A*, **1998**, *102*, 7787.

12. Z. Markovic, J. Tošovic, D. Milenkovic, S. Markovic, *Comput. Theor. Chem.*, **2016**, *1077*, 11.

APPENDIX D: COPYRIGHT PERMISSION LETTER

Chapter 2 Reprinted with permission from (Page 1 of 1):

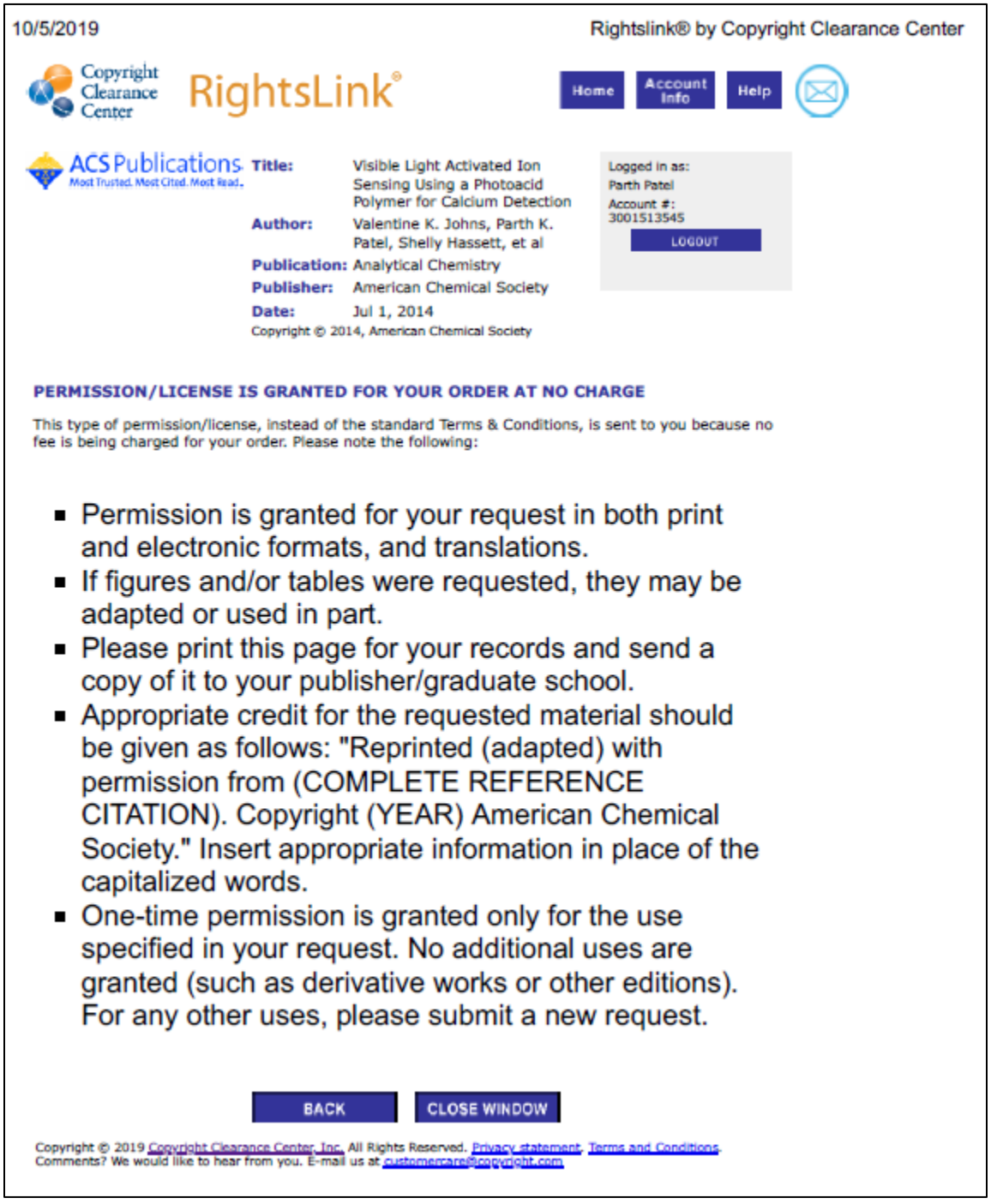

10/5/2019 Rightslink® by Copyright Clearance Center

Copyright Clearance Center RightsLink®

Home | Account Info | Help

ACS Publications Most Trusted. Most Cited. Most Read.

Title: Visible Light Activated Ion Sensing Using a Photoacid Polymer for Calcium Detection

Author: Valentine K. Johns, Parth K. Patel, Shelly Hassett, et al

Publication: Analytical Chemistry

Publisher: American Chemical Society

Date: Jul 1, 2014

Copyright © 2014, American Chemical Society

Logged in as: Parth Patel
Account #: 3001513545
LOGOUT

PERMISSION/LICENSE IS GRANTED FOR YOUR ORDER AT NO CHARGE

This type of permission/license, instead of the standard Terms & Conditions, is sent to you because no fee is being charged for your order. Please note the following:

- Permission is granted for your request in both print and electronic formats, and translations.
- If figures and/or tables were requested, they may be adapted or used in part.
- Please print this page for your records and send a copy of it to your publisher/graduate school.
- Appropriate credit for the requested material should be given as follows: "Reprinted (adapted) with permission from (COMPLETE REFERENCE CITATION). Copyright (YEAR) American Chemical Society." Insert appropriate information in place of the capitalized words.
- One-time permission is granted only for the use specified in your request. No additional uses are granted (such as derivative works or other editions). For any other uses, please submit a new request.

BACK | CLOSE WINDOW

Copyright © 2019 Copyright Clearance Center, Inc. All Rights Reserved. Privacy statement. Terms and Conditions.
Comments? We would like to hear from you. E-mail us at customercare@copyright.com

Chapter 3 Reproduced with permission from: (Page 1 of 5)

JOHN WILEY AND SONS LICENSE TERMS AND CONDITIONS

Sep 06, 2019

This Agreement between Mr. Parth Patel ("You") and John Wiley and Sons ("John Wiley and Sons") consists of your license details and the terms and conditions provided by John Wiley and Sons and Copyright Clearance Center.

License Number	4663190653894
License date	Sep 06, 2019
Licensed Content Publisher	John Wiley and Sons
Licensed Content Publication	Electroanalysis
Licensed Content Title	Tuning the Equilibrium Response Time of Meta-Stable Photoacids in Ion-Sensors by Appropriate Functionalization
Licensed Content Author	Parth K. Patel, Valentine K. Johns, Dawn M. Mills, et al
Licensed Content Date	Jan 16, 2015
Licensed Content Volume	27
Licensed Content Issue	3
Licensed Content Pages	7
Type of use	Dissertation/Thesis
Requestor type	Author of this Wiley article
Format	Print and electronic
Portion	Full article
Will you be translating?	No
Title of your thesis / dissertation	Metastable-state Photoacid: Synthesis, Properties, and Applications
Expected completion date	Dec 2019
Expected size (number of pages)	150
Requestor Location	Mr. Parth Patel 1283 Lexington Ave DAVENPORT, FL 33837 United States Attn: Mr. Parth Patel
Publisher Tax ID	EU826007151
Total	0.00 USD
Terms and Conditions	

TERMS AND CONDITIONS

This copyrighted material is owned by or exclusively licensed to John Wiley & Sons, Inc. or one of its group companies (each a"Wiley Company") or handled on behalf of a society with which a Wiley Company has exclusive publishing rights in relation to a particular work (collectively "WILEY"). By clicking "accept" in connection with completing this licensing transaction, you agree that the following terms and conditions apply to this transaction (along with the billing and payment terms and conditions established by the Copyright

Chapter 3 Reproduced with permission from: (Page 2 of 5)

Clearance Center Inc., ("CCC's Billing and Payment terms and conditions"), at the time that you opened your RightsLink account (these are available at any time at http://myaccount.copyright.com).

Terms and Conditions

- The materials you have requested permission to reproduce or reuse (the "Wiley Materials") are protected by copyright.
- You are hereby granted a personal, non-exclusive, non-sub licensable (on a stand-alone basis), non-transferable, worldwide, limited license to reproduce the Wiley Materials for the purpose specified in the licensing process. This license, **and any CONTENT (PDF or image file) purchased as part of your order**, is for a one-time use only and limited to any maximum distribution number specified in the license. The first instance of republication or reuse granted by this license must be completed within two years of the date of the grant of this license (although copies prepared before the end date may be distributed thereafter). The Wiley Materials shall not be used in any other manner or for any other purpose, beyond what is granted in the license. Permission is granted subject to an appropriate acknowledgement given to the author, title of the material/book/journal and the publisher. You shall also duplicate the copyright notice that appears in the Wiley publication in your use of the Wiley Material. Permission is also granted on the understanding that nowhere in the text is a previously published source acknowledged for all or part of this Wiley Material. Any third party content is expressly excluded from this permission.
- With respect to the Wiley Materials, all rights are reserved. Except as expressly granted by the terms of the license, no part of the Wiley Materials may be copied, modified, adapted (except for minor reformatting required by the new Publication), translated, reproduced, transferred or distributed, in any form or by any means, and no derivative works may be made based on the Wiley Materials without the prior permission of the respective copyright owner.**For STM Signatory Publishers clearing permission under the terms of the STM Permissions Guidelines only, the terms of the license are extended to include subsequent editions and for editions in other languages, provided such editions are for the work as a whole in situ and does not involve the separate exploitation of the permitted figures or extracts,** You may not alter, remove or suppress in any manner any copyright, trademark or other notices displayed by the Wiley Materials. You may not license, rent, sell, loan, lease, pledge, offer as security, transfer or assign the Wiley Materials on a stand-alone basis, or any of the rights granted to you hereunder to any other person.
- The Wiley Materials and all of the intellectual property rights therein shall at all times remain the exclusive property of John Wiley & Sons Inc, the Wiley Companies, or their respective licensors, and your interest therein is only that of having possession of and the right to reproduce the Wiley Materials pursuant to Section 2 herein during the continuance of this Agreement. You agree that you own no right, title or interest in or to the Wiley Materials or any of the intellectual property rights therein. You shall have no rights hereunder other than the license as provided for above in Section 2. No right, license or interest to any trademark, trade name, service mark or other branding ("Marks") of WILEY or its licensors is granted hereunder, and you agree that you shall not assert any such right, license or interest with respect thereto
- NEITHER WILEY NOR ITS LICENSORS MAKES ANY WARRANTY OR REPRESENTATION OF ANY KIND TO YOU OR ANY THIRD PARTY, EXPRESS, IMPLIED OR STATUTORY, WITH RESPECT TO THE MATERIALS

Chapter 3 Reproduced with permission from: (Page 3 of 5)

OR THE ACCURACY OF ANY INFORMATION CONTAINED IN THE MATERIALS, INCLUDING, WITHOUT LIMITATION, ANY IMPLIED WARRANTY OF MERCHANTABILITY, ACCURACY, SATISFACTORY QUALITY, FITNESS FOR A PARTICULAR PURPOSE, USABILITY, INTEGRATION OR NON-INFRINGEMENT AND ALL SUCH WARRANTIES ARE HEREBY EXCLUDED BY WILEY AND ITS LICENSORS AND WAIVED BY YOU.

- WILEY shall have the right to terminate this Agreement immediately upon breach of this Agreement by you.
- You shall indemnify, defend and hold harmless WILEY, its Licensors and their respective directors, officers, agents and employees, from and against any actual or threatened claims, demands, causes of action or proceedings arising from any breach of this Agreement by you.
- IN NO EVENT SHALL WILEY OR ITS LICENSORS BE LIABLE TO YOU OR ANY OTHER PARTY OR ANY OTHER PERSON OR ENTITY FOR ANY SPECIAL, CONSEQUENTIAL, INCIDENTAL, INDIRECT, EXEMPLARY OR PUNITIVE DAMAGES, HOWEVER CAUSED, ARISING OUT OF OR IN CONNECTION WITH THE DOWNLOADING, PROVISIONING, VIEWING OR USE OF THE MATERIALS REGARDLESS OF THE FORM OF ACTION, WHETHER FOR BREACH OF CONTRACT, BREACH OF WARRANTY, TORT, NEGLIGENCE, INFRINGEMENT OR OTHERWISE (INCLUDING, WITHOUT LIMITATION, DAMAGES BASED ON LOSS OF PROFITS, DATA, FILES, USE, BUSINESS OPPORTUNITY OR CLAIMS OF THIRD PARTIES), AND WHETHER OR NOT THE PARTY HAS BEEN ADVISED OF THE POSSIBILITY OF SUCH DAMAGES. THIS LIMITATION SHALL APPLY NOTWITHSTANDING ANY FAILURE OF ESSENTIAL PURPOSE OF ANY LIMITED REMEDY PROVIDED HEREIN.
- Should any provision of this Agreement be held by a court of competent jurisdiction to be illegal, invalid, or unenforceable, that provision shall be deemed amended to achieve as nearly as possible the same economic effect as the original provision, and the legality, validity and enforceability of the remaining provisions of this Agreement shall not be affected or impaired thereby.
- The failure of either party to enforce any term or condition of this Agreement shall not constitute a waiver of either party's right to enforce each and every term and condition of this Agreement. No breach under this agreement shall be deemed waived or excused by either party unless such waiver or consent is in writing signed by the party granting such waiver or consent. The waiver by or consent of a party to a breach of any provision of this Agreement shall not operate or be construed as a waiver of or consent to any other or subsequent breach by such other party.
- This Agreement may not be assigned (including by operation of law or otherwise) by you without WILEY's prior written consent.
- Any fee required for this permission shall be non-refundable after thirty (30) days from receipt by the CCC.
- These terms and conditions together with CCC's Billing and Payment terms and conditions (which are incorporated herein) form the entire agreement between you and WILEY concerning this licensing transaction and (in the absence of fraud) supersedes

Chapter 3 Reproduced with permission from: (Page 4 of 5)

all prior agreements and representations of the parties, oral or written. This Agreement may not be amended except in writing signed by both parties. This Agreement shall be binding upon and inure to the benefit of the parties' successors, legal representatives, and authorized assigns.

- In the event of any conflict between your obligations established by these terms and conditions and those established by CCC's Billing and Payment terms and conditions, these terms and conditions shall prevail.
- WILEY expressly reserves all rights not specifically granted in the combination of (i) the license details provided by you and accepted in the course of this licensing transaction, (ii) these terms and conditions and (iii) CCC's Billing and Payment terms and conditions.
- This Agreement will be void if the Type of Use, Format, Circulation, or Requestor Type was misrepresented during the licensing process.
- This Agreement shall be governed by and construed in accordance with the laws of the State of New York, USA, without regards to such state's conflict of law rules. Any legal action, suit or proceeding arising out of or relating to these Terms and Conditions or the breach thereof shall be instituted in a court of competent jurisdiction in New York County in the State of New York in the United States of America and each party hereby consents and submits to the personal jurisdiction of such court, waives any objection to venue in such court and consents to service of process by registered or certified mail, return receipt requested, at the last known address of such party.

WILEY OPEN ACCESS TERMS AND CONDITIONS

Wiley Publishes Open Access Articles in fully Open Access Journals and in Subscription journals offering Online Open. Although most of the fully Open Access journals publish open access articles under the terms of the Creative Commons Attribution (CC BY) License only, the subscription journals and a few of the Open Access Journals offer a choice of Creative Commons Licenses. The license type is clearly identified on the article.

The Creative Commons Attribution License

The Creative Commons Attribution License (CC-BY) allows users to copy, distribute and transmit an article, adapt the article and make commercial use of the article. The CC-BY license permits commercial and non-

Creative Commons Attribution Non-Commercial License

The Creative Commons Attribution Non-Commercial (CC-BY-NC)License permits use, distribution and reproduction in any medium, provided the original work is properly cited and is not used for commercial purposes.(see below)

Creative Commons Attribution-Non-Commercial-NoDerivs License

The Creative Commons Attribution Non-Commercial-NoDerivs License (CC-BY-NC-ND) permits use, distribution and reproduction in any medium, provided the original work is properly cited, is not used for commercial purposes and no modifications or adaptations are made. (see below)

Use by commercial "for-profit" organizations

Use of Wiley Open Access articles for commercial, promotional, or marketing purposes requires further explicit permission from Wiley and will be subject to a fee.

Further details can be found on Wiley Online Library

http://olabout.wiley.com/WileyCDA/Section/id-410895.html

Chapter 3 Reproduced with permission from: (Page 5 of 5)

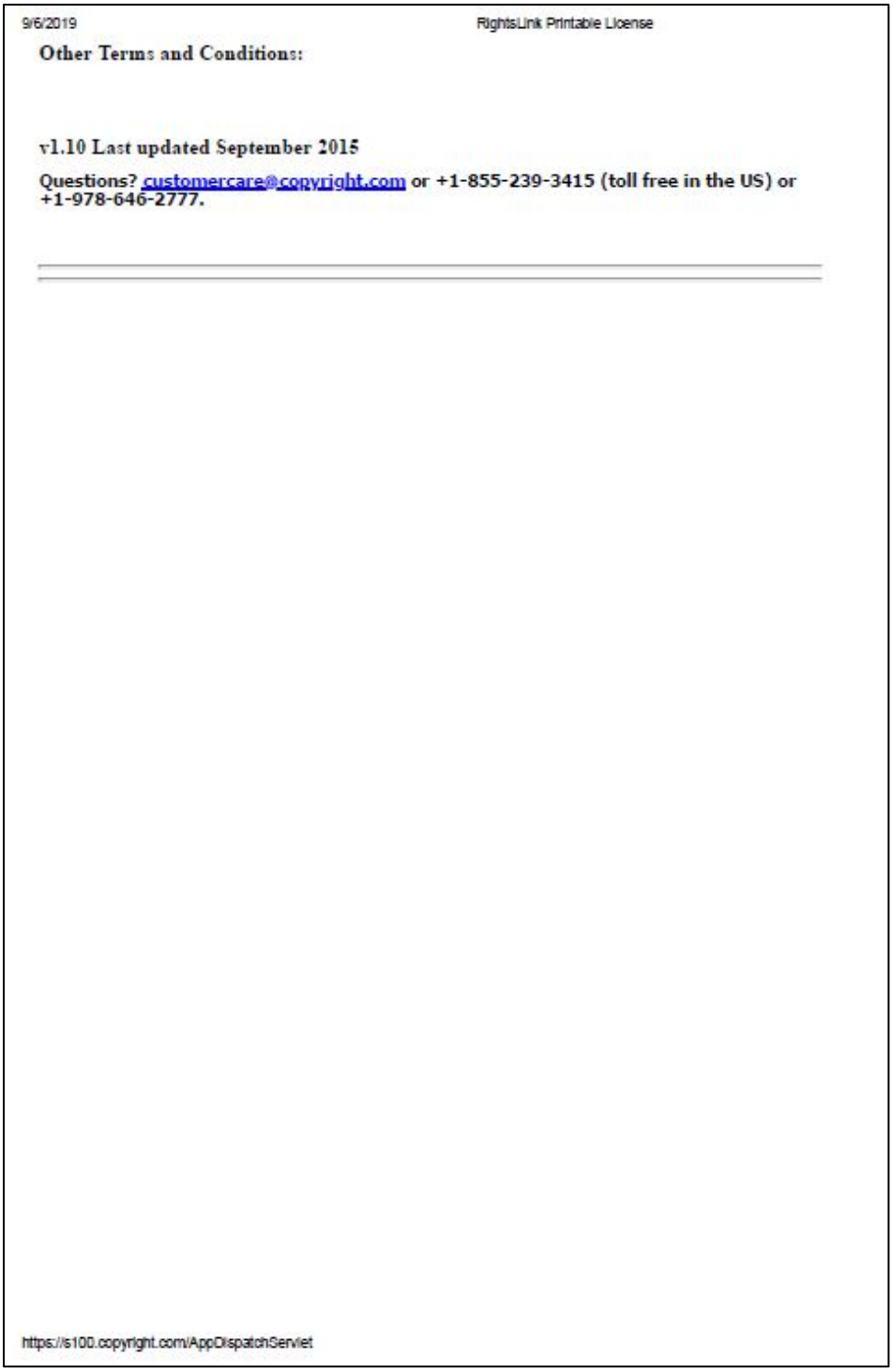

9/6/2019 RightsLink Printable License

Other Terms and Conditions:

v1.10 Last updated September 2015

Questions? customercare@copyright.com or +1-855-239-3415 (toll free in the US) or +1-978-646-2777.

https://s100.copyright.com/AppDispatchServlet

Chapter 4 Reproduced with permission from: (Page 1 of 5)

Royal Society of Chemistry LICENSE TERMS AND CONDITIONS

Oct 02, 2019

This is a License Agreement between Mr. Parth Patel ("You") and Royal Society of Chemistry ("Royal Society of Chemistry") provided by Copyright Clearance Center ("CCC"). The license consists of your order details, the terms and conditions provided by Royal Society of Chemistry, and the payment terms and conditions.

All payments must be made in full to CCC. For payment instructions, please see information listed at the bottom of this form.

License Number	4680740048047
License date	Oct 01, 2019
Licensed content publisher	Royal Society of Chemistry
Licensed content title	The analyst online
Licensed content date	Jan 1, 1876
Type of Use	Thesis/Dissertation
Requestor type	Academic institution
Format	Print, Electronic
Portion	chapter/article
The requesting person/organization is:	Parth K. Patel
Title or numeric reference of the portion(s)	Visible light-induced ion-selective optodes based on a metastable photoacid for cation detection
Title of the article or chapter the portion is from	Visible light-induced ion-selective optodes based on a metastable photoacid for cation detection
Editor of portion(s)	N/A
Author of portion(s)	N/A
Volume of serial or monograph.	N/A
Page range of the portion	
Publication date of portion	16 Nov 2015
Rights for	Main product
Duration of use	Life of current edition
Creation of copies for the disabled	no
With minor editing privileges	no
For distribution to	Worldwide
In the following language(s)	Original language of publication
With incidental promotional use	no
The lifetime unit quantity of new product	Up to 499
Title	Metastable-state Photoacid: Synthesis, Properties, and Applications
Institution name	University of Central Florida
Expected presentation date	Oct 2019
Billing Type	Invoice
Billing Address	Mr. Parth Patel 1283 Lexington Ave DAVENPORT, FL 33837 United States Attn: Mr. Parth Patel
Total (may include CCC user fee)	0.00 USD
Terms and Conditions	

TERMS AND CONDITIONS

The following terms are individual to this publisher:

None

Other Terms and Conditions:

STANDARD TERMS AND CONDITIONS

1. Description of Service; Defined Terms. This Republication License enables the User to obtain licenses for republication of one or more copyrighted works as described in detail on the relevant Order Confirmation (the "Work(s)"). Copyright Clearance Center, Inc. ("CCC")

Chapter 4 Reproduced with permission from: (Page 2 of 5)

grants licenses through the Service on behalf of the rightsholder identified on the Order Confirmation (the "Rightsholder"). "Republication", as used herein, generally means the inclusion of a Work, in whole or in part, in a new work or works, also as described on the Order Confirmation. "User", as used herein, means the person or entity making such republication.

2. The terms set forth in the relevant Order Confirmation, and any terms set by the Rightsholder with respect to a particular Work, govern the terms of use of Works in connection with the Service. By using the Service, the person transacting for a republication license on behalf of the User represents and warrants that he/she/it (a) has been duly authorized by the User to accept, and hereby does accept, all such terms and conditions on behalf of User, and (b) shall inform User of all such terms and conditions. In the event such person is a "freelancer" or other third party independent of User and CCC, such party shall be deemed jointly a "User" for purposes of these terms and conditions. In any event, User shall be deemed to have accepted and agreed to all such terms and conditions if User republishes the Work in any fashion.

3. Scope of License; Limitations and Obligations.

3.1 All Works and all rights therein, including copyright rights, remain the sole and exclusive property of the Rightsholder. The license created by the exchange of an Order Confirmation (and/or any invoice) and payment by User of the full amount set forth on that document includes only those rights expressly set forth in the Order Confirmation and in these terms and conditions, and conveys no other rights in the Work(s) to User. All rights not expressly granted are hereby reserved.

3.2 General Payment Terms: You may pay by credit card or through an account with us payable at the end of the month. If you and we agree that you may establish a standing account with CCC, then the following terms apply: Remit Payment to: Copyright Clearance Center, 29118 Network Place, Chicago, IL 60673-1291. Payments Due: Invoices are payable upon their delivery to you (or upon our notice to you that they are available to you for downloading). After 30 days, outstanding amounts will be subject to a service charge of 1-1/2% per month or, if less, the maximum rate allowed by applicable law. Unless otherwise specifically set forth in the Order Confirmation or in a separate written agreement signed by CCC, invoices are due and payable on "net 30" terms. While User may exercise the rights licensed immediately upon issuance of the Order Confirmation, the license is automatically revoked and is null and void, as if it had never been issued, if complete payment for the license is not received on a timely basis either from User directly or through a payment agent, such as a credit card company.

3.3 Unless otherwise provided in the Order Confirmation, any grant of rights to User (i) is "one-time" (including the editions and product family specified in the license), (ii) is non-exclusive and non-transferable and (iii) is subject to any and all limitations and restrictions (such as, but not limited to, limitations on duration of use or circulation) included in the Order Confirmation or invoice and/or in these terms and conditions. Upon completion of the licensed use, User shall either secure a new permission for further use of the Work(s) or immediately cease any new use of the Work(s) and shall render inaccessible (such as by deleting or by removing or severing links or other locators) any further

Chapter 4 Reproduced with permission from: (Page 3 of 5)

copies of the Work (except for copies printed on paper in accordance with this license and still in User's stock at the end of such period).
3.4 In the event that the material for which a republication license is sought includes third party materials (such as photographs, illustrations, graphs, inserts and similar materials) which are identified in such material as having been used by permission, User is responsible for identifying, and seeking separate licenses (under this Service or otherwise) for, any of such third party materials; without a separate license, such third party materials may not be used.
3.5 Use of proper copyright notice for a Work is required as a condition of any license granted under the Service. Unless otherwise provided in the Order Confirmation, a proper copyright notice will read substantially as follows: "Republished with permission of [Rightsholder's name], from [Work's title, author, volume, edition number and year of copyright]; permission conveyed through Copyright Clearance Center, Inc. " Such notice must be provided in a reasonably legible font size and must be placed either immediately adjacent to the Work as used (for example, as part of a by-line or footnote but not as a separate electronic link) or in the place where substantially all other credits or notices for the new work containing the republished Work are located. Failure to include the required notice results in loss to the Rightsholder and CCC, and the User shall be liable to pay liquidated damages for each such failure equal to twice the use fee specified in the Order Confirmation, in addition to the use fee itself and any other fees and charges specified.
3.6 User may only make alterations to the Work if and as expressly set forth in the Order Confirmation. No Work may be used in any way that is defamatory, violates the rights of third parties (including such third parties' rights of copyright, privacy, publicity, or other tangible or intangible property), or is otherwise illegal, sexually explicit or obscene. In addition, User may not conjoin a Work with any other material that may result in damage to the reputation of the Rightsholder. User agrees to inform CCC if it becomes aware of any infringement of any rights in a Work and to cooperate with any reasonable request of CCC or the Rightsholder in connection therewith.
4. Indemnity. User hereby indemnifies and agrees to defend the Rightsholder and CCC, and their respective employees and directors, against all claims, liability, damages, costs and expenses, including legal fees and expenses, arising out of any use of a Work beyond the scope of the rights granted herein, or any use of a Work which has been altered in any unauthorized way by User, including claims of defamation or infringement of rights of copyright, publicity, privacy or other tangible or intangible property.
5. Limitation of Liability. UNDER NO CIRCUMSTANCES WILL CCC OR THE RIGHTSHOLDER BE LIABLE FOR ANY DIRECT, INDIRECT, CONSEQUENTIAL OR INCIDENTAL DAMAGES (INCLUDING WITHOUT LIMITATION DAMAGES FOR LOSS OF BUSINESS PROFITS OR INFORMATION, OR FOR BUSINESS INTERRUPTION) ARISING OUT OF THE USE OR INABILITY TO USE A WORK, EVEN IF ONE OF THEM HAS BEEN ADVISED OF THE POSSIBILITY OF SUCH DAMAGES. In any event, the total liability of the Rightsholder and CCC (including their respective employees and directors) shall not exceed the total amount actually paid by User for this license. User

Chapter 4 Reproduced with permission from: (Page 4 of 5)

assumes full liability for the actions and omissions of its principals, employees, agents, affiliates, successors and assigns.

6. Limited Warranties. THE WORK(S) AND RIGHT(S) ARE PROVIDED "AS IS". CCC HAS THE RIGHT TO GRANT TO USER THE RIGHTS GRANTED IN THE ORDER CONFIRMATION DOCUMENT. CCC AND THE RIGHTSHOLDER DISCLAIM ALL OTHER WARRANTIES RELATING TO THE WORK(S) AND RIGHT(S), EITHER EXPRESS OR IMPLIED, INCLUDING WITHOUT LIMITATION IMPLIED WARRANTIES OF MERCHANTABILITY OR FITNESS FOR A PARTICULAR PURPOSE. ADDITIONAL RIGHTS MAY BE REQUIRED TO USE ILLUSTRATIONS, GRAPHS, PHOTOGRAPHS, ABSTRACTS, INSERTS OR OTHER PORTIONS OF THE WORK (AS OPPOSED TO THE ENTIRE WORK) IN A MANNER CONTEMPLATED BY USER; USER UNDERSTANDS AND AGREES THAT NEITHER CCC NOR THE RIGHTSHOLDER MAY HAVE SUCH ADDITIONAL RIGHTS TO GRANT.

7. Effect of Breach. Any failure by User to pay any amount when due, or any use by User of a Work beyond the scope of the license set forth in the Order Confirmation and/or these terms and conditions, shall be a material breach of the license created by the Order Confirmation and these terms and conditions. Any breach not cured within 30 days of written notice thereof shall result in immediate termination of such license without further notice. Any unauthorized (but licensable) use of a Work that is terminated immediately upon notice thereof may be liquidated by payment of the Rightsholder's ordinary license price therefor; any unauthorized (and unlicensable) use that is not terminated immediately for any reason (including, for example, because materials containing the Work cannot reasonably be recalled) will be subject to all remedies available at law or in equity, but in no event to a payment of less than three times the Rightsholder's ordinary license price for the most closely analogous licensable use plus Rightsholder's and/or CCC's costs and expenses incurred in collecting such payment.

8. **Miscellaneous.**

8.1 User acknowledges that CCC may, from time to time, make changes or additions to the Service or to these terms and conditions, and CCC reserves the right to send notice to the User by electronic mail or otherwise for the purposes of notifying User of such changes or additions; provided that any such changes or additions shall not apply to permissions already secured and paid for.

8.2 Use of User-related information collected through the Service is governed by CCC's privacy policy, available online here: http://www.copyright.com/content/cc3/en/tools/footer/privacypolicy.html.

8.3 The licensing transaction described in the Order Confirmation is personal to User. Therefore, User may not assign or transfer to any other person (whether a natural person or an organization of any kind) the license created by the Order Confirmation and these terms and conditions or any rights granted hereunder; provided, however, that User may assign such license in its entirety on written notice to CCC in the event of a transfer of all or substantially all of User's rights in the new material which includes the Work(s) licensed under this Service.

8.4 No amendment or waiver of any terms is binding unless set forth in writing and signed by the parties. The Rightsholder and CCC hereby

Chapter 4 Reproduced with permission from: (Page 5 of 5)

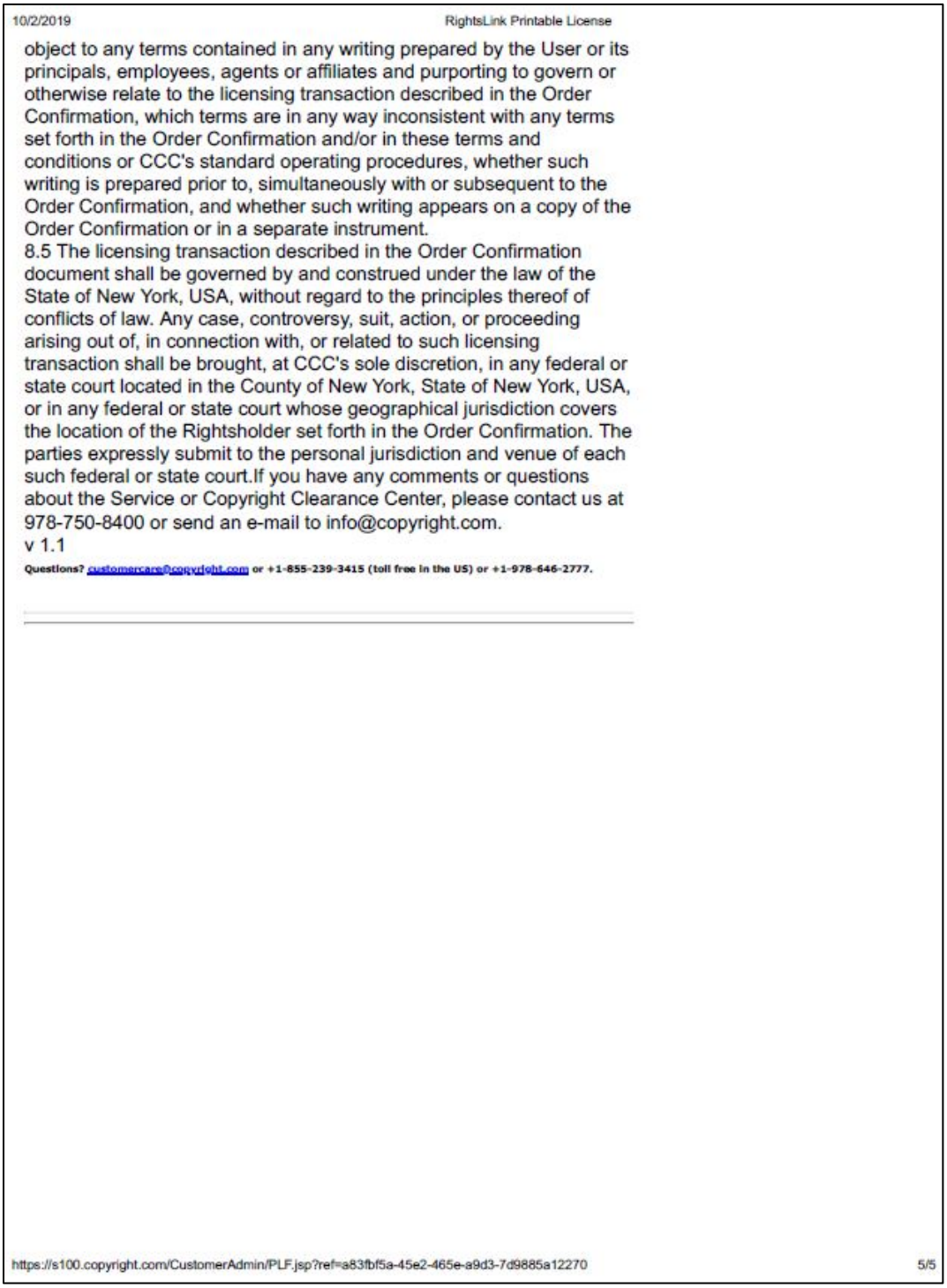

10/2/2019 RightsLink Printable License

object to any terms contained in any writing prepared by the User or its principals, employees, agents or affiliates and purporting to govern or otherwise relate to the licensing transaction described in the Order Confirmation, which terms are in any way inconsistent with any terms set forth in the Order Confirmation and/or in these terms and conditions or CCC's standard operating procedures, whether such writing is prepared prior to, simultaneously with or subsequent to the Order Confirmation, and whether such writing appears on a copy of the Order Confirmation or in a separate instrument.

8.5 The licensing transaction described in the Order Confirmation document shall be governed by and construed under the law of the State of New York, USA, without regard to the principles thereof of conflicts of law. Any case, controversy, suit, action, or proceeding arising out of, in connection with, or related to such licensing transaction shall be brought, at CCC's sole discretion, in any federal or state court located in the County of New York, State of New York, USA, or in any federal or state court whose geographical jurisdiction covers the location of the Rightsholder set forth in the Order Confirmation. The parties expressly submit to the personal jurisdiction and venue of each such federal or state court.If you have any comments or questions about the Service or Copyright Clearance Center, please contact us at 978-750-8400 or send an e-mail to info@copyright.com.

v 1.1

Questions? customercare@copyright.com or +1-855-239-3415 (toll free in the US) or +1-978-646-2777.

https://s100.copyright.com/CustomerAdmin/PLF.jsp?ref=a83fbf5a-45e2-465e-a9d3-7d9885a12270 5/5

Chapter 5 Reproduced with permission from: (Page 1 of 5)

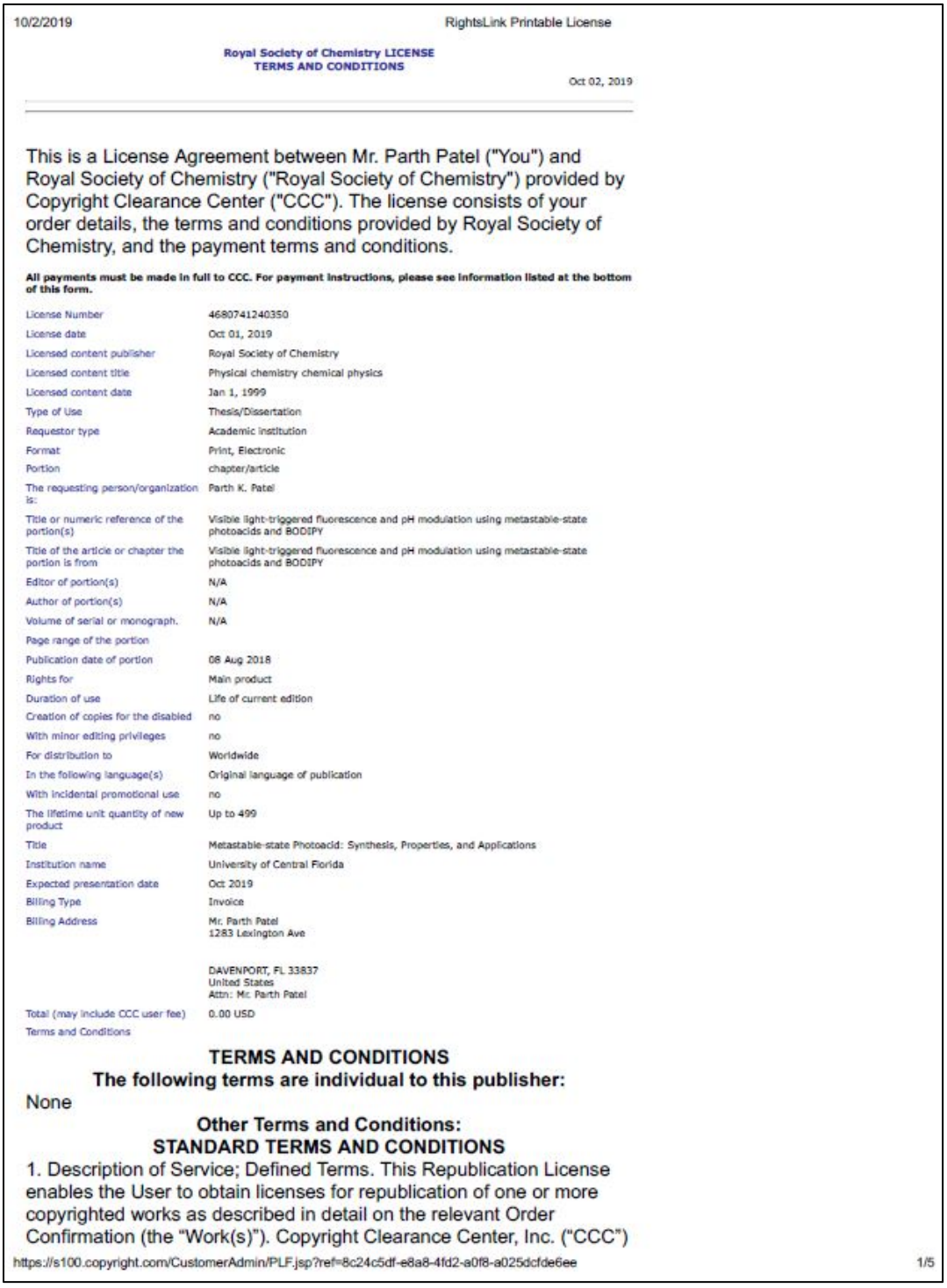

10/2/2019 RightsLink Printable License

Royal Society of Chemistry LICENSE TERMS AND CONDITIONS

Oct 02, 2019

This is a License Agreement between Mr. Parth Patel ("You") and Royal Society of Chemistry ("Royal Society of Chemistry") provided by Copyright Clearance Center ("CCC"). The license consists of your order details, the terms and conditions provided by Royal Society of Chemistry, and the payment terms and conditions.

All payments must be made in full to CCC. For payment instructions, please see information listed at the bottom of this form.

License Number	4680741240350
License date	Oct 01, 2019
Licensed content publisher	Royal Society of Chemistry
Licensed content title	Physical chemistry chemical physics
Licensed content date	Jan 1, 1999
Type of Use	Thesis/Dissertation
Requestor type	Academic institution
Format	Print, Electronic
Portion	chapter/article
The requesting person/organization is:	Parth K. Patel
Title or numeric reference of the portion(s)	Visible light-triggered fluorescence and pH modulation using metastable-state photoacids and BODIPY
Title of the article or chapter the portion is from	Visible light-triggered fluorescence and pH modulation using metastable-state photoacids and BODIPY
Editor of portion(s)	N/A
Author of portion(s)	N/A
Volume of serial or monograph.	N/A
Page range of the portion	
Publication date of portion	08 Aug 2018
Rights for	Main product
Duration of use	Life of current edition
Creation of copies for the disabled	no
With minor editing privileges	no
For distribution to	Worldwide
In the following language(s)	Original language of publication
With incidental promotional use	no
The lifetime unit quantity of new product	Up to 499
Title	Metastable-state Photoacid: Synthesis, Properties, and Applications
Institution name	University of Central Florida
Expected presentation date	Oct 2019
Billing Type	Invoice
Billing Address	Mr. Parth Patel 1283 Lexington Ave DAVENPORT, FL 33837 United States Attn: Mr. Parth Patel
Total (may include CCC user fee)	0.00 USD
Terms and Conditions	

TERMS AND CONDITIONS

The following terms are individual to this publisher:

None

Other Terms and Conditions:

STANDARD TERMS AND CONDITIONS

1. Description of Service; Defined Terms. This Republication License enables the User to obtain licenses for republication of one or more copyrighted works as described in detail on the relevant Order Confirmation (the "Work(s)"). Copyright Clearance Center, Inc. ("CCC")

https://s100.copyright.com/CustomerAdmin/PLF.jsp?ref=8c24c5df-e8a8-4fd2-a0f8-a025dcfde6ee 1/5

Chapter 5 Reproduced with permission from: (Page 2 of 5)

grants licenses through the Service on behalf of the rightsholder identified on the Order Confirmation (the "Rightsholder"). "Republication", as used herein, generally means the inclusion of a Work, in whole or in part, in a new work or works, also as described on the Order Confirmation. "User", as used herein, means the person or entity making such republication.

2. The terms set forth in the relevant Order Confirmation, and any terms set by the Rightsholder with respect to a particular Work, govern the terms of use of Works in connection with the Service. By using the Service, the person transacting for a republication license on behalf of the User represents and warrants that he/she/it (a) has been duly authorized by the User to accept, and hereby does accept, all such terms and conditions on behalf of User, and (b) shall inform User of all such terms and conditions. In the event such person is a "freelancer" or other third party independent of User and CCC, such party shall be deemed jointly a "User" for purposes of these terms and conditions. In any event, User shall be deemed to have accepted and agreed to all such terms and conditions if User republishes the Work in any fashion.

3. Scope of License; Limitations and Obligations.

3.1 All Works and all rights therein, including copyright rights, remain the sole and exclusive property of the Rightsholder. The license created by the exchange of an Order Confirmation (and/or any invoice) and payment by User of the full amount set forth on that document includes only those rights expressly set forth in the Order Confirmation and in these terms and conditions, and conveys no other rights in the Work(s) to User. All rights not expressly granted are hereby reserved.

3.2 General Payment Terms: You may pay by credit card or through an account with us payable at the end of the month. If you and we agree that you may establish a standing account with CCC, then the following terms apply: Remit Payment to: Copyright Clearance Center, 29118 Network Place, Chicago, IL 60673-1291. Payments Due: Invoices are payable upon their delivery to you (or upon our notice to you that they are available to you for downloading). After 30 days, outstanding amounts will be subject to a service charge of 1-1/2% per month or, if less, the maximum rate allowed by applicable law. Unless otherwise specifically set forth in the Order Confirmation or in a separate written agreement signed by CCC, invoices are due and payable on "net 30" terms. While User may exercise the rights licensed immediately upon issuance of the Order Confirmation, the license is automatically revoked and is null and void, as if it had never been issued, if complete payment for the license is not received on a timely basis either from User directly or through a payment agent, such as a credit card company.

3.3 Unless otherwise provided in the Order Confirmation, any grant of rights to User (i) is "one-time" (including the editions and product family specified in the license), (ii) is non-exclusive and non-transferable and (iii) is subject to any and all limitations and restrictions (such as, but not limited to, limitations on duration of use or circulation) included in the Order Confirmation or invoice and/or in these terms and conditions. Upon completion of the licensed use, User shall either secure a new permission for further use of the Work(s) or immediately cease any new use of the Work(s) and shall render inaccessible (such as by deleting or by removing or severing links or other locators) any further

Chapter 5 Reproduced with permission from: (Page 3 of 5)

copies of the Work (except for copies printed on paper in accordance with this license and still in User's stock at the end of such period).
3.4 In the event that the material for which a republication license is sought includes third party materials (such as photographs, illustrations, graphs, inserts and similar materials) which are identified in such material as having been used by permission, User is responsible for identifying, and seeking separate licenses (under this Service or otherwise) for, any of such third party materials; without a separate license, such third party materials may not be used.
3.5 Use of proper copyright notice for a Work is required as a condition of any license granted under the Service. Unless otherwise provided in the Order Confirmation, a proper copyright notice will read substantially as follows: "Republished with permission of [Rightsholder's name], from [Work's title, author, volume, edition number and year of copyright]; permission conveyed through Copyright Clearance Center, Inc. " Such notice must be provided in a reasonably legible font size and must be placed either immediately adjacent to the Work as used (for example, as part of a by-line or footnote but not as a separate electronic link) or in the place where substantially all other credits or notices for the new work containing the republished Work are located. Failure to include the required notice results in loss to the Rightsholder and CCC, and the User shall be liable to pay liquidated damages for each such failure equal to twice the use fee specified in the Order Confirmation, in addition to the use fee itself and any other fees and charges specified.
3.6 User may only make alterations to the Work if and as expressly set forth in the Order Confirmation. No Work may be used in any way that is defamatory, violates the rights of third parties (including such third parties' rights of copyright, privacy, publicity, or other tangible or intangible property), or is otherwise illegal, sexually explicit or obscene. In addition, User may not conjoin a Work with any other material that may result in damage to the reputation of the Rightsholder. User agrees to inform CCC if it becomes aware of any infringement of any rights in a Work and to cooperate with any reasonable request of CCC or the Rightsholder in connection therewith.
4. Indemnity. User hereby indemnifies and agrees to defend the Rightsholder and CCC, and their respective employees and directors, against all claims, liability, damages, costs and expenses, including legal fees and expenses, arising out of any use of a Work beyond the scope of the rights granted herein, or any use of a Work which has been altered in any unauthorized way by User, including claims of defamation or infringement of rights of copyright, publicity, privacy or other tangible or intangible property.
5. Limitation of Liability. UNDER NO CIRCUMSTANCES WILL CCC OR THE RIGHTSHOLDER BE LIABLE FOR ANY DIRECT, INDIRECT, CONSEQUENTIAL OR INCIDENTAL DAMAGES (INCLUDING WITHOUT LIMITATION DAMAGES FOR LOSS OF BUSINESS PROFITS OR INFORMATION, OR FOR BUSINESS INTERRUPTION) ARISING OUT OF THE USE OR INABILITY TO USE A WORK, EVEN IF ONE OF THEM HAS BEEN ADVISED OF THE POSSIBILITY OF SUCH DAMAGES. In any event, the total liability of the Rightsholder and CCC (including their respective employees and directors) shall not exceed the total amount actually paid by User for this license. User

Chapter 5 Reproduced with permission from: (Page 4 of 5)

assumes full liability for the actions and omissions of its principals, employees, agents, affiliates, successors and assigns.

6. Limited Warranties. THE WORK(S) AND RIGHT(S) ARE PROVIDED "AS IS". CCC HAS THE RIGHT TO GRANT TO USER THE RIGHTS GRANTED IN THE ORDER CONFIRMATION DOCUMENT. CCC AND THE RIGHTSHOLDER DISCLAIM ALL OTHER WARRANTIES RELATING TO THE WORK(S) AND RIGHT(S), EITHER EXPRESS OR IMPLIED, INCLUDING WITHOUT LIMITATION IMPLIED WARRANTIES OF MERCHANTABILITY OR FITNESS FOR A PARTICULAR PURPOSE. ADDITIONAL RIGHTS MAY BE REQUIRED TO USE ILLUSTRATIONS, GRAPHS, PHOTOGRAPHS, ABSTRACTS, INSERTS OR OTHER PORTIONS OF THE WORK (AS OPPOSED TO THE ENTIRE WORK) IN A MANNER CONTEMPLATED BY USER; USER UNDERSTANDS AND AGREES THAT NEITHER CCC NOR THE RIGHTSHOLDER MAY HAVE SUCH ADDITIONAL RIGHTS TO GRANT.

7. Effect of Breach. Any failure by User to pay any amount when due, or any use by User of a Work beyond the scope of the license set forth in the Order Confirmation and/or these terms and conditions, shall be a material breach of the license created by the Order Confirmation and these terms and conditions. Any breach not cured within 30 days of written notice thereof shall result in immediate termination of such license without further notice. Any unauthorized (but licensable) use of a Work that is terminated immediately upon notice thereof may be liquidated by payment of the Rightsholder's ordinary license price therefor; any unauthorized (and unlicensable) use that is not terminated immediately for any reason (including, for example, because materials containing the Work cannot reasonably be recalled) will be subject to all remedies available at law or in equity, but in no event to a payment of less than three times the Rightsholder's ordinary license price for the most closely analogous licensable use plus Rightsholder's and/or CCC's costs and expenses incurred in collecting such payment.

8. **Miscellaneous.**

8.1 User acknowledges that CCC may, from time to time, make changes or additions to the Service or to these terms and conditions, and CCC reserves the right to send notice to the User by electronic mail or otherwise for the purposes of notifying User of such changes or additions; provided that any such changes or additions shall not apply to permissions already secured and paid for.

8.2 Use of User-related information collected through the Service is governed by CCC's privacy policy, available online here: http://www.copyright.com/content/cc3/en/tools/footer/privacypolicy.html.

8.3 The licensing transaction described in the Order Confirmation is personal to User. Therefore, User may not assign or transfer to any other person (whether a natural person or an organization of any kind) the license created by the Order Confirmation and these terms and conditions or any rights granted hereunder; provided, however, that User may assign such license in its entirety on written notice to CCC in the event of a transfer of all or substantially all of User's rights in the new material which includes the Work(s) licensed under this Service.

8.4 No amendment or waiver of any terms is binding unless set forth in writing and signed by the parties. The Rightsholder and CCC hereby

Chapter 5 Reproduced with permission from: (Page 5 of 5)

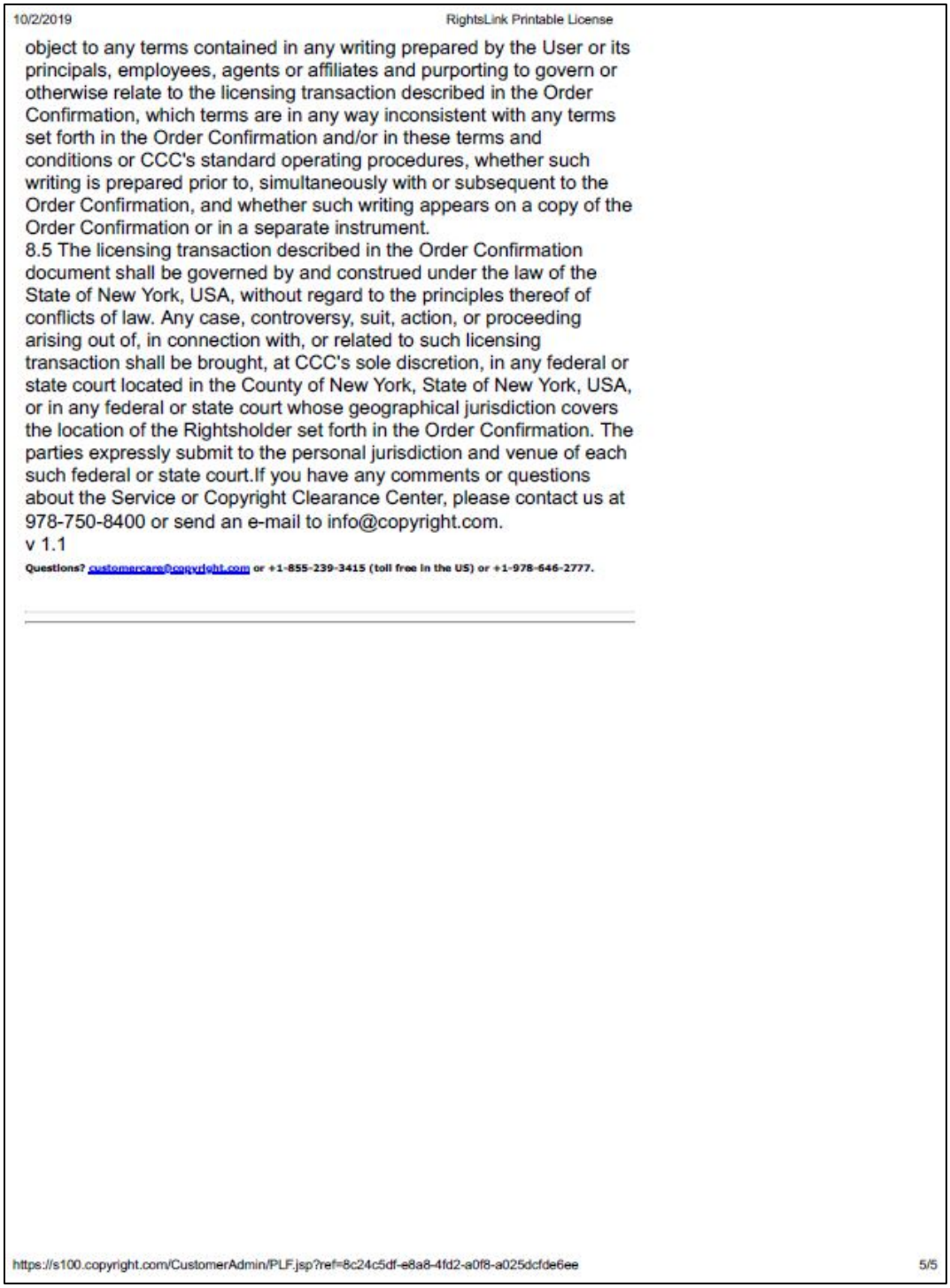

object to any terms contained in any writing prepared by the User or its principals, employees, agents or affiliates and purporting to govern or otherwise relate to the licensing transaction described in the Order Confirmation, which terms are in any way inconsistent with any terms set forth in the Order Confirmation and/or in these terms and conditions or CCC's standard operating procedures, whether such writing is prepared prior to, simultaneously with or subsequent to the Order Confirmation, and whether such writing appears on a copy of the Order Confirmation or in a separate instrument.

8.5 The licensing transaction described in the Order Confirmation document shall be governed by and construed under the law of the State of New York, USA, without regard to the principles thereof of conflicts of law. Any case, controversy, suit, action, or proceeding arising out of, in connection with, or related to such licensing transaction shall be brought, at CCC's sole discretion, in any federal or state court located in the County of New York, State of New York, USA, or in any federal or state court whose geographical jurisdiction covers the location of the Rightsholder set forth in the Order Confirmation. The parties expressly submit to the personal jurisdiction and venue of each such federal or state court.If you have any comments or questions about the Service or Copyright Clearance Center, please contact us at 978-750-8400 or send an e-mail to info@copyright.com.

v 1.1

Questions? customercare@copyright.com or +1-855-239-3415 (toll free in the US) or +1-978-646-2777.